A common European approach to the regulatory testing of nanomaterials

NANoREG

Grant Agreement Number 310584

Deliverable D 2.08

Protocols for exposure-fate characterization in ecotoxicity and in vitro studies

Due date of deliverable: *2016/01/31*

Actual submission date: *2016/09/02*

Author(s) and company:	Jorge Mejia, Stéphane Lucas (UNamur) Andy Booth, Julia Farkas (SINTEF) Stefania Sabella, Pasquale Bove, Mariada Malvindi (IIT) Keld Alstrup Jensen, Yahia Kembouche, Emilie Da Silva, Ulla Tegner (NRCWE) David Gonzales, Camilla Delpivo, Socorro Vazquez-Campos (LEITAT) Carlos Rey-Castro, Josep Galcerán, Calin A. David (UdL) Diana Boraschi, Alessandro Ponti (CNR) Jenny Rissler, Anders Gudmundsson (LTH) Deborah Oughton (NMBU)
Work package/task:	WP2 / Task 2.4
Document status:	draft / final
Confidentiality:	confidential / restricted / public
Key words:	

This project has received funding from the European Union Seventh Framework Programme (FP7/2007-2013) under grant agreement no 310584

DOCUMENT HISTORY

Version	*Date*	*Reason of change*
1	2015/11/10	First internal draft
2	2016/05/24	Second internal draft
3	2016/08/15	Revision by WP2 leader and request for input
4	2016/08/30	Final draft for WP leader review
5	2016/09/02	Final draft for MC pre-approval and last group circulation
6	2016/09/09	Final version
7	2016/10/07	Final version with amendments demanded by MC
8	2017/03/07	Project Office harmonized lay-out

Lead beneficiary for this deliverable: University of Namur, UNamur, 22

Owner(s) of this document	
Owner of the content	UNamur, 22
Co-Owner 1	IIT, 28
Co-Owner 2	UdL, 43
Co-Owner 3	NRCWE, 4
Co-Owner 4	CNR, 31
Co-Owner 5	LEITAT, 20
Co-Owner 6	SINTEF, 44
Co-Owner 7	NMBU, 50
Co-Owner 8	LTH, 37

Table of Content

1. DESCRIPTION OF TASK 10

2. DESCRIPTION OF WORK & MAIN ACHIEVEMENTS 10

2.1. SUMMARY 10

2.2. BACKGROUND OF THE TASK 13

2.2.1. Ecotoxicity studies 13

2.2.2. In vitro studies 14

2.2.3. Hydrochemical reactivity 15

2.3. DESCRIPTION OF THE WORK CARRIED OUT 16

2.3.1. Task 2.4 e) Procedures for quantification of MNM exposure and fate in dispersions for ecotoxicological studies 17

Recommendations and prerequisites 18

Overview of NANoREG ECOTOX Dispersion Characterisation TGD contents and approaches 18

Overview of test MNMs and ecotoxicity test set ups employed 20

Preparation of MNM stock dispersions 21

Characterisation of MNM exposure dispersions 21

MNM stability pre-test for exposure characterisation 21

2.3.2. Task 2.4 f) Procedures for quantification of MNM exposure and fate in dispersions for in vitro studies 22

2.3.3. Task 2.4 i) Characterization of MNM hydrochemical reactivity in synthetic biological fluids 24

2.4. RESULTS 25

2.4.1. Task 2.4 e) Procedures for quantification of MNM exposure and fate in dispersions for ecotoxicological studies 25

MNM stock dispersion verification 25

Influence of MNM exposure dispersion concentration on Z-ave values and PDI 25

MNM stability pre-test for exposure characterisation 30

2.4.2. Task 2.4 f) Procedures for quantification of MNM exposure and fate in dispersions for in vitro studies 37

NRCWE DLS procedure for assessment of sedimentation rate and agglomeration in exposure mediums 37

Experimental evaluation of LEITAT SOPs 39

Results from particle size determination (CLS) and concentration determination for fate-exposure of MNM dispersion during in vitro tests (sedimented dose) 44

Particle size distribution determination by CLS of MNM dispersions during in vitro assays 47

IIT procedure and relative protocol for characterization of MNM surface charge by zeta potential in synthetic human body fluids (simulating the human digestive compartments) or cellular biological media. 49

IIT procedure and protocol for characterization of MNM size and aggregation by DLS in cellular biological media 50

IIT procedure and relative protocol for characterization of MNM dissolution by ICP-AES in cellular biological media. 53

NRCWE procedure for assessing the hydrochemical reactivity and dissolution of MNM in vitro using the Sensor Dish Reader (SDR) method. 54
NRCWE procedure for assessing the particle adsorption of BSA, LDH and interleukins during incubation with MNM in in vitro exposure mediums 61
NRCWE method for Atmosphere-Temperature-pH-controlled Stirred Batch Reactor procedure for determination of hydrochemical reactivity and dissolution of MNM in phagolysomal cell fluids 66
IIT procedure and relative protocol for characterization of MNM size and aggregation by DLS in synthetic human body fluids (simulating the human digestive compartments). 68
IIT procedure and relative protocol for characterization of MNM size and aggregation by TEM in synthetic human body fluids (simulating the human digestive compartments). 69
IIT procedure for characterization of MNM dissolution by UF-ICP-AES in synthetic human body fluids (simulating the human digestive compartments) 70
2.5. Evaluation and conclusions 77
2.5.1. Task 2.4 e) Procedures for quantification of MNM exposure and fate in dispersions for ecotoxicological studies 77
2.5.2. Task 2.4 f) Procedures for quantification of MNM exposure and fate in dispersions for in vitro studies; 78
2.5.3. Task 2.4 i) Characterization of MNM hydrochemical reactivity in synthetic biological fluids. 78
2.6. Data management 78
3. DEVIATIONS FROM THE WORK PLAN 79
3.1. Task 2.4 e) Procedures for quantification of MNM exposure and fate in dispersions for ecotoxicological studies 79
3.2. Task 2.4 f) Procedures for quantification of MNM exposure and fate in dispersions for in vitro studies 79
3.3. Task 2.4 i) Characterization of MNM hydrochemical reactivity in synthetic biological fluids 79
4. REFERENCES / SELECTED SOURCES OF INFORMATION (OPTIONAL) 79

List of Figures

Figure 1. Schematic showing the preparation steps required for producing reproducible MNM dispersion for aquatic ecotoxicity testing. Recommended SOP are given in the blue boxes. 18

Figure 2. Schematic showing the relationship between the terms $C_{nominal}$, C_{total}, $C_{dissolved}$ and $C_{particulate}$. 19

Figure 3. Decision tree for assessing the degree of monitoring of MNM Z-ave required in ecotoxicity studies. 20

Figure 4. Decision tree for assessing the degree of monitoring of MNM dissolution required in ecotoxicity studies. 20

Figure 5. Strategy for the evaluation of exposure fate of MNMs during in vitro assessment. 23

Figure 6. Differences in NM-100 Z(ave) values in the two different test media, TG201 (algae) and MHRW (*D. magna*), and across the concentration range employed. 30

Figure 7. Z(ave) of metal oxide and metal particles (10 mg/L) in the algae test medium TG201 after 0 h and 72 h. 31

Figure 8. Z(ave) of metal oxide particles (10 mg/L) in the *D. magna* test medium MHRW after 0 h, 48 h and 72 h. 31

Figure 9. Graph showing the percentage of the metal oxide and metal MNM (NM-100, NM-101, NM-103 and NM-300K) in algae media (TG201) after 72 h. * NM-300K data not available. 34

Figure 10. Graph showing the percentage of the metal oxide MNM (NM-100, NM-101 and NM-103) in *D. magna* media (MHRW) after 72 h. 35

Figure 11. Graph showing the percentage of the CNT MNM (NM-400, NM-401 and NM-411) in algae media (TG201) after 72 h. 35

Figure 12. Graph showing the percentage of the CNT MNM (NM-400, NM-401 and NM-411) in *D. magna* media (MHRW) after 72 h. 36

Figure 13. a) Temporal evolution of the relative intensity; LOG(I/Io); and size; LOG(Z/Zo); of NM-101, NM-110 and NM-400 dispersed in RPMI with 0.2% glutamax (w/v). b) Regression curves (user defined models) for the three MNM for assessment of fractional deposition in 38

Figure 14. Dispersed particle settling assessment diagram plotting LOG(Z/Zo) versus LOG(I/Io). The graph shows the settling results from experiments with NM-101, NM-110, and NM-400 showing different evolution paths during the 24-hour incubation. The behaviour of NM-101 is dominated by deposition while first sedimentation followed by combined sedimentation and agglomeration plays an important role for NM-110. The NM-400 sample is first affected by slight deposition followed by accumulation and agglomeration at the vial bottom. 39

Figure 15. Z-ave of NM-200 in the stock solution and in the concentration series in DMEM 41

Figure 16. Z-ave of NM-101 dispersed at 100 ppm in complete culture medium DMEM at time 0, 3, 6, 24 h. The blue curve is obtained after sample homogenization ("dynamic" conditions), while the red one is obtained storing the sample to be tested inside the DLS cuvette, to ensure "static" condition. 42

Figure 17. Z-ave of NM-212 dispersed at 100 ppm in complete culture medium DMEM at time 0, 3, 6, 24h. .. 43

Figure 18. PdI of NM-212 dispersed at 100 ppm in complete culture medium DMEM at time 0, 3, 6, and 24h. 43

Figure 19. Zeta potential of NM-212 dispersed at 100 ppm in complete culture medium DMEM at time 0, 3, 6, and 24h. 43

Figure 20. Evolution of hydrodynamic diameter of main peak of ZnO MNM (NM-110) measured by CLS. Results are the average +/- standard deviation from two series of triplicates per condition. 45

Figure 21. Sedimented dose of ZnO MNM in culture medium with cells at different incubation times calculated from CLS measurements. 45

Figure 22. Sedimented dose of ZnO MNM in culture medium with cells at different incubation times calculated from PIXE measurements 47

Figure 23. Evolution of the concentration of ZnO MNM (NM-110) traced by the quantity of Zn by PIXE. Results are the weighted average +/- weighted standard deviation from a series of triplicates per condition. 47

Figure 24. Size distribution analysis of sonicated and stirred ZnO MNM in stock solutions or in Caco-2 cell culture medium by centrifugal liquid sedimentation. A) Agglomeration state profiles were obtained for sonicated and stirred ZnO MNM in water-BSA stock solutions or after dilution at 100 µg/ml in Caco-2 cell culture medium. B) Size distribution profiles of sonicated and stirred SiO_2 MNM after dilution at 100 µg/ml in Caco-2 cell culture medium were compared after 0h or 24h of incubation. Results are displayed as relative ZnO MNM weight distribution against the hydrodynamic diameter. Maximal values in each sample were arbitrarily normalized to 100. 48

Figure 25. Size distribution analysis of sonicated and stirred ZnO MNM in stock solutions or in Caco-2 cell culture medium by centrifugal liquid sedimentation. A) Agglomeration state profiles were obtained for sonicated and stirred ZnO MNM in water-BSA stock solutions or after dilution at 100 µg/ml in Caco-2 cell culture medium. B) Agglomeration state profiles were obtained for sonicated and stirred ZnO MNM after dilution at 100 or 10 µg/ml in Caco-2 cell culture medium. C) Size distribution profiles of sonicated and stirred ZnO MNM after dilution at 100 µg/ml in Caco-2 cell culture medium were compared after 0h or 24h of incubation. D) Size distribution profiles of both sonicated and stirred ZnO MNM (100 or 10 µg/ml) after 24h incubation in Caco-2 cell culture medium. Results are displayed as relative ZnO MNM weight distribution against the hydrodynamic diameter. Maximal values in each sample were arbitrarily normalized to 100. 49

Figure 26. Representative DLS spectra of NM-300K in biological cell media (DMEM and RPMI). 51

Figure 27. NM-300K size profile. The plot reports the size trend of Peak 1 over time (the deviation standard bars are relative to 10 runs) 51

Figure 28. Representative DLS spectra of NM-200 in biological cell media (DMEM and RPMI). 52

Figure 29. NM-200 size profile. The plot reports the size trend of Peak 3 (error bar are relative to 10 runs). ... 52

Figure 30. Representative DLS spectra of NM-110 in biological cell media (DMEM and RPMI). ... 53

Figure 31. NM-110 size profile. The plot reports the size trend of Peak 3 (error bar are relative to 10 runs). ... 53

Figure 32. Dissolution of NM-200 in DMEM and RPMI at the concentration of 20 nM for 0-48 hours by UF/ICP-OES. ... 54

Figure 33: SDR Sensor Dish Reader and illustration of the SDR measurement principle. In this study we used the 24-well Oxy- and HydroDish for O_2 and pH monitoring, respectively. Source: PreSens Precision Sensing GmbH, Germany. ... 55

Figure 34. a) dpH and b) dO_2 reactivity plots for NM-200 in HAMs F12 +10%FBS. A minor increase in both pH and O_2 is observed within the first 400 minutes of the test. The temperature fluctuations are due to sampling of mediums for dissolution studies. The temperature fluctuations are due to sampling of mediums for dissolution studies and to have some effect on the reactivity measurements. ... 56

Figure 35. a) dpH and b) dO_2 reactivity plots for NM-110 in HAMs F12 +10%FBS. A high increase in both pH and O_2 is observed at the start of the experiment and slowly diminishes during the entire experiment. The temperature fluctuations are due to sampling of mediums for dissolution studies. The temperature fluctuations are due to sampling of mediums for dissolution studies and appear to affect reactivity the measurements. ... 57

Figure 36. a) dpH and b) dO_2 reactivity plots for NM-111 in HAMs F12 +10%FBS. An increase in both pH and O_2 is observed at immediate the start of the experiment and slowly diminishes during mainly the first 800 min of the entire experiment. The temperature fluctuations are due to sampling of mediums for dissolution studies and appear to affect reactivity the measurements. ... 58

Figure 37. a) dpH and b) dO_2 reactivity plots for NM-300K in HAMs F12 +10%FBS. A weak increase in pH and a greater increase in O_2 is observed at immediate the start of the experiment and slowly diminishes during mainly the first 400 (dpH) to 800 (dO_2) min of the entire experiment. The temperature fluctuations are due to sampling of mediums for dissolution studies and appear to affect the reactivity measurements. ... 58

Figure 38. Concentration of Si dissolved during incubation [Si[NM-200]] compared to the measured [Si (NM-200)*] and calculated total Si dissolved from NM-200 [Si (NM-200)]** in HAM's F12+10%FBS cell medium during dissolution and hydrochemical reactivity testing of NM-200 plotted as function of time. The data fit a sub-linear power function suggesting a slowly decreasing dissolution rate within the 24-hour incubation time. The sampling time-points are added 0.50±0.25 hour to include time and uncertainty for dosing, sampling and centrifugal centrifugation. The estimated start concentration is calculated from the measured Si-concentration in HAMs F12 + 10% FBS (1.2 g/mL) and the batch dispersion (0.41 mg/L). ... 59

Figure 39. Temporal evolution in dissolved Zn [Zn (NM-110)] during incubation as compared to the measured [Zn (NM-110)*] and calculated total dissolved Zn [Zn (NM-110)**] in HAM's F12+10%FBS cell medium during dissolution and hydrochemical reactivity testing of NM-110. The data show a slightly irregular evolution during time which can be partially fitted to a sub-linear power function. A very high initial dissolution rate appears to rapidly decreasing within the first four-hour incubation time followed by a slight increase in the Zn release rate between 4 and 24 hours incubation. The sampling time-points are added 0.50±0.25 hour to include time and uncertainty for dosing, sampling and centrifugal centrifugation. The estimated start concentration is calculated from the measured Zn-concentration in HAMs F12 + 10% FBS (49.6 µg/L) and the batch dispersion (904.3 µg/L). ... 60

Figure 40. Temporal evolution of dissolved Zn [Zn (NM-111)] as compared to the measured [Zn (NM-111)*] and calculated total dissolved Zn from ZnO [Zn (NM-111)**] in HAM's F12+10%FBS cell medium during dissolution and hydrochemical reactivity testing of NM-111. The data show a slightly irregular evolution during time which can be partially fitted to a sub-linear power function. A very high initial dissolution rate appears to rapidly decreasing within the first four-hour incubation time followed by a slight increase in the Zn release rate between 4 and 24 hours incubation. The sampling time-points are added 0.50±0.25 hour to include time and uncertainty for dosing, sampling and centrifugal centrifugation. The estimated start concentration is calculated from the measured Zn-concentration in HAMs F12 + 10% FBS (49.6 µg/L) and the batch dispersion (904.3 µg/L). ... 60

Figure 41. Temporal evolution in the dissolved Ag-concentration during incubation [Ag (NM-300K)] of NM-300K in HAM's F12+10%FBS cell medium as compared to the measured Ag-concentration [Ag (NM-300K)*] during dissolution and hydrochemical reactivity testing of NM-300K. The data show a slightly irregular evolution as function of time which can be partially fitted to a sub-linear power function. Dissolution appears to occur within the first four-hour incubation time followed by stagnation or potentially even re-precipitation of Ag between 4 and 24 hours incubation. The sampling time-points are added 0.50±0.25 hour to include time and

uncertainty for dosing, sampling and centrifugal centrifugation. The estimated start concentration is calculated from the measured Ag-concentration in HAMs F12 + 10% FBS (3.4 µg/L). 61

Figure 42. Concentration of BSA adsorbed onto the NANoREG core MNM compared to the relative percentage of BSA present in the NANOGENOTOX dispersion medium with 2.56 mg MNM/mL. 62

Figure 43. Loss in LDH-concentration from HAMs F12+10%FBS cell medium after 24-hours incubation in a cell incubator plotted as function of MNM dose. All NANoREG core MNM were tested and data are only plotted for experiments where the LDH concentration difference exceed the standard deviation of the controls. The LDH loss is assumed to be due to adsorption onto the MNM test materials. 63

Figure 44. Loss in IL-6-concentration from HAMs F12+10%FBS cell medium after 24-hours incubation in a cell incubator plotted as function of MNM dose. All NANoREG core MNM were tested and data are only plotted for experiments where the IL-6 concentration difference exceed the standard deviation of the controls. The IL-6 loss is assumed to be due to adsorption onto the MNM test materials. 64

Figure 45. Loss in IL-8-concentration from HAMs F12+10%FBS cell medium after 24-hours incubation in a cell incubator plotted as function of MNM dose. All NANoREG core MNM were tested and data are only plotted for experiments where the IL-8 concentration difference exceed the standard deviation of the controls. For NM-101, the regression curve is only calculated in the linear range in the first four doses only, before the medium starts to be depleted. The IL-8 loss is assumed to be due to adsorption onto the MNM test materials. 64

Figure 46. Temporal evolution in pH and Eh coupled with measured titrant volume in tests with NM-110 and NM-300K and the reference medium PSF. Addition of NM-110 causes immediate increase in Eh and pH and counterbalancing titration, which suggests an acute strong reaction. Addition of NM-300K results in a long-term addition of titrant with reduction in Eh and no increase in pH, which suggests a long-term slow reaction. 67

Figure 47. Temporal evolution of Zn and Ag concentrations in PSF kept at pH and Eh conditions plotted above. All concentrations are almost constant in the measured samples suggesting very rapid dissolution of most of the soluble fraction in both NM-110 and NM-300K. However, a clear increase is also observed from 24 hours to 48 hours, where the blind-control background concentration also increases slightly for both Zn and Ag. 67

Figure 48. MNM size profile in the human digestive juices. The plots report the size trend of DLS Peak 1 possibly related to primary MNM (deviation standard bars are relative to 10 runs). Body compartments are the size signals detected for inorganic/organic/protein components of the *in vitro* human digestive compartments. 69

Figure 49. TEM images of MNM in synthetic human digestive juices: Images show MNM dissolution in the stomach and a partial re-aggregation in the intestine-bile compartments for NM-300K. For the NM-200 and NM-110 MNM, it was possible observing only aggregation by this technique. 70

Figure 50. Histograms reporting the dissolution efficiency (mg/mL) of NM-300k at two concentration values into the human body compartments simulating the oral exposure of NMs. Note: results are affected by down-estimation due to the partial filter clogging. 71

Figure 51. Histograms reporting the dissolution rate (mg/mL) of NM-200 at two concentration values into the human body compartments simulating the oral exposure of NMs. Note: results are affected by down-estimation due to the partial filter clogging. 71

Figure 52. Histograms reporting the dissolution rate (mg/mL) of NM-110 at two concentration values into the human body compartments simulating the oral exposure of NMs. Note: results are affected by down-estimation due to the partial filter clogging. 72

Figure 53. UV-Vis spectra of NM300K in water. 73

Figure 54. UV-Vis spectra of NM-300K in saliva compartment. 73

Figure 55. Characterization of NM-300K in saliva. 74

Figure 56. UV-Vis spectra of NM-300K in stomach compartment 75

Figure 57. Characterization of NM-300K in stomach 75

Figure 58. UV-Vis spectra of NM-300K in intestine compartment 76

List of Tables

Table 1. Minimum characterization requirements for *in vitro* and ecotoxicologial studies in NANoREG 17

Table 2. Z-ave of stock solutions of the metal and metal oxide particles NM-100, NM-101, NM-103 and NM-300K..... 25

Table 3. Z-ave of stock solutions of CNTs NM-400, NM-401 and NM-411 25

Table 4. Z-ave and zeta potential values of NM-300K in the range-finding concentration series in TG201 (algae media, no NOM). 26

Table 5. Z-ave and zeta potential values of NM-100 in the range-finding concentration series in TG201 (algae media, no NOM) and MHRW (*D. magna*, no NOM). 26

Table 6. Z-ave and zeta potential values of NM-101 in the range-finding concentration series in TG201 (algae media, no NOM) and MHRW (*D. magna*, no NOM). 27

Table 7. Z-ave and zeta potential values of NM-103 in the range-finding concentration series in TG201 (algae media, no NOM) and MHRW (*D. magna*, no NOM). 27

Table 8. Z-ave and zeta potential values of NM-400 in the range-finding concentration series in TG201 (algae media, NOM) and MHRW (*D. magna*, NOM). 28

Table 9. Z-ave and zeta potential values of NM-401 in the range-finding concentration series in TG201 (algae media, NOM) and MHRW (*D. magna*, NOM). 28

Table 10. Z-ave and zeta potential values of NM-411 in the range-finding concentration series in TG201 (algae media, NOM) and MHRW (*D. magna*, NOM). 29

Table 11. NM-300K concentration in the algae ecotoxicity range-finding test at 0 h and 72 h (in TG201 algae media, no NOM). 31

Table 12. NM-100 concentration in the algae ecotoxicity range-finding test at 0 h and 72 h (in TG201 algae media, no NOM) and in the daphnia ecotoxicity range-finding test at 0 h, 48, and 72 h (in MHRW, no NOM). 32

Table 13. NM-101 concentration in the algae ecotoxicity range-finding test at 0 h and 72 h (in TG201 algae media, no NOM) and in the daphnia ecotoxicity range-finding test at 0 h, 48, and 72 h (in MHRW, no NOM). 32

Table 14. NM-103 concentration in the algae ecotoxicity range-finding test at 0 h and 72 h (in TG201 algae media, no NOM) and in the daphnia ecotoxicity range-finding test at 0 h, 48, and 72 h (in MHRW, no NOM). 32

Table 15. NM-400 concentration in the algae ecotoxicity range-finding test at 0 h and 72 h (in TG201 algae media, no NOM) and in the daphnia ecotoxicity range-finding test at 0 h, 48, and 72 h (in MHRW, no NOM). 33

Table 16. NM-401 concentration in the algae ecotoxicity range-finding test at 0 h and 72 h (in TG201 algae media, no NOM) and in the daphnia ecotoxicity range-finding test at 0 h, 48, and 72 h (in MHRW, no NOM). 33

Table 17. NM-411 concentration in the algae ecotoxicity range-finding test at 0 h and 72 h (in TG201 algae media, no NOM) and in the daphnia ecotoxicity range-finding test at 0 h, 48, and 72 h (in MHRW, no NOM). 33

Table 18. Dissolved concentrations of NM-300K, NM-100, NM-101 and NM-103 in the algae ecotoxicity range-finding test at 0 h and 72 h (in TG201 algae media, no NOM) and in the daphnia ecotoxicity range-finding test at 0 h, 48, and 72 h (in MHRW, no NOM). Data generated at 50 mg/L (NM-300K) and 100 mg/L (NM-100, NM-101 and NM-103) exposure concentrations. 36

Table 19. Calculated fractional deposition time in hours for NM-101, NM-110, and NM-400 calculated from equations in Figure 12. 38

Table 20. Z-ave of NM-200 in the stock solution and in the concentration series in DMEM..... 40

Table 21. Z-ave of NM-200 stock dispersions. 44

Table 22. Z-ave, PdI and zeta potential of NM-200 dispersed at 100 ppm in complete culture medium DMEM at time 0, 3, 6, and 24 h. 44

Table 23. Surface charge of MNM in the biological media DMEM and RPMI supplemented with 10% of proteins. CTRL refers to surface charge of MNM after the dispersion by NANOGENOTOX protocol (with 0.05 % of BSA) 50

Table 24. MNM surface charges in the human *in vitro* digestive compartments. CTRL refers to surface charge of MNM after the dispersion by NANOREGONOTOX protocol (with 0.05 % of BSA) 50

Table 25. Dissolution of NM-300K, NM-110, and NM-200 in DMEM and RPMI at the concentration of 20 nM for 0-48 hours by UF/ICP-OES. 54

Table 26. Colour-coded relative scale for the fraction of BSA adsorbed and the percentage doses-adsorption slope for LDH, IL-6 and IL-8. Green indicates lowest values (minimum) and red highest values (maximum). For samples were the LDH, IL-6 or IL-8 is depleted the slopes were calculated based on the data that show linear dose-response behaviour. 65

Table 27. Elemental concentrations measured at different time-points during dissolution of NM-110 and NM-300K in PSF (n = 2) 67

1. Description of task

This task focuses on the development of measurement procedures for accurate quantification of MNM exposure concentrations and characteristics, including MNM fate, in ecotoxicological and *in vitro* test media.

Mediums used for dispersions should have no or limited disturbing interaction with the MNM, the bio-assays and its end-points analysis. Dispersion stabilities and potential use-constraints will be characterized. Methods for dispersion of MNM in air will be evaluated for their ability to generate nm-size particle and mimic characteristics in the exposure scenarios identified in WP3. In both cases experience from previous studies will be taken into account.

Procedures for exposure measurements of both liquid-dispersed (e.g., DLS) and airborne MNM dust (e.g., SMPS) including an analysis of reliability of unit conversions (e.g., size-distribution to surface area to mass or vice versa) will be evaluated for and potential SOPs developed with explanation on measurement limitations.

Moreover the importance of direct-contact-dose is unclear for some end-points. The exposure and dose may also be due to hydrochemical reactions (redox-activity, acidity, formation of reactive oxygen species, dissolution/dissociation/biodurability) where direct particle-cell interaction is not needed. The procedures will be developed and validated in close collaboration with WP3, WP4 and WP5.

SOPs for description of particle fate in environmental and biological systems will also be implemented in the project following recommendations from task 3.1.3. New procedures for characterization of NM-induced oxidative stress in the test systems as well as the biodurability of NM in synthetic biological fluids (e.g, lung lining, lysosome, and gastric fluids) will be established. Initial protocols for such analyses are underway in connection with a number of EU FP7 projects.

2. Description of work & main achievements

2.1. Summary

The information reported in Deliverable 2.8 derives from 3 related sub-tasks conducted as part of NANoREG WP2:

Task 2.4e) procedures for quantification of MNM exposure and fate in dispersions for ecotoxicologial studies (lead partner SINTEF)

Task 2.4f) procedures for quantification of MNM exposure and fate in *in vitro* exposure mediums. (Lead partner UNamur)*

Task 2.4i) characterization of MNM hydrochemical reactivity in synthetic biological fluids (lead partner NRCWE?)*

* Task2.4g use similar SOPs and is not further described.

Although many of the challenges associated with the analysis and quantification of MNM dispersions, exposure, fate and reactivity in ecotoxicity and *in vitro* tests are similar, methods do sometimes differ and a separation into tasks facilitated a more focused work approach, description of procedures and ultimately results that optimized to each experimental system. A brief overview of the each aforementioned tasks is provided below:

Task 2.4e) Procedures for quantification of MNM exposure and fate dispersion for ecotoxicological studies

Partners SINTEF, NMBU, UdL and LEITAT developed a Technical Guidance Document (TGD) describing a physicochemical characterisation strategy for MNM in aquatic environmental fate and ecotoxicity exposure

media. The TGD is developed to provide researchers and scientists with a framework for conducting and generating a necessary level of physicochemical MNM characterisation during aquatic ecotoxicity studies for assessment of MNMs. The TGD was developed by NANoREG partners who have significant experience and competence in conducting both aquatic ecotoxicity studies and MNM characterisation in such studies.

Many laboratories conducting ecotoxicity studies have a limited amount of characterisation instrumentation available. Furthermore, such analyses can be come at a considerable cost on top of the 'standard' costs associated with conducting ecotoxicity studies. The TGD contains a detailed overview of both the **'Minimum'** and **'Additional/Desirable'** MNM characterisation requirements for exposure and fate in ecotoxicity studies. The TGD has been structured in this way in order to try and make such work an affordable/viable element of conducting ecotoxicity studies.
In particular, the TGD describes a procedure for the characterisation of test MNMs at the start and end of the exposure study in order to determine changes in particle size and morphology over time and provide appropriate data for a meaningful interpretation of the ecotoxicological endpoints determined. Importantly, the TGD has been developed in such a way as to make it applicable to any aquatic ecotoxicity test. The TGD has been evaluated during its implementation in the aquatic ecotoxicity studies conducted with WP4 of NANoREG. Two of the partners (SINTEF and NMBU) also have significant activity and roles within conducting aquatic ecotoxicity studies within WP4 of NANoREG. As a result, example data and an evaluation of the performance and suitability of the TGD are provided in this report.

Task 2.4f) Procedures for quantification of MNM exposure and fate in in vitro exposure mediums

In this deliverable, methods for assessing the particle dispersion stabilities in *in vitro* and *In vitro* batch dispersions as well as *in vitro* exposure mediums where established and / or documented. The methods applied for the analysis are conceptually similar; but examples are primarily given using *in vitro* exposure mediums as demonstration of dispersion stabilities in NANOGENOTOX batch dispersions have been demonstrated previously (www.nanogenotox.eu).

NRCWE, further improved the procedures, previously developed as part of the ENPRA and NANOGENOTOX projects, to assess the sedimentation rates and level of agglomeration of nanomaterials in *in vitro* test mediums using the DLS under fixed measurement parameters. This procedure can be used to assess the dose rate of sedimenting particles dispersed at the beginning of the tests and. The procedure was developed as a sub-chapter in the NANoREG DLS protocol for toxicological studies and suggested in the technical guidance document for the NANoREG toxicological studies. There has not yet been an attempt to compare the results obtained by this method with results from other methods developed within the task.

Minor revision of the data-treatment for describing agglomeration and sedimentation rates in situ was made as part of NANoREG and exemplified. The method relies on the relative intensity of the light scattered from the sample when incubated in a DLS cuvette and kept for a certain time-period (here 24 hours) at fixed test temperatures (here 37°C) to simulate the conditions of the *in vitro* test. At the same time, coupling the change in intensity with changes in average zeta-size gives indication on whether the material, near the bottom of the cell-vial undergo agglomeration, accumulation or fining during the sedimentation.

Recalculating results obtained during testing of a number of NANoREG MNM (NM-101, NM-110, and NM-400) in previous work, demonstrate the ability of the method to estimate the level of sedimentation and sedimentation and agglomeration behaviour of nanomaterials in specific cell mediums as function of time. Limitations may be different behaviour of dispersions in cell incubation plates and effects caused by presence of controlled CO_2 concentrations in cell incubators.

LEITAT performed a series of experiments focused on three core MNM (NM-101 NM-200 and NM-212) that were investigated in term of size, pH and zeta potential (Zetasizer nano ZS series, Malvern Instruments) as function of time, simulating the "condition" (preparation, timing, dilution in Dulbecco's Modified Eagle's medium (DMEM) as cell culture medium...) of *in vitro* assays.

UNamur developed two protocols for exposure-fate characterization of MNMs dispersions in *in vitro* studies. The first protocol is to determine the particle size distribution of a given MNM in cell culture media by the Centrifuge Liquid Sedimentation (CLS) technique. A second protocol is to quantify the concentration of a given MNM in cell culture media with the Particle-Induced X-ray Emission (PIXE) technique. A methodology is proposed to calculate the sedimentation dose from data obtained using both techniques. Results of the evaluation of MNMs in contact with cells in culture medium during *in vitro* assessment have shown that effective doses are significantly smaller than nominal doses. Values of about 50% for the sedimented dose

with respect to the nominal dose were observed. A time dependent behaviour was also observed. Furthermore, a correlation is observed between results from both techniques, which indicate that a validation using similar techniques, such as DLS, could be stablished. Using this approach, the determination of a correction factor for the nominal dose used in an in vitro experiment can be stablished.

IIT performed studies to investigate NM exposure and fate in biological media of relevance for *in vitro* cell studies particularly focusing on tracing changes of two physical properties of MNM that are surface charge and size. To do so, a multi-technique based method was developed that employ zeta-potential, DLS, UF/ICP-AES.

Results show that MNM (NM-300K, NM-200, NM-110), once incubated in these synthetic fluids, do not maintain their primary properties. Size changes were due to aggregation/agglomeration and to dissolution. Overall, these changes lead to a formation of complex mixtures of bio-transformed products including different organic, inorganic and ion molecular species, which are the actual species responsible of sedimented dose, cellular permeability and uptake *in vitro*/*In vitro*.

Task 2.4i) Characterization of MNM hydrochemical reactivity in synthetic biological fluid

NRCWE established a procedure to test and quantify the interaction between test materials and LDH, IL-6 and IL-8 in HAMs F12 with 10% Foetal Bovine Serum for correction of toxicological test results and further fate (uptake) assessments. The method is based on incubation of test materials with LDH and interleukin-doped cell medium and quantification of LDH and interleukin-loss by the use of suitable ELISA assays. Tests were made on all NANoREG core MNM. The results show variable levels of BSA-adsorption across the sample suite. Some materials also adsorb interleukins and LDH and in a few cases (NM-300K, NM-110 and NM-111). The results from these tests can be used directly to correct for interaction between LDH and interleukins and test materials, which is especially important in colorimetric ELISA assays.

NRCWE also further refined two previously established procedures to quantify the acid-base and oxidative-reductive reactivity and the test- and medium-specific dissolution rate of MNM during *in vitro* cell incubation as well as in phagolysosomal fluid (PSF) after potential cellular uptake. The SDR (Sensor Dish Reader Method) is used to investigate the medium-specific fate of MNM in situ during the exact incubation conditions applied in *in vitro* studies. Reactivity is quantified as the pH and O_2 concentration change in the cell medium doped with a MNM dose as compared to the effect in reference mediums. The ATempH SBR (Atmosphere-Temperature-pH controlled Stirred Batch Reactor) Method is applied to investigate the MNM fate during specific biological conditions. In this case, we established and demonstrated the method to investigate the reactivity and dissolution of MNM in the PSF. The reactivity in the ATempH SBR method is investigated by the amount of titrant required to maintain the PSF system at pH = 4.5 and direct measurement of the redox potential (E_h) in the medium. Results are to be compared with the reference medium. In both systems, the dissolution of the test materials is quantified based on elemental analysis of 3KDa centrifuge-filtered medium samples (as established in D2.9). Modifications include time-point sampling of liquids to assess the dissolution rate rather than a single time-point measurement and particle separation in liquid samples by 3kDa centrifugal filtering as agreed also in D2.9.

Results testing the dissolution behaviour of NM-200, NM-110, and NM-300K showed that it is possible to describe the acid-base and oxidative-reductive behaviour of the test materials in a cell medium and in PSF. In addition, due to sampling of exposure / test mediums at different time-points during testing reveals the medium-and test-specific dissolution rates. However, the results also show that critical care must be made in regards to interaction with *in vitro* systems during incubation as repeated interruptions appears to potentially affect the reactive behaviour.

IIT performed studies to investigate MNM exposure and fate in *synthetic biological fluid* particularly focusing on tracing changes of MNM size and quantifying dissolution. To do so, a multi-technique based method was developed that employ DLS, TEM, UF/ICP-AES, UV-Vis and using synthetic human body fluids (simulating the human digestive compartments). Results show that MNM (NM-200, NM-110, and NM-300K), once incubated in these synthetic fluids, do not maintain their primary properties but most of them agglomerate and dissolve in the corresponding ions. Size changes were due to aggregation/agglomeration and to dissolution. Overall, these changes lead to a formation of complex mixtures of bio-transformed products including different organic, inorganic and ion molecular species (free and bound to matrix), which are the actual species responsible of sedimented / effective dose, cellular permeability and uptake *in vitro*/*In vitro*.

2.2. Background of the task

2.2.1. Ecotoxicity studies

A number of comprehensive reviews are available that provide in depth discussions of the advantages and disadvantages of a range of analytical techniques available for the characterisation and analysis of engineered nanomaterials (MNM) (Wigginton, Haus et al. 2007, Tiede, Hassellöv et al. 2009, Paterson, Macken et al. 2011, Weinberg, Galyean et al. 2011). Environmental fate and effects research of MNM has highlighted the need for comprehensive characterisation of nanomaterials in order to draw conclusive results from the data. In addition to characterisation of the pure MNM, assessment of their behaviour in relevant ecotoxicity exposure media (biological tissues, natural surface waters, soils and sediments) is necessary. MNM properties including particle size and size distribution, surface charge and shape properties, solubility and agglomeration and aggregation states in environmental and experimental media are known to change substantially relative to mono-dispersed controlled media suspensions (Warheit 2008, Domingos, Baalousha et al. 2009, Paterson, Macken et al. 2011). The complexity of test media clearly introduces additional challenges for the extraction and detection of MNM in such matrices (Paterson, Macken et al. 2011). Furthermore, the difficulties associated with distinguishing between naturally occurring and anthropogenically generated nanomaterials adds greatly to these analytical challenges (Paterson, Macken et al. 2011). Previously, critical MNM characteristics that should be determined for toxicological assessments include particle size/size distribution, surface chemistry, surface area and the particle chemical composition and concentration (Warheit 2008, Domingos, Baalousha et al. 2009, Paterson, Macken et al. 2011).

A large number of MNM have been investigated in environmental fate and effects studies. Reviews are available that discuss the environmental behaviour and ecotoxicity of MNM towards aquatic and terrestrial organisms such as algae, crustaceans, ciliates, fish, bacteria, fungi, plants, nematodes and earthworms (Baun, Hartmann et al. 2008, Navarro, Baun et al. 2008, Kahru and Dubourguier 2010, Handy, Cornelis et al. 2012, Miralles, Church et al. 2012). A wide range of lethal and sub lethal endpoints have been investigated (Baun, Hartmann et al. 2008), but reported ecotoxicity data is often inconsistent due to the use of different exposure conditions and limited understanding of MNM physical and chemical properties. The majority of these studies have concerned mammals (including mammalian cell cultures) and aquatic species, with comparatively few studies conducted using terrestrial species (e.g. soil invertebrates, soil microorganisms or plants) (Klaine, Alvarez et al. 2008). Whilst there has been much focus on 'first generation' MNM (Baun, Hartmann et al. 2008), for some commercially available MNM already utilised in specific technologies there is little or no ecotoxicity data available. Furthermore, environmental conditions both aquatic (NOM concentration, ionic strength, pH) and terrestrial (soil cation exchange capacity, pH, clay content, organic matter content) can significantly influence the ecotoxicological impacts of MNM, but this is still poorly understood (Peijnenburg, Baalousha et al. 2015, Sajid, Ilyas et al. 2015, Simonin and Richaume 2015) (Baun, Hartmann et al. 2008, Klaine, Alvarez et al. 2008). Importantly, the issue of dosimetry in ecotoxicity studies is yet to be addressed satisfactorily for MNM. To date most studies have used concentration values based on mass to quantify exposure. New approaches to address this issue are urgently required.

Physical and chemical modification of MNM is routinely used to improve the material properties, yet these same MNM modifications can also affect their potential for adverse effects on human health or the environment. Size, shape and surface chemistry modification all appear to affect human-related toxicity and ecotoxicity of MNM. The effect of surface chemistry modifications (e.g. -COOH, -NH2, -OH residues, PEGylation) has been studied for silica, carbon nanotubes (CNTs) and silver MNM, both *in vitro* and *In vitro* (Jain, Thakare et al. 2011, Ilknur, Mine et al. 2012, Lankoff, Arabski et al. 2012, Morishige, Yoshioka et al. 2012, Nangia and Sureshkumar 2012). Some surface modifications have reduced toxicity whilst preserving the nano-scaled technological properties (i.e. Al-Si surface-coated TiO_2 MNM in human sunscreens). However, many experiments show inconsistent and disputed patterns (e.g. carboxylated CNTs showed increased and decreased toxicity), which may result from CNT purity/metal content, length and use of *in vitro* versus *In vitro* models (Patlolla, Hussain et al. 2010, Jain, Thakare et al. 2011, Jensen, Larsen et al. 2012). Particle shape has been shown to effect the toxicity of silver MNM to fish gill cell lines and zebrafish embryos (George, Lin et al. 2012) and silver MNM preparation methods elicit differences in ecotoxicological endpoints in Salmon (Farmen, Mikkelsen et al. 2012). In general, a lack of detailed ecotoxicological research on the effects of MNM physical and chemicals properties means current knowledge regarding MNM modification and corresponding effects on human health and the environmental is poorly understood.

2.2.2. *In vitro studies*

Validated methods for quantification of MNM exposure dose and fate in *in vitro* assays using in dispersions is lacking. The challenges are principally related to the complexity, in terms of chemistry, concentration, heterogeneity, and the media used for studies. Moreover, there is a current need for the development of infrastructure for the characterisation of MNM in complex matrices and the development of reference materials for the calibration of instruments used for assessing exposure and dosimetry. For example quantification of CNT exposure in (eco-) toxicity testing remains a significant challenge, and is not possible using methods suitable for metallic nanomaterials (e.g. ICP-MS). Furthermore, current quantification methods for MNM do not suitably address the issue of dosimetry and consider the nominal dose as the effective dose uptake.

The current need to move towards predictive hazard assessments is driven by a requisite to develop better and faster screening methods to better evaluate the potential risk associated to products susceptible of entering markets. A success in the former will help to prevent risk beforehand and to control exposure of MNM. However, there are some significant gaps in knowledge that need to be addressed. A substantial part of the missing knowledge could be obtained with the harmonization of protocols for exposure and fate of MNM. The outcomes of these actions will constitute a base for such guidelines.

The evaluation of the potential toxicity of MNM with *in vitro* assays is of extreme importance. Careful studies have been designed to test specific parameters (Laloy, Robert et al. 2012)). However, characterization of relevant physicochemical characteristics during *in vitro* evaluations and methods to do so is highly understudied. Similarly, only a limited number of studies have been conducted to thoroughly investigate the dependence of the exposure characteristics and effects on different dispersion protocol and test procedures. Case studies have demonstrated that the preparation methods of MNM dispersions can drastically influence their properties and their derived toxicity (Lankoff, Arabski et al. 2012, Nangia and Sureshkumar 2012, Mejia, Piret et al. 2013). Likewise, the application of small variations in dispersion mediums and test mediums as well as the order of events in the test procedures can also result in significant differences in the toxicological response (e.g., (Corradi, Gonzalez et al. 2012, Vranic, Gosens et al. 2016).

The interaction of a MNM with compounds in a relevant biological media (i.e. high protein media for cell culture, blood plasma, etc.) has been a subject of recent interest (Lynch, Salvati et al. 2009). It is not clear whether a similarly dispersed MNM will have the same agglomeration state in different biological media (absorption phenomena). Another question of relevance, for *in vitro* toxicological testing, is the quantification of exposure dose of MNMs that interact with cells and their state of agglomeration. The effect of an external change in the level of MNM agglomeration and their dissolution during transport in the body is not well understood (i.e. MNM passing through the stomach). These questions can be assessed by testing the state and transformations of the MNM by using different dispersion protocols and incubate the resulting MNM dispersions with relevant biological media for toxicological testing.

To conduct such tests, it is crucial to carefully select the most relevant parameters to be investigated and traced during the experiments. Quantification of dose available for the cells and/or internalized needs to be adequately quantified to improve the interpretation of *in vitro* toxicological studies. The primary physicochemical characteristics such as the effective size and surface charge of MNM are rarely the same in exposure mediums and inside cells (Fubini et al. 2010).

The dispersion protocol used need to be carefully selected considering the intended use and aims of the study. The applied dispersion principles and mediums will in part determine the dispersion quality and particle size-distributions and fate in the exposure mediums (Hartmann, Jensen et al. 2015). It is known that, the concentrations of suspended MNM, but also their level agglomeration, very often evolves during the *in vitro* assay (e.g., (Jackson, Kling et al. 2015, Vranic, Gosens et al. 2016). Therefore, the definition of nominal dose should be re-evaluated, given that a fraction of the MNMs does not reach the cells if cultivated at the bottom. MNM remaining in the culture medium do not directly affect cells if cultivated at the well-bottom and therefore skew the dose-effect assessment. Vice-versa suspended cells are not exposed to the average dispersion MNM concentrations, if sedimentation occurs.

It is also important to consider the potential interactions between MNM and cell medium constituents. Proteins and nutrients may adsorb onto MNM surfaces resulting in a shortage of the available nutrients, which can affect the cells in the assay. Not only, have different protein coronas changed the original MNM size in different cellular media, but also influencing the MNM cellular uptake and toxicity (Maiorano et al. ACS Nano 2010; (Corradi, Gonzalez et al. 2012, Vranic, Gosens et al. 2016)). Moreover, MNM may partially or completely dissolve in specific environments and/or matrixes. The released ions (or correspondent

constituents) may interfere with the subsequent cells interactions or even be the direct cause of toxicity. MNM dissolution has also been demonstrated occurring in the lysosomes and is demonstrated to be the cause of intracellular toxicity for many types of MNM (Sabella et al. Nanoscale 2014). Thus, relationship of MNM dosimetry to exposure conditions should be evaluated. In addition, the temporal evolution of some MNM properties may drastically interfere with the determination of the effective MNM concentration in the matrixes as well as the effective internal dose that cells receive. It has been determined that size and charge parameters mainly control the extent of variation of MNM internalization and final concentrations in cells (Nangia and Sureshkumar 2012).

Measuring the fraction of intracellular MNM is useful to understand the real dose responsible of a certain toxic effect. However, many critical technical issues are related to methods and instrumentation for the quantification of the internal amount of MNM in the cell. For instance, the most used methods currently available are fluorescence based microscopy, ICP-AES, flow cytometry. However, these methods may sometimes produce a certain overestimation of MNM measurement due to MNM sticking on the cellular external membranes(Ahmad Khanbeigi, Kumar et al. 2012).

An important effort towards the homogenisation of methods for exposure and fate in MNM dispersions for *in vitro* and ecotoxicity studies is needed to achieve solid bases for strong regulatory initiatives.

2.2.3. Hydrochemical reactivity

The reactivity of materials is considered key information and one of the key drivers for the observed increased toxicities of MNM as compared to bulk materials as well as ultrafine air-pollution particles. However, the term particle reactivity is not specifically defined and it cannot be considered as one parameter alone (Jensen, Pojana et al. 2014). In this work, the hydrochemical reactivity of MNM are considered to include the causticity (acid-base-reactivity) and oxidative-reductive activity as well as dissolution, transformation and interactions between particles and medium constituents in specific test item preparation and exposure mediums. Moreover, determination of these reactivity end-points in intracellular/ intraorganism compartments is also of critical importance as discussed above. Even-though the mentioned reactivity end-points are not fundamentally new, there are no standardized methods or protocols established in toxicology to measure and determine them for application in exposure characterization and hazard assessment. The lack of harmonized standard methods is an obstacle for establishment of potential causal relationships between the different reactivity phenomena and toxicological effects.

However, as can be anticipated from chemical modeling, the solubility and reactivity of (at least some) materials are very sensitive to variations in the test conditions. For example, it has been demonstrated that the solubility of ZnO and speciation of dissolved Zn varies with the composition of the mediums, but also with the CO_2 concentrations in the test atmosphere (David, Galceran et al. 2012, Li, Lin et al. 2013, Wang, Tong et al. 2016). Consequently, to understand the true (or the most likely fate) of a test material in a specific test system; or in a cell or an organism; it is essential to study the reactivity in the specific mediums of interest and under the exact conditions of the test or exposure. Therefore, a generic in situ measurement methods are needed that can be used to detect and quantify the relevant reactivity parameters real-time at the specific exposure conditions. If successful, such methodologies can serve as a future high-throughput screening methods.

At this point in time, the particle reactivity is usually only considered to be the surface reactivity and ability of the test materials to produce reactive oxygen species, such as superoxide and hydroxyl radicals (e.g., Nel et al., 2006;(Xia, Kovochich et al. 2006, Arts, Irfan et al. 2016). It is well-known that the practical use of many frequently applied probes to quantify ROS-production is not straightforward to apply due to interaction with test materials ((Wardman 2007). Therefore, direct measurement of the redox potential (or related oxygen-concentration) to quantify the source-term needed for radical formation may give more accurate and sufficient information for evaluation of the reductive-oxidative potential of the MNM. This may be an important change in metrics as electrons may not be biologically active only through formation of reactive oxygen species, but also through direct disturbance of the electron transport across the cell membrane and cellular respiration (Flaherty, Chandrasekaran et al. 2015, Wu, Li et al. 2016).

The causticity of particulate materials is rarely discussed in particle toxicology even-though hydrolysis occurs on material surfaces and dissolution may result in significant pH-changes while an adequate pH is crucial during *in vitro* testing (e.g., (Varnes, Dethlefsen et al. 1986). Despite the fact that *in vitro* mediums usually

contain a buffer, there may be threshold doses for certain MNM that exceed the buffer capacity of the cell mediums.

Several different methods and approaches have been previously applied to investigate the solubility of MNM in different test mediums (e.g., (Ellegaard-Jensen, Jensen et al. 2012, Nymark, Catalan et al. 2013, Gittings, Turnbull et al. 2015). However, it is a current opinion that in addition to solubility limits, it is possibly even more important to understand the dissolution rates of MNM during testing. Such principles for dissolution rate testing were also discussed in D2.9 and are under scientific discussion.

2.3. Description of the work carried out

The NANoREG technical guideline (TG) for *in vitro* and ecotoxicological exposure and fate characterization contained a number of methods proposed for establishing the key requested and recommended end-points (Table 1). This list is already advanced considering typical toxicological studies and methods generally needs further developed. Moreover, additional end-points are of interest for better exposure fate characterization of MNM, which may also have use for grouping and future regulatory risk assessment, have been further elaborated as part of the work in Task 2.4.

Table 1. Minimum characterization requirements for *in vitro* and ecotoxicologial studies in NANoREG

Element in the workflow	Recommendation (R) and Mandatory requirement (M); Optional (O)
Batch dispersion	Ten repeated measurements of hydrodynamic size (DLS) are made without pause in combination with verification or measurement with TEM, SEM or AFM which-ever is most suitable. *In vitro* (M) and eco-tox (M).
Initial exposure medium	Ten consecutive measurements of hydrodynamic size (DLS) are made (if technically possible) without pause on the same sample in combination with verification or measurement with TEM, SEM or AFM which-ever is most suitable. *In vitro* (M) and eco-tox (M)
Final exposure medium	Ten consecutive measurements of hydrodynamic size (DLS) are made (if technically possible) without pause on the same sample in combination with verification or measurement with TEM, SEM or AFM which-ever is most suitable. *In vitro* (M) and eco-tox (M).
Stability of dispersion during assay	It is recommended to follow size distribution and sedimentation of MNM in the exposure medium during the test. (R) Sedimentation rates can be assessed from calculations, analytical centrifugation or tests using the DLS. By DLS one may analyze both agglomeration and sedimentation. From experience, a time-resolution of 20 minutes after the first hour is a suitable time-resolution (e.g., 20 min.). Within the first hour a time-resolution of 10 minutes is normally suitable.
Contextual conditions and reactivity in the during testing	Measure several of the following parameters (pH, T, conductivity, redox potential and the CO_2/O_2 concentrations) during testing. *In vitro* (R) and eco-toxicity (M).
Dissolution in batch dispersion and test media	Dissolution can be assessed by taking hydrous samples from the test or parallel tests conducted at the same conditions as the exposure conditions. The residual test material must be removed from the medium immediate after taking the sample. (R)*

* Conclusions from D2.9 results in a recommendation for using a 3kDa centrifuge filter for particle separation immediately after the liquid sample is extracted to avoid influence of particles in suspension.

2.3.1. Task 2.4 e) Procedures for quantification of MNM exposure and fate in dispersions for ecotoxicological studies

An outline of the key elements of the NANoREG TGD for ecotoxicity exposure dispersion characterisation is provided in the current Deliverable Report document. In addition, example data generated through implementation of the TGD in aquatic ecotoxicity studies conducted as part of NANoREG WP4 are presented. Both characterisation data and the suitability of the TGD are evaluated. Full details of the recommended MNM characterisation procedure for quantifying exposure in aquatic ecotoxicity studies can be found in the TGD document ( ).

Recommendations and prerequisites

It is strongly recommended that all MNM test materials are subjected to a thorough physicochemical characterisation of their pristine form prior to utilisation in aquatic ecotoxicity studies. The following physicochemical properties should be determined:

- Particle size and morphology (e.g. using transmission electron microscopy)
- Particle specific surface area (SSA) (e.g. using BET methodology)
- Any other relevant physicochemical properties such as chemical composition and impurities should also be considered.

Implementation of the developed NANoREG ECOTOX Dispersion Characterisation TGD is strongly recommended in conjunction with the following documents prepared and benchmarked for aquatic ecotoxicology studies as part of the EU FP7 Project NANoREG (WP2, Task 2.4a; 'Validation of test item preparation for ecotoxicological studies'):

- Probe sonication calibration SOP
- NANoREG ECOTOX Dispersion SOP

Together, these 3 documents for the summary output representing NANoREG's goal for improved reproducibility, relevancy and implementation of aquatic ecotoxicity studies for MNM assessment. An overview of how each document contributes to this goal and how they combine in a work flow for conducting aquatic ecotoxicity tests is shown in Figure 1.

Figure 1. Schematic showing the preparation steps required for producing reproducible MNM dispersion for aquatic ecotoxicity testing. Recommended SOPs are given in the blue boxes.

N.B. A detailed characterisation of the media being utilised in the specific aquatic ecotoxicity test should be conducted as this will vary depending on the species being tested. Furthermore, no time points for conducting characterisation for any ecotoxicity study are proposed in the TGD as this will be test specific depending on the organisms being used.

Overview of NANoREG ECOTOX Dispersion Characterisation TGD contents and approaches

The TGD provides a recommendation and framework or conducting aquatic ecotoxicology studies with MNM whereby the following information and data will be determined in order to improve interpretation of the ecotoxicity endpoint data generated:

- Characterisation of the test MNMs at the start and end of the exposure study in order to determine changes in particle size and morphology over time
- The nominal concentration of MNM ($C_{nominal}$) in both mass on MNM (e.g. mg/L) and SSA (cm^3/L)
- The total concentration of MNM (C_{total}) present in the water phase of the exposure at both the start and end of the experiment (in SSA and mass)
- The concentration of both dissolved MNM ($C_{dissolved}$) and particulate MNM ($C_{particulate}$) in the water phase (actual) present in the water phase of the exposure at both the start and end of the experiment (in SSA and mass)
- Estimation of the amount of test MNM which has either sedimented out of the water phase or adsorbed to the surfaces of the exposure system (in SSA and mass)

An overview of the relationship between the terms outlined above is given in Figure 2.

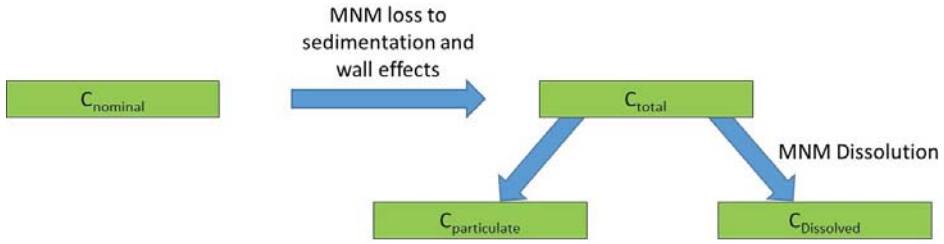

Figure 2. Schematic showing the relationship between the terms $C_{nominal}$, C_{total}, $C_{dissolved}$ and $C_{particulate}$.

The TGD contains sections and information related to the following aspects of MNM characterisation in aquatic ecotoxicity studies:

- Size and morphology characterisation.
- Determination of nominal concentration of MNM ($C_{nominal}$) in the water phase.
- Determination of total MNM concentration (C_{total}) remaining dispersed in water phase during and at the end of the study.
- Determination of the dissolved ($C_{dissolved}$) and particulate ($C_{particulate}$) fractions which comprise C_{total}.
- Procedure for conducting an MNM pre-test for aggregation and sedimentation.
- Procedure for conducting an MNM pre-test for dissolution.
- Procedure for conducting MNM sampling for aggregation determination in an ecotoxicity test.
- Procedure for conducting MNM sampling for determination of dissolution in an ecotoxicity test.
- Quantification methods for determining MNM aggregation and sedimentation.
- Quantification methods for determining MNM dissolution.

The NANoREG ECOTOX Dispersion Characterization TGD provides a simple procedure for the characterization of MNM dispersions throughout the duration of an aquatic ecotoxicity test. The procedure has been developed to be sufficiently general that it can be applied to all standard aquatic ecotoxicity tests. The key characterization end points included in the TGD are aggregation, sedimentation and dissolution of MNM during aquatic ecotoxicity studies. The procedure has been developed with the aim of minimizing the amount of characterization work where possible, but at the same time maintaining a sufficient level of characterization to permit a clearer interpretation of ecotoxicity data generated. To this end, simple pre-tests using MNM dispersions in the relevant ecotoxicity media, but with no organisms present, are described for both aggregation/sedimentation and dissolution. Here, the aim is to identify, and minimize where possible, the level of characterization detail required when conducting full aquatic ecotoxicity studies. The TGD contains defined parameters for each of the pre-tests which allow the user to make decisions on the subsequent level of characterization required in the full ecotoxicity study. Figure 3 shows the decision tree for conducting characterization of MNM aggregation and sedimentation. Figure 4 shows the decision tree for conducting characterization of MNM dissolution.

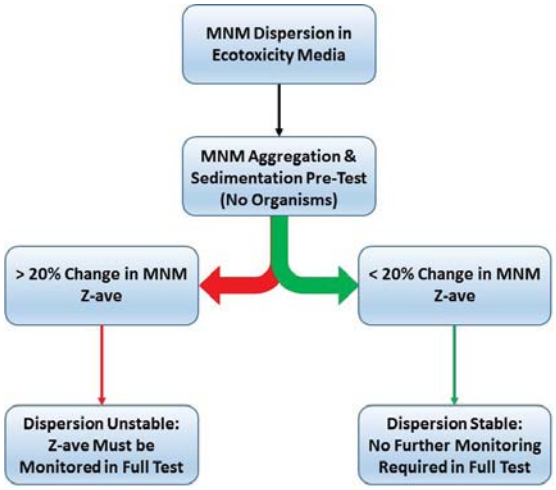

Figure 3. Decision tree for assessing the degree of monitoring of MNM Z-ave required in ecotoxicity studies.

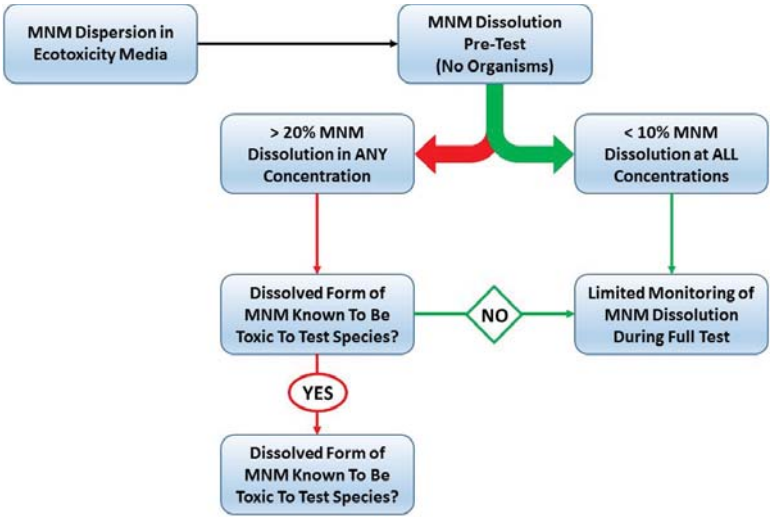

Figure 4. Decision tree for assessing the degree of monitoring of MNM dissolution required in ecotoxicity studies.

Example physicochemical characterisation data determined in aquatic ecotoxicity studies conducted within NANoREG WP4 are presented in Section 0. An evaluation of the suitability and performance of the TGD is also provided in Section 2.5.1.

Overview of test MNMs and ecotoxicity test set ups employed

In total, 7 of the core NANoREG MNM were utilised by partner SINTEF in aquatic ecotoxicity studies in NANoREG WP4. The test materials comprised 3 TiO_2 MNMs (NM-100, NM-101 and NM-103), 3 CNTs MNM (NM-400, NM-401 and NM-411), and 1 Ag MNM (NM-300K). The aquatic ecotoxicity studies conducted were for freshwater algae (*Pseudokirchneriella subcapitata*) and for *Daphnia magna*. Each of the test species had a specific media type, TG201 and MHRW for algae and *D. magna*, respectively. The NANoREG ECOTOX Dispersion Characterisation TGD was applied to all materials during the ecotoxicity tests conducted (range finding pre-test and full tests) and the data are presented here. The z-average diameter, polydispersity index, zeta potential, MNM concentration and, where applicable, ionic releases were monitored to determine dispersion stability and organism exposure during toxicity testing.

Preparation of MNM stock dispersions

A stock dispersion of each MNM was prepared according to the "NANoREG-ECOTOX dispersion protocol" according to:

a) The 'Standard Dispersion Procedure' was used for easily dispersible materials (NM-100, NM-101, NM-103 and NM-300K)

b) The 'Enhanced Dispersion Procedure' (ethanol pre-wetting, MilliQ water plus 20 mg/L NOM) was used for materials that are difficult to disperse (NM-400, NM-401, and NM-411).

The dispersion step was conducted with care and the quality controlled by measuring the z-ave size of 1 mL of each stock dispersion by DLS (dispersion quality control, NANoREG-ECOTOX dispersion protocol). A comparison/verification was made between the determined z-ave for the dispersions with recorded z-ave data for the same materials. Stock dispersions were only used for further testing if they passed the quality control step above. In cases where a stock dispersion was determined as being too different from the reference value, a new stock dispersion was prepared.

Characterisation of MNM exposure dispersions

- The media used in the aquatic ecotoxicity tests were pH-adjusted before preparing the working dispersions.
- Media containing 10 mg/L NOM for enhanced dispersion was filtered repeatedly until determined z-average was below 120 nm.
- Concentrations used in the preliminary stability test reflected the concentrations used in the respective aquatic ecotoxicity range-finding tests (usually 5 to 6 concentrations) and were prepared by diluting the correct amount of stock solution in the respective media.
- The influence of MNM exposure dispersion concentration on z-ave, PDI and zeta potential were determined immediately after preparation.

MNM stability pre-test for exposure characterisation

- The test dispersions were mixed well and samples to determine aggregation and dispersion concentration were taken immediately after preparation (time 0 h). Thereafter, the MNM dispersions were left standing still for the same period of time as the planned ecotoxicity tests (e.g. 72 h for *D. magna* and 72 h for algae) test duration. In order to determine MNM exposure concentration, aggregation and sedimentation samples for size (z-average), PDI, zeta potential, and, where applicable, ionic release were taken from the middle region of the sample at allocated sampling time points. Samples were measured according to the "NANoREG ECOTOX Dispersion Characterisation TGD".
- Z-average, PDI and zeta potential were determined with a Zetasizer nano ZS series (Malvern Instruments, UK).
- MNM concentration of metal and metal oxide MNM was determined using ICP-MS and using UV-vis (spectrophotometrically) for carbon-based MNM. Metal and metal oxide samples for ICP-MS analysis were stabilised in 5% (final concentration) ultrapure HNO_3 immediately after sampling. For spectrophotometric analysis, absorbance of the respective samples was determined at 800 nm as well as the absorbance peak.

  NOTE: For accurate concentration analysis of TiO_2 MNMs with ICP-MS, a hydrofluoric acid digestion step is recommended.
- Ionic release was evaluated for metal and metal oxide MNM by filtering samples through 3kDa filters and subsequent ICP-MS analysis. Samples were stabilised in 5% ultrapure HNO_3 after filtration.

The obtained data was evaluated in order to decide/identify whether a full characterisation or a more limited characterisation of MNM stability is necessary during the definitive aquatic ecotoxicity test(s) (Figure 3, Figure 4).

2.3.2. Task 2.4 f) Procedures for quantification of MNM exposure and fate in dispersions for in vitro studies

In task 2.4f the focus was set on developing and/or demonstrating experimental methods to characterize and analyse the interaction between MNM and biomolecules, their hydrodynamic particle size-distributions as well as the dispersion stabilities or sedimentation/deposition rates in exposure mediums for improved exposure dose assessments. Quantification of the suspended particle size and the deposited fraction is considered to be the most crucial information for the interpretation of *in vitro* toxicological results (Cohen, DeLoid et al. 2015). However, newer research also point to the particle protein interaction as determinant for the particle uptake and fate *in vitro*. Furthermore, interactions have been documented for cytotoxicity and toxicological signal molecules such lactate dehydrogenase (LDH) and interleukins (IL-6 and IL-8). First this information is of help to correct for adsorption phenomena. However, if understood, the role of such phenomena can also be considered in future work. Finally, information of the MNM hydrochemical reactivity and dissolution behaviour of MNM in *in vitro* toxicological test mediums is essential to understand whether an observed biological effect is due to direct particle exposure of exposure to dissolved ions, secondary phases or simple hydro- or electro-chemical reaction products. Consequently, the main objective of this task is to establish procedures to provide information to both toxicologists and regulators to better qualify and assess *in vitro* toxicological test results for biological endpoints obtained.

Regarding sizing and dispersion stability assessments of exposure mediums, this task already contributed to the NANOREG Technical Guidance document. In this work a DLS procedure was proposed for assessment of the MNM size and the agglomeration and sedimentation behaviour of MNM during incubation in *in vitro* studies. The key aim in this task was to investigate the applicability ranges of the DLS method suggested in the NANoREG Technical Guidance document, but also to investigate the applicability and data obtained using other (and maybe more quantitative) methods to quantify hydrodynamic size-distribution and contact dose.

In the first part the NRCWE method proposed in the NANoREG Technical Guidance document was further documented. The method applies the DLS intensity data and the average zeta-size collected at fixed measurement conditions in a DLS. The relative changes in these parameters are used for the interpretations. Experiments were conducted with NM-101, NM-110 and NM-400 dispersed into RPMI cell medium with 0.2% (w/v) glutamax. Samples were incubated in a DLS cuvette for a duration of 24 hours or until measurements stopped. The results demonstrate the ability to monitor the size- and apparent concentration development at the vial bottom, which allows understanding of both accumulation at the vial bottom and full sedimentation. Estimation of the deposition time reveals that 25% of the NM-101, NM-110 and NM-400, have deposited in the test mediums at 0.2; 1, and 8.4 hours, respectively. For NM-400, initial sedimentation is followed by accumulation of CNT at the bottom layer. The procedure appears applicable for the intermediate exposure concentrations investigated.

LEITAT further investigated the particle-size characteristics and sedimentation behaviour of MNM as function of particle dose in *in vitro* mediums as function of time, under carefully simulated *in vitro* assays (preparation, timing, dilution in Dulbecco's Modified Eagle's medium (DMEM) and RPMI as cell culture mediums...). In addition to deposited fraction, quantification of deposited contact dose was also demonstrated by the use PIXE analysis.

- ZnO MNM (NM-110) was used as a test material for the characterization protocols. Dispersions of were prepared using the NANoREG dispersion protocol. *In vitro* assays with CaCo2 cells were performed adding the ZnO dispersion to obtain a final concentration of 50 µg/mL. The cells were incubated during 6, 24, 48 or 72 hours. Afterwards the culture media was carefully removed and stored in vials for both CLS and PIXE characterizations.
- SiO_2 and TiO_2 and carbides (SiC, TiC) MNM (not from NANoREG's core materials) were used to demonstrate protocols proposed for fate assessment of MNM during *in vitro* exposure, following incubation times up to 72h. In order to validate the methodology, three cell lines with their respective culture media have been selected. These cell models are representatives of the lungs, skin and sébocytes, which are the A549, NhTERT and SZ95 cell lines. The MNM fate was characterized by the

sedimented dose, the dose arriving in contact (or penetrating) to the cells. This fate characterization was done in terms of: 1) concentration using the technique PIXE (Particle-Induced X-ray Emission) and, 2) particle size distribution using the technique CLS (Centrifuge Liquid Sedimentation). The protocol used in this study was recently published (Lozano, Mejia et al. 2013). Data for 6, 24, 48 and 72 hours of incubation time and for two fractions were measured: sedimented and dispersed fractions. The MNM sedimented dose and its particle size distribution were measured for each incubation time. In general, no significant variations in PSD were observed for SiO_2 MNM during incubation with A549 cells and TiO_2 MNM with the three tested cell lines. Indeed, the slight variations observed for the size are mostly due to the adsorption of proteins and/or molecules from the culture medium. Some interaction as function of the specific surface area was observed in the three studied culture media. Globally, different trends, in terms of the sedimented dose were observed with each cell line, with their specific culture media and with the MNM concentration used.

UNamur worked with colleagues from Task 5.3 to establish particle size determination of MNM during *in vitro* assessment using Centrifugal Liquid Sedimentation (CLS). The materials used were the fluorescent positively and negatively charged SiO_2 (specifically used in task 5.3), SiO_2 (NM-200) and ZnO (NM-110) dispersed in BSA-water stock dispersions and in different cell culture media (used in *in vitro* assays –tasks 5.3 and 5.5) Comparison of sonicated (following the NANOGENOTOX dispersion protocol) or only stirred MNM was done. The work demonstrates the higher dispersibility achieved by sonication. The following strategy was followed for the evaluation of the in vitro test.

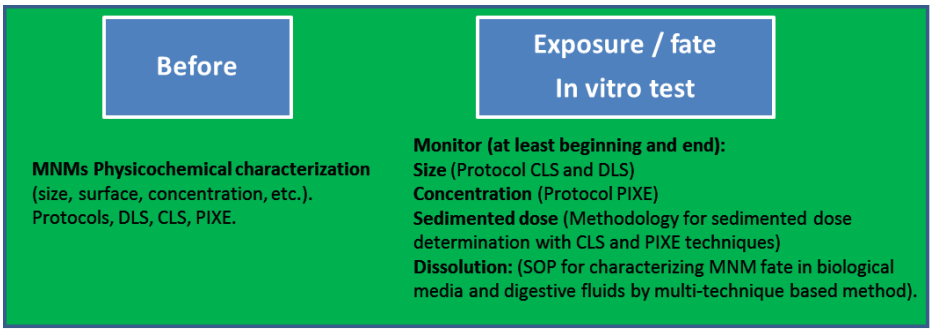

Figure 5. Strategy for the evaluation of exposure fate of MNMs during in vitro assessment.

Partner IIT performed studies to investigate MNM exposure and fate in biological media of relevance for *in vitro* cell studies particularly focusing on tracing changes of hydrodynamic size and surface charge. A multi-instrumental technique method was developed that employ zeta-potential, DLS, and UF/ICP-AES. Results show that MNM (NM-300K, NM-200, NM-110), once incubated in the tested cell mediums (and synthetic fluids), do not maintain their primary properties. Size changes were due to aggregation/agglomeration and to dissolution. Overall, these changes lead to formation of complex mixtures of bio-transformed products including different organic, inorganic and ion molecular species, which are the actual species responsible of effective dose, cellular permeability and uptake *in vitro*/*In vitro*.

Methods for measurement of MNM reactivity and dissolution behaviour were applied to demonstrate the type of information that can be obtained to provide new critical information for assessment and interpretation of *in vitro* toxicological test results.

IIT used an UF/ICP-AES method to quantify the dissolution of NM-200, NM-110 and NM-300K in RPMI and DMEM supplemented with 10% FBS. It was found that neither NM-300K nor NM-110 were dissolved to any significance in any of the two mediums. NM-200 on the other hand was found to dissolve completely in DMEN, but only partially in RPMI.

NRCWE further refined the methodology for measurement of MNM reactivity and dissolution using the Sensor Dish Reader method, which is currently under CEN standardization with support from funding from the NANoREG project. The procedure allows real-time measurement of pH and O_2 in the exposure mediums added MNM during (simulated) incubation in a cell incubator. Liquid samples were drawn at specific time-points (“0”, “1”, “2”, “4”, and “24” hour) during incubation to understand the temporal dissolution behaviour. Liquid samples were filtered using 3KDa centrifuge filters as agreed between partners conducting the

dissolution experiments in NANoREG. The protocol was demonstrated NM-200; NM-110; NM-111; and NM-300K were tested at 0.32 mg/mL HAMs F12+10%(w/v) FBS cell medium. The concentration of dissolved elements was quantified by ICP-MS and GC (Si). The results showed highly variable reactivity of the different MNM. The silica (NM-200) showed little reactivity and low dissolution over the 24-hour. The ZnO MNM were highly pH-reactive and caused initial pH increases above pH 9, which demonstrates that the pH buffer in HAMs F12 is not sufficient to maintain the desired *in vitro* conditions. The silver sample (NM-300K) showed little pH reactivity, but clear redox activity resulting in an increase in free O_2. The O_2 concentration also increased in the test of NM-110, but less in the test with NM-111. Considering their dissolution behaviour all samples were partially dissolved during 24-hour incubation in HAMs F12 + 10% FBS. Taken together, the results from IIT and NRCWE, shows that it is currently necessary to assess the MNM solubility in the specific test mediums studies to understand and interpret the MNM specific test results.

Finally in this task, the protocols were established to quantify the adsorption interaction between MNM and BSA and secreted biomolecules (LDH, IL-6, and IL-8). The methods and results were established to:

1) Determine the amount of BSA that is bound to the MNM when dosing MNM into the *in vitro* test mediums when using the NANOGENOTOX dispersion protocol 2)
2) Determine the signal biomolecule interaction for immediate correction in analysis of secreted IL-6; IL-8 and LDH cytotoxicity measurements and potential use in future predictive risk assessment.

Tests were performed on all NANoREG core MNM using ELISA kits and shows highly variable ability of the MNM to adsorb the tested biomolecules. NM-203, NM-110, NM-111; NM-212; and NM-400 were shown to adsorb high amounts of BSA. LDH was to high extent adsorbed onto NM-300K and to a lesser extent to NM-110 and NM-111. NM-411 was the most significant adsorber of IL-6 and IL-8 as well as NM-101. IL-6 and IL-8 generally adsorbed well to TiO_2 and silica, whereas no LDH or interleukin adsorbed to cellulose. The results need to be coupled with *in vitro* toxicological results to investigate the importance of these results. The anticipation is that the specific types of interaction can be used for future predictive fate and hazard assessment.

All together the results from this task demonstrate several different techniques to assess particle deposition and exposure dose in *in vitro* studies as well as MNM-biomolecule interaction and dissolution. Whereas the methods are capable of generating plausible results for the MNM sizing and sedimentation rates as well as contact exposure dose to cells in *in vitro* studies, further work is needed to confirm the applicability of the different methods as well as their comparability between laboratories. Similar, it was not possible to perform interlaboratory comparison tests for any of the SOPs described. This is needed in future work.

All the SOPs developed / tested in task 2.4f are available (Methodology for sedimented dose determination, NRCWE SOP for measurement of hydrodynamic size distribution, protocol for particle size determination of a given MNM, Protocol to quantify the concentration, SOP for test item preparation).

2.3.3. Task 2.4 i) Characterization of MNM hydrochemical reactivity in synthetic biological fluids

Knowledge on the MNM exposure-fate and reactivity in *synthetic biological fluid* provides critical information for interpretation of toxicological test results and as input parameters for predictive risk assessment. Currently the hydrochemical reactivity is not well-defined. In this task, we consider reactivity to include pH and redox potential as well as dissolution and phase transformation.

NRCWE, applied a stirred-batch reactor method for assessing the solubility and reactivity (pH and redox activity) of MNM in lung-lining (Gambles solution) and phagolysosome simulant fluids (PSF). The system was demonstrated for PSF using NM-110 and NM-300K. The results show that NM-110 dissolves rapidly in the pH 4.5 PSF resulting in a short-term pH-increase and increased redox potential while NM-300K dissolves slowly and has lowering effect on the redox potential and requires extensive pH buffering with HCl at these conditions.

Another approach was developed for tracing changes of MNM size and quantifying dissolution through the gastro-intestinal tract. This is multi-technique based method using DLS, TEM, UF/ICP-AES, UV-Vis after incubation in synthetic human body fluids (simulating the human digestive compartments). Results show that MNM (NM-200, NM-110 and NM-300K) once incubated in these synthetic fluids, do not maintain their primary properties but most of them agglomerate and dissolve in the corresponding ions. Size changes were due to

aggregation/agglomeration and to dissolution. Overall, these changes lead to a formation of complex mixtures of bio-transformed products including different organic, inorganic and ion molecular species (free and bound to matrix), which are the actual species responsible of effective dose, cellular permeability and uptake *in vitro*/*In vitro*.

Protocols used and / or developed in task 2.4i are available in the CIRCABC platform (IIT SOP, NRCWE protocol for determination LDH, NRCWE protocol for hydrochemical reactivity, NRCWE protocol for SDR).

2.4. Results

2.4.1. Task 2.4 e) Procedures for quantification of MNM exposure and fate in dispersions for ecotoxicological studies

MNM stock dispersion verification

The tested metal and metal oxide MNM (NM-100, NM-101, NM-103 and NM-300K) dispersed readily with the 'Standard Dispersion Procedure' and determined Z(ave) values were in agreement with those previously reported. PDI values indicated a reasonably homogenous dispersion was achieved (

Table 2 and Table 3). Pre-wetting and the presence of NOM improved the dispersibility of the carbon-based MNM (NM-400, NM-401 and NM-411), however, the materials did not form stable homogenous dispersions. The information on dispersion qualities given by the Z (ave) values and PDI measurements for the stock dispersions of NM-400, NM-401 and NM-411 is limited (

Table 2 and Table 3). In addition to limitations regarding the suitability of DLS for filamentous materials, PDI values were very high and frequent measurement error messages occurred.

Table 2. Z-ave of stock solutions of the metal and metal oxide particles NM-100, NM-101, NM-103 and NM-300K

MNM	Z-average	PDI
NM-100	317.0	0.2
NM-101	489.87	0.3
NM-103	155.3	0.3
NM-300K	67.2	0.3

Table 3. Z-ave of stock solutions of CNTs NM-400, NM-401 and NM-411

MNM	Z-average (nm)	PDI
NM-400	36057.8	1.0
NM-401	874.9	0.8
NM-411	55724.3	1.0

Influence of MNM exposure dispersion concentration on Z-ave values and PDI

Exposure dispersions for all MNM types were determined in both TG201 (algae) and MHRW (*D. magna*) media type. Concentration ranges prepared reflected the concentrations used in the subsequent ecotoxicity range- finding tests. Immediately after preparation of the exposure dispersions, z-ave and MNM. Table 4 to

Table 10 show z-average, PDI and zeta potential values for each MNM in the two different media types over the concentration ranges selected. In addition, the percentage change in z-ave and zeta potential at each of the exposure dispersion concentrations relative to the equivalent values determined for the individual stock dispersions are presented. N.B. z-ave and zeta potential values for each of the stock dispersions (concentration 2560 mg/L) are in MilliQ only (no media or NOM).

Table 4. Z-ave and zeta potential values of NM-300K in the range-finding concentration series in TG201 (algae media, no NOM).

Media Type	Dispersion Concentration (mg/L)	Z-Ave (nm)	% change Z-Ave compared to stock dispersion	PDI	Zeta Potential (ZP)
TG201	**50.0**	67.6	0.6	0.3	-11.6
TG201	**10.0**	65.1	-3.1	0.3	-11.9
TG201	**1.0**	72.7	8.2	0.4	-9.8
TG201	**0.1**	72.2	7.4	0.5	-9.1
TG201	**0.01**	127.3	89.3	0.5	-9.1

Table 5. Z-ave and zeta potential values of NM-100 in the range-finding concentration series in TG201 (algae media, no NOM) and MHRW (*D. magna*, no NOM).

Media Type	Dispersion Concentration (mg/L)	Z-Ave (nm)	% change Z-Ave compared to stock dispersion	PDI	Zeta Potential (ZP)
TG201	**100.0**	317.0	34.0	0.2	-22.1
TG201	**50.0**	251.4	6.3	0.2	-23.8
TG201	**10.0**	246.6	4.2	0.2	-27.3
TG201	**1.0**	235.4	-0.5	0.2	-28.6
TG201	**0.1**	279.7	18.3	0.4	-23.0
MHRW	**100.0**	961.4	306.5	0.2	0.5
MHRW	**50.0**	643.6	172.1	0.2	-1.6
MHRW	**10.0**	381.8	61.4	0.3	-7.2
MHRW	**1.0**	558.1	136.0	0.5	-20.8
MHRW	**0.1**	689.3	191.4	0.4	-20.4

Table 6. Z-ave and zeta potential values of NM-101 in the range-finding concentration series in TG201 (algae media, no NOM) and MHRW (*D. magna*, no NOM).

Media Type	Dispersion Concentration (mg/L)	Z-Ave (nm)	% change Z-Ave compared to stock dispersion	PDI	Zeta Potential (ZP)
TG201	**100.0**	519.9	6.1	0.4	-23.4
TG201	**50.0**	539.7	10.2	0.4	-22.3
TG201	**10.0**	402.7	-17.8	0.4	-21.9
TG201	**1.0**	470.1	-4.0	0.5	-25.8
TG201	**0.1**	505.0	3.1	0.6	-20.4
MHRW	**100.0**	2026.3	313.6	0.5	-5.9
MHRW	**50.0**	1373.3	180.3	0.5	-6.0
MHRW	**10.0**	970.7	98.2	0.5	-5.4
MHRW	**1.0**	933.7	90.6	0.5	-14.1
MHRW	**0.1**	1136.7	132.0	0.5	-12.1

Table 7. Z-ave and zeta potential values of NM-103 in the range-finding concentration series in TG201 (algae media, no NOM) and MHRW (*D. magna*, no NOM).

Media Type	Dispersion Concentration (mg/L)	Z-Ave (nm)	% change Z-Ave compared to stock dispersion	PDI	Zeta Potential (ZP)
TG201	**100.0**	3592.7	2212.9	0.4	-7.5
TG201	**50.0**	1044.6	572.5	0.3	-9.4
TG201	**10.0**	455.8	193.4	0.3	-16.6
TG201	**1.0**	268.8	73.1	0.4	-22.5
TG201	**0.1**	551.6	255.1	0.6	-24.3
MHRW	**100.0**	2416.0	1455.4	0.4	7.3
MHRW	**50.0**	1432.3	822.1	0.4	7.1
MHRW	**10.0**	641.4	312.9	0.5	3.5
MHRW	**1.0**	545.8	251.4	0.5	-10.3
MHRW	**0.1**	775.2	399.0	0.6	-8.9

Table 8. Z-ave and zeta potential values of NM-400 in the range-finding concentration series in TG201 (algae media, NOM) and MHRW (*D. magna*, NOM).

Media Type	Dispersion Concentration (mg/L)	Z-Ave (nm)	% change Z-Ave compared to stock dispersion	PDI	Zeta Potential (ZP)
TG201	**50.0**	7215.0	-80.0	0.9	-
TG201	**20.0**	9959.3	-72.4	1.0	-19.2
TG201	**10.0**	64113.3	77.8	0.8	-
TG201	**5.0**	65220.0	80.9	0.7	-
TG201	**2.0**	2412.6	-93.3	0.5	-11.8
MHRW	**50.0**	24650.3	-31.6	0.7	-
MHRW	**20.0**	62406.7	73.1	0.9	-10.9
MHRW	**10.0**	65376.7	81.3	0.8	-
MHRW	**5.0**	4058.3	-88.7	1.0	-
MHRW	**2.0**	35846.7	-0.6	0.9	-9.6

Table 9. Z-ave and zeta potential values of NM-401 in the range-finding concentration series in TG201 (algae media, NOM) and MHRW (*D. magna*, NOM).

Media Type	Dispersion Concentration (mg/L)	Z-Ave (nm)	% change Z-Ave compared to stock dispersion	PDI	Zeta Potential (ZP)
TG201	**50.0**	7633.7	772.5	1.0	-
TG201	**20.0**	6138.0	601.6	0.9	-23.2
TG201	**10.0**	16658.3	1804.0	1.0	-
TG201	**5.0**	17210.7	1867.2	0.9	-
TG201	**2.0**	756.2	-13.6	0.4	-11.9
MHRW	**50.0**	4925.0	462.9	0.5	-
MHRW	**20.0**	6316.7	622.0	1.0	-9.9
MHRW	**10.0**	8041.3	819.1	1.0	-
MHRW	**5.0**	36932.3	4121.3	0.8	-
MHRW	**2.0**	9810.2	1021.3	0.8	-7.8

Table 10. Z-ave and zeta potential values of NM-411 in the range-finding concentration series in TG201 (algae media, NOM) and MHRW (*D. magna*, NOM).

Media Type	Dispersion Concentration (mg/L)	Z-Ave (nm)	% change Z-Ave compared to stock dispersion	PDI	Zeta Potential (ZP)
TG201	**50.0**	55724.3	n.d.*	1.0	-
TG201	**20.0**	57943.3	n.d.*	1.0	-11.9
TG201	**10.0**	72206.7	n.d.*	0.6	-
TG201	**5.0**	36813.3	n.d.*	1.0	-
TG201	**2.0**	15665.3	n.d.*	0.5	-18.9
MHRW	**50.0**	43180.0	n.d.*	0.7	-
MHRW	**20.0**	47790.0	n.d.*	0.8	-6.8
MHRW	**10.0**	92853.3	n.d.*	0.9	-
MHRW	**5.0**	59003.3	n.d.*	0.7	-
MHRW	**2.0**	25389.7	n.d.*	0.9	-3.3

* Percentage change in z-ave was not determined as the z-ave size was so large and the DLS instrument was not able to generate any meaningful data.

MNM concentration appears to play an important role in the resulting Z(ave) size for MNM in the two ecotoxicity media used in the study. An effect of the test medium, e.g. increased aggregation (z-ave), was found for most MNM immediately after the MNM stock dispersion was diluted into the ecotoxicity test media selected. A comparison of the z-ave sizes determined for NM-100 (selected as a representative MNM to provide an example) at each of the concentrations used and for both media types is presented in Figure 6. In all MNM tested, and in both media types, decreasing concentration across the range-finding values used resulted in significant changes in the Z(ave) for each material. This indicates that the exposure conditions are therefore varying across the test system meaning that those organisms used in low exposures are exposed to different Z(ave) dispersions than those organisms used in the higher concentration exposures. Furthermore, low MNM exposure dispersion concentrations present challenges for the DLS instrument as they approach or reach the limit of quantification/sensitivity. Using the data generated here as a basis, it recommended that exposure dispersion concentrations below 0.1 mg/L are not included in ecotoxicity tests investigating NM-300K, NM-100 and NM-101. Concentration limits for other MNM are higher. Importantly, significant differences in the Z(ave) values for the same material at the same exposure dispersion concentration were observed across the two media types. This clearly shows the importance of determining Z(ave) and zeta potential values for all the different test systems used in ecotoxicity studies (i.e. data cannot be generated in one media type and applied directly to other media types). Importantly, these data confirm the acknowledged limitations of DLS for determining Z(ave) data for high aspect ratio nanomaterials (HARN) such as carbon nanotubes (CNTs).

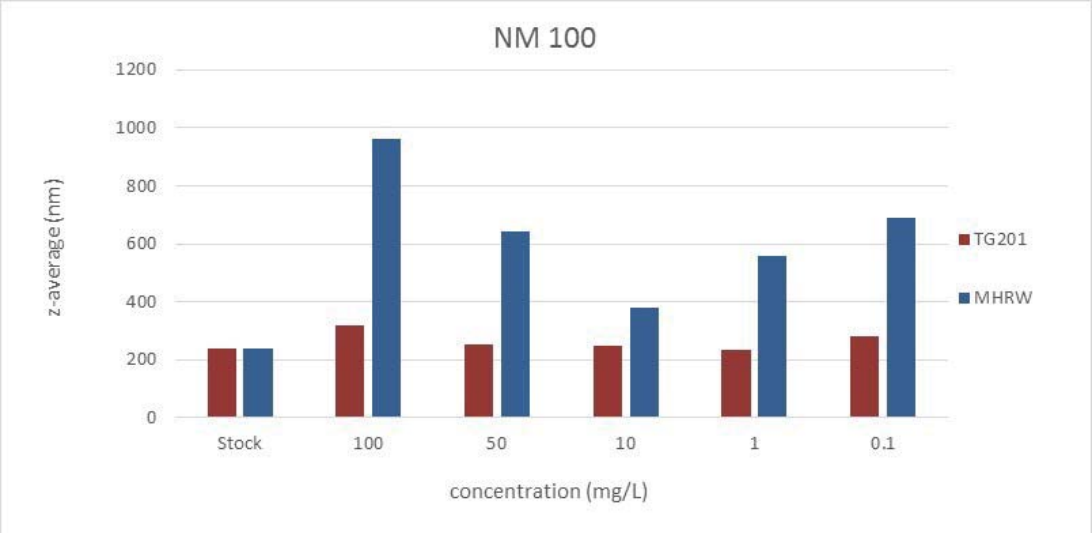

Figure 6. Differences in NM-100 Z(ave) values in the two different test media, TG201 (algae) and MHRW (*D. magna*), and across the concentration range employed.

MNM stability pre-test for exposure characterisation

MNM Aggregation behaviour over time

Z(ave), PDI and zeta potential were determined at the beginning (0 h) and the end time points (48/72 h for *D. magna*; 72 h for algae) for all concentrations utilised in the ecotoxicity range-finding test. Samples were taken from the middle of the sample vials to obtain samples of dispersed material and to avoid any large aggregates that may have formed and which settled out of dispersion to the bottom of the test vessel. Figure 7 shows the changes in Z (ave) over time (72 h) for metal and metal oxide MNM (NM-100, NM-101, NM-103 and NM-300K) in the algae media TG201. Figure 8 shows the changes in Z (ave) over time (72 h) for metal oxide MNM (NM-100, NM-101, NM-103) in the *D. magna* media MHRW. Z(ave) values were found to be dependent on both the MNM type (and physicochemical properties) and media type. Z(ave) values were typically higher in MHRW than in TG201. Most materials showed some degree of aggregation over time, although the exact level was material specific. For example NM-100, NM-101 and NM-300K showed little or no aggregation over 72 in TG201. In contrast, NM-103 showed significant aggregation during the same time period in the same media. NM-100, NM-101 and NM103 all showed a gradual increase in z-ave value over a 72 duration in MHRW, but in this case NM-100 appears to undergo the most significant degree of aggregation. Owing to the lack of suitability of DLS for the determination of Z(ave) values for HARN materials such as CNTs, data for NM-400, NM-401 and NM-411 are not presented.

MNM concentration was determined at the beginning (0 h) and the end time points (48/72 h for *D. magna*; 72 h for algae) for all concentrations utilised in the ecotoxicity range-finding test. The exposure system contained only MNM and the respective test media (TG201 or MHRW) under static conditions; no organisms were included in these tests. Samples were taken from the middle of the sample vials to obtain a samples of dispersed material and to avoid any large aggregates that may have formed and which settled out of dispersion to the bottom of the test vessel. MNM concentration and MNM sedimentation/removal from dispersion was evaluated by determining the individual MNM concentration of the samples by using either ICP-MS (metal oxides and metal MNM) or UV-vis (carbon-based MNM). Table 11 to Table 17 show the dispersion concentrations (mg/L) for each MNM in the two different media types at time 0 h, 48 h (*D. magna* only) and 72 h. NM-300K was only used in algae ecotoxicity studies and was therefore not tested in the D. magna media (MHRW). All MNM concentrations presented represent total MNM concentration (i.e. no distinction between dissolved and particulate contribution).

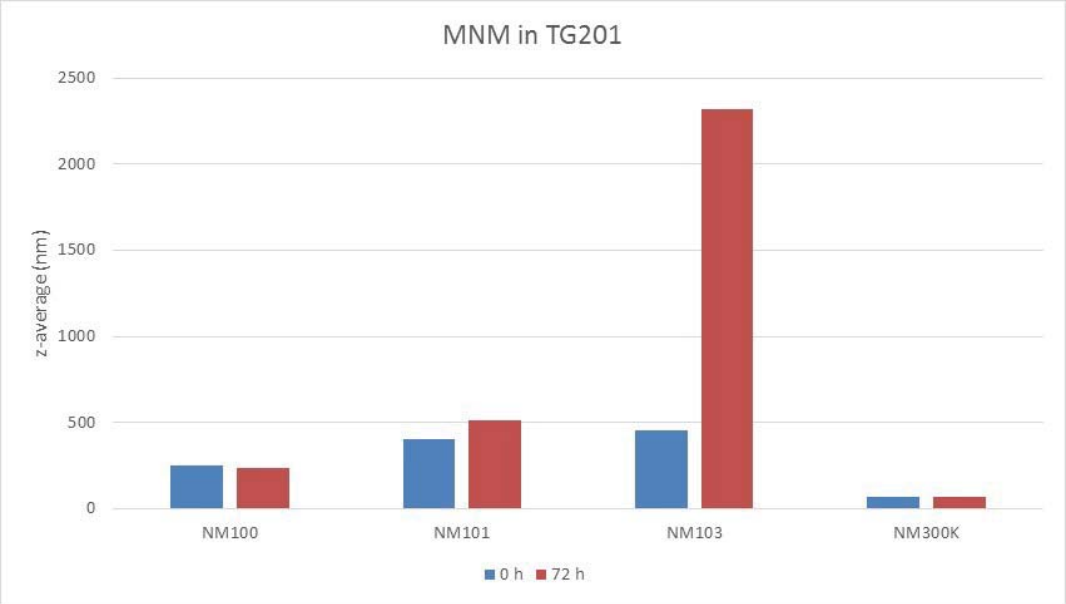

Figure 7. Z(ave) of metal oxide and metal particles (10 mg/L) in the algae test medium TG201 after 0 h and 72 h.

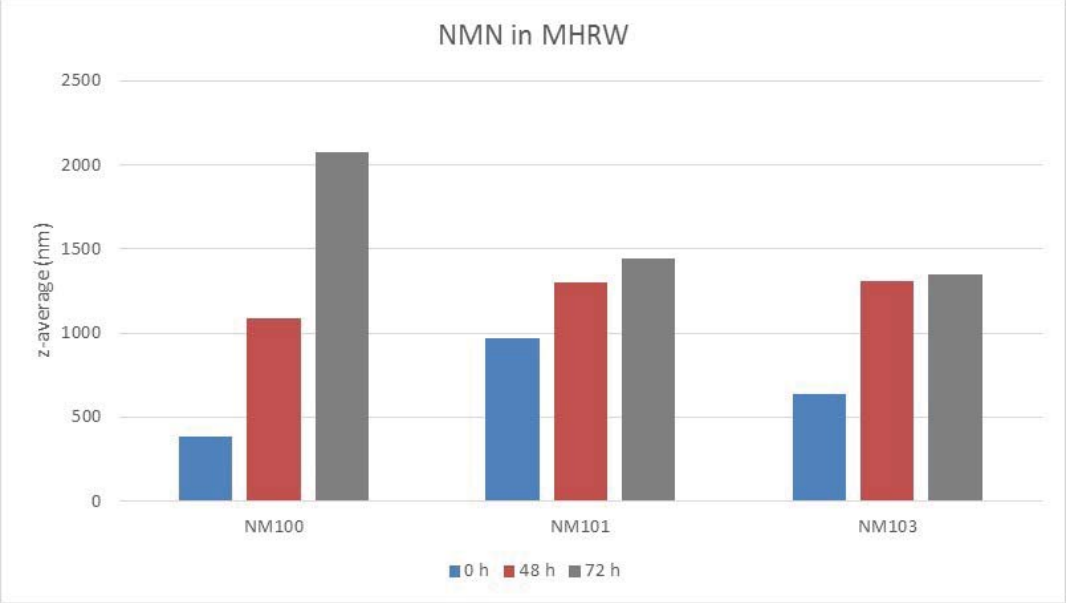

Figure 8. Z(ave) of metal oxide particles (10 mg/L) in the *D. magna* test medium MHRW after 0 h, 48 h and 72 h.

MNM concentration

Table 11. NM-300K concentration in the algae ecotoxicity range-finding test at 0 h and 72 h (in TG201 algae media, no NOM).

Media Type	Nominal Dispersion	Dispersion	Dispersion	Percentage

	Concentration (mg/L)	Concentration 0 h (mg/L)	Concentration 72 h (mg/L)	Decrease
TG201	0.01	*0.018**	*0.014**	*22.2**
TG201	0.1	*0.146**	*0.136**	*6.8**
TG201	1	*0.188**	*0.165**	*12.2**
TG201	10	*0.480**	*0.628**	*-30.8**
TG201	50	*1.928**	*2.700**	*-40.0**

*Relative to the nominal dispersion concentration, a significant loss of NM-300K was observed in the sample preparation process and data for these samples is not considered reliable. Accurate NM-300K data was generated in the full algae ecotoxicity test and are reported as part of NANoREG WP4.

Table 12. NM-100 concentration in the algae ecotoxicity range-finding test at 0 h and 72 h (in TG201 algae media, no NOM) and in the daphnia ecotoxicity range-finding test at 0 h, 48, and 72 h (in MHRW, no NOM).

Media Type	Nominal Dispersion Concentration (mg/L)	Dispersion Concentration 0 h (mg/L)	Dispersion Concentration 48 h (mg/L)	Dispersion Concentration 72 h (mg/L)	Percentage Decrease
TG201	0.1	0.02	-	0.01	22.9
TG201	10	1.16	-	0.47	59.7
TG201	100	50.91	-	0.25	99.5
MHRW	0.1	0.06	0.02	0.01	74.7
MHRW	10	5.18	0.21	0.09	98.3
MHRW	100	56.36	0.08	0.03	99.9

Table 13. NM-101 concentration in the algae ecotoxicity range-finding test at 0 h and 72 h (in TG201 algae media, no NOM) and in the daphnia ecotoxicity range-finding test at 0 h, 48, and 72 h (in MHRW, no NOM).

Media Type	Nominal Dispersion Concentration (mg/L)	Dispersion Concentration 0 h (mg/L)	Dispersion Concentration 48 h (mg/L)	Dispersion Concentration 72 h (mg/L)	Percentage Decrease
TG201	0.1	0.02	-	0.01	35.5
TG201	10	3.67	-	0.23	93.8
TG201	100	45.77	-	0.25	99.5
MHRW	0.1	0.06	0.04	0.02	69.1
MHRW	10	4.63	0.43	0.10	97.8
MHRW	100	46.65	0.24	0.20	99.6

Table 14. NM-103 concentration in the algae ecotoxicity range-finding test at 0 h and 72 h (in TG201 algae media, no NOM) and in the daphnia ecotoxicity range-finding test at 0 h, 48, and 72 h (in MHRW, no NOM).

Media Type	Nominal Dispersion Concentration (mg/L)	Dispersion Concentration 0 h (mg/L)	Dispersion Concentration 48 h (mg/L)	Dispersion Concentration 72 h (mg/L)	Percentage Decrease
TG201	0.1	0.02	-	0.01	59.2
TG201	10	4.60	-	0.05	98.9

TG201	100	53.24	-	0.12	99.8
MHRW	0.1	0.05	0.02	0.01	71.6
MHRW	10	5.63	0.24	0.13	97.8
MHRW	100	54.04	0.33	0.22	99.6

Table 15. NM-400 concentration in the algae ecotoxicity range-finding test at 0 h and 72 h (in TG201 algae media, no NOM) and in the daphnia ecotoxicity range-finding test at 0 h, 48, and 72 h (in MHRW, no NOM).

Media Type	Nominal Dispersion Concentration (mg/L)	Dispersion Concentration 0 h (mg/L)	Dispersion Concentration 48 h (mg/L)	Dispersion Concentration 72 h (mg/L)	Percentage Decrease
TG201	**2**	1	-	0.23	77.0
TG201	**20**	11.9	-	0.58	95.1
TG201	**50**	29.7	-	0.3	99.0
MHRW	**2**	1	0.25	0.23	77.0
MHRW	**20**	14	0.28	0.31	97.8
MHRW	**50**	35	0.26	0.27	99.2

Table 16. NM-401 concentration in the algae ecotoxicity range-finding test at 0 h and 72 h (in TG201 algae media, no NOM) and in the daphnia ecotoxicity range-finding test at 0 h, 48, and 72 h (in MHRW, no NOM).

Media Type	Nominal Dispersion Concentration (mg/L)	Dispersion Concentration 0 h (mg/L)	Dispersion Concentration 48 h (mg/L)	Dispersion Concentration 72 h (mg/L)	Percentage Decrease
TG201	**2**	0.1	-	0	100.0
TG201	**20**	6.3	-	0.04	99.4
TG201	**50**	9.7	-	0.15	98.5
MHRW	**2**	0.4	0.16	0.21	47.5
MHRW	**20**	9	0.16	0.16	98.2
MHRW	**50**	22	0.16	0.1	99.5

Table 17. NM-411 concentration in the algae ecotoxicity range-finding test at 0 h and 72 h (in TG201 algae media, no NOM) and in the daphnia ecotoxicity range-finding test at 0 h, 48, and 72 h (in MHRW, no NOM).

Media Type	Nominal Dispersion Concentration (mg/L)	Dispersion Concentration 0 h (mg/L)	Dispersion Concentration 48 h (mg/L)	Dispersion Concentration 72 h (mg/L)	Percentage Decrease
TG201	**2**	0.3	-	0	100.0
TG201	**20**	8.5	-	0	100.0
TG201	**50**	20.5	-	0	100.0
MHRW	**2**	0.4	0.16	0.21	47.5
MHRW	**20**	9	0.16	0.16	98.2
MHRW	**50**	22	0.16	0.1	99.5

Owing to the unexpected complications in analysis of the NM-300K samples, these data are not accurate and cannot be discussed in detail (Table 11). In the case of the TiO_2 MNM used in the study, all three types (NM-100, NM-101 and NM-103) exhibited significant decreases in dispersed concentration after 72 h. At nominal exposure concentrations of 10 and 100 mg/L all three TiO_2 MNM exhibited a significant decrease in dispersion concentration after 72 h (

Table 5 to Table 7). In most cases removal of TiO_2 MNM from the water column was over 90% efficient. At the lowest nominal concentration tested (0.1 mg/L), the percentage decrease is much less than 100% (ranging from 22.9 mg/L to 74.7 mg/L). The results for the 0.1 mg/L exposures may be the result of (i) operating near the instrumental limits of detection and (ii) the low exposure concentration at 0 h resulting in less aggregation and sedimentation over a 72 h period.

There was no clear difference in MNM dispersion decrease between the two media types studied at exposure concentrations of 100 mg/L (Figure 9 and Figure 10). However, at exposure concentrations of 10 and 0.1 mg/L, there are indications that dispersions of NM-100 and NM-101 are more stable in TG201 algal media. The decrease in TiO_2 MNM dispersion concentration corresponded with an increase in TiO_2 z-ave values, especially in MHRW (Figure 7 and Figure 8). The results show that all 3 TiO_2 materials tested rapidly aggregate in the two standard ecotoxicity media and that the selected test organisms (*algae and D. magna*) will not undergo exposure to these types of materials at the nominal exposure concentrations used in such studies. It should be noted that non-static studies (e.g. algae test) will result in re-suspension of the TiO_2 MNM and increase the final exposure concentrations. Importantly, the method described highlights the importance of quantifying MNM dispersion concentrations throughout the duration of ecotoxicity tests rather than using the nominal exposure values determined at the start of a study.

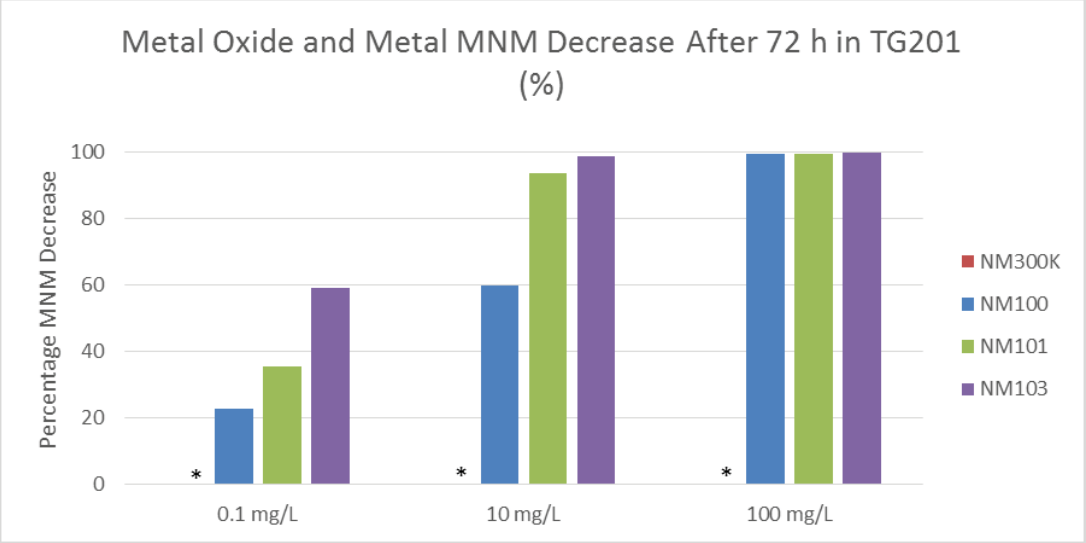

Figure 9. Graph showing the percentage of the metal oxide and metal MNM (NM-100, NM-101, NM-103 and NM-300K) in algae media (TG201) after 72 h. * NM-300K data not available.

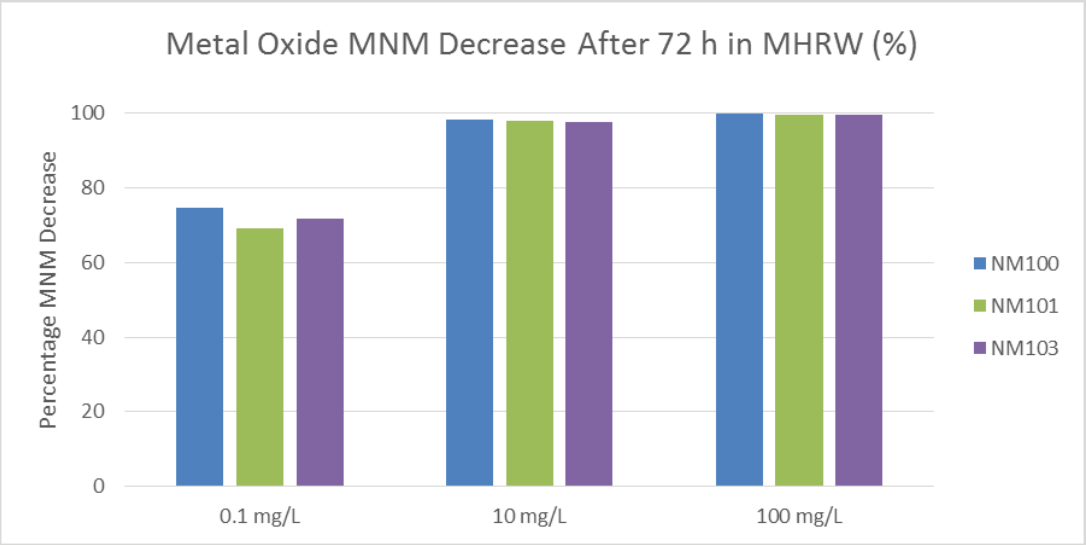

Figure 10. Graph showing the percentage of the metal oxide MNM (NM-100, NM-101 and NM-103) in *D. magna* media (MHRW) after 72 h.

In the case of the CNT MNM used in the study, all three types (NM-400, NM-401 and NM-411) exhibited significant decreases in dispersed concentration after 72 h. There was no clear difference in CNT concentration between the two media types studied (Figure 11 and Figure 12). The decrease in CNT dispersion concentration corresponded with an increase in CNT z-ave values. The results show that CNTs rapidly aggregate in the two standard ecotoxicity media and that the selected test organisms (*algae and D. magna*) will not undergo exposure to these types of materials at the nominal exposure concentrations used in such studies. It should be noted that non-static studies (e.g. algae test) might result in re-suspension of the CNTs and increase the final exposure concentrations. Although UV-vis was found to be a very reliable method for determining CNT dispersion concentration in a quick and cost effect way, the limits of quantification may be an issue if testing such materials at environmentally relevant concentrations. Importantly, the method described highlights the importance of quantifying MNM dispersion concentrations throughout the duration of ecotoxicity tests rather than using the nominal exposure values determined at the start of a study.

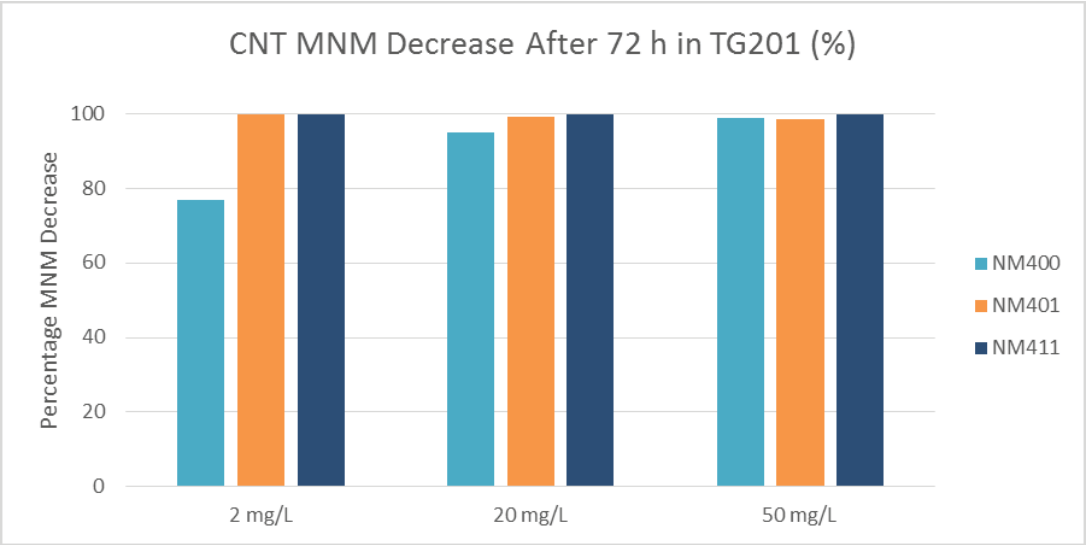

Figure 11. Graph showing the percentage of the CNT MNM (NM-400, NM-401 and NM-411) in algae media (TG201) after 72 h.

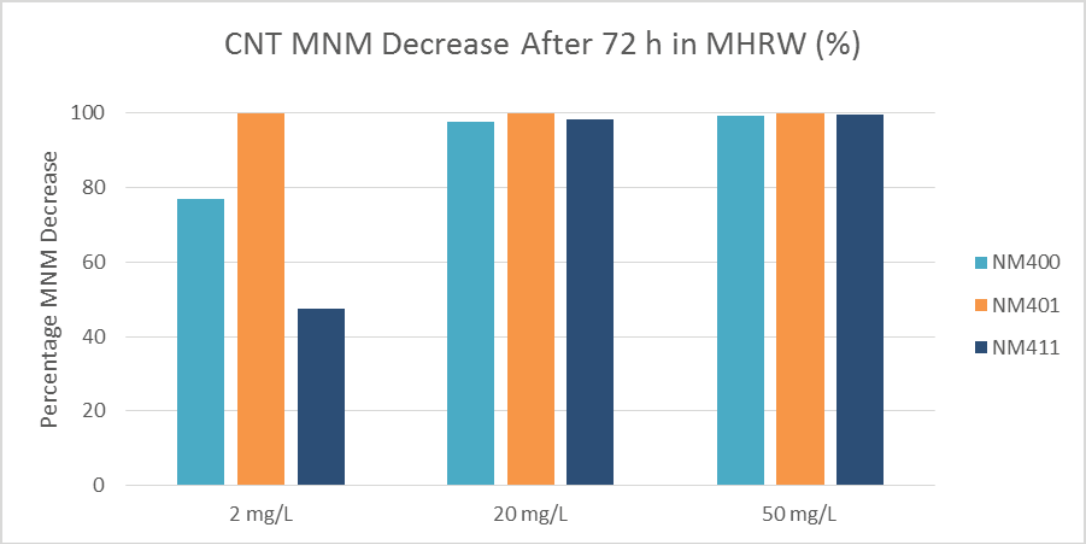

Figure 12. Graph showing the percentage of the CNT MNM (NM-400, NM-401 and NM-411) in *D. magna* media (MHRW) after 72 h.

MNM dispersion concentration and dispersion stability was found to vary significantly between the different materials types used in this study. MNM concentration also appears to play an important role in the percentage amount of MNM remaining in dispersion, with low exposure concentrations (e.g. 0.1 – 2 mg/L) resulting in a relatively lower percentage decrease (Figure 9 to Figure 12). However, this must be considered from the perspective of total amount of MNM remaining in dispersion after 72 h and in most cases for the MNM tested the amount was virtually zero (except NM-300K).

MNM ionic release

Ionic release was evaluated for metal oxide (NM-100, NM-101, NM-103) and metal (NM-300K) MNM in the ecotoxicity range-finding tests. Dissolution was determined by filtering samples taken at each defined time point through 3kDa filters and subsequent ICP-MS analysis. Only samples from the highest exposure concentrations were taken for dissolution analysis. Samples were analysed at 0 h to determine the dissolved concentration at the start of the exposure study. Samples were then analysed at 72 h (also 48 h for *D. magna*) to determine the dissolved concentration at the end of the study. The exposure system contained only MNM and the respective test media (TG201 or MHRW) under static conditions; no organisms were included in these tests. Table 18 shows the dissolved concentrations (mg/L) for each MNM in the two different media types at time 0 h, 48 h (*D. magna* only) and 72 h. NM-300K was only used in algae ecotoxicity studies and was therefore not tested in the *D. magna* media (MHRW). The change in percentage dissolved concentration is determined for each test MNM.

Table 18. Dissolved concentrations of NM-300K, NM-100, NM-101 and NM-103 in the algae ecotoxicity range-finding test at 0 h and 72 h (in TG201 algae media, no NOM) and in the daphnia ecotoxicity range-finding test at 0 h, 48, and 72 h (in MHRW, no NOM). Data generated at 50 mg/L (NM-300K) and 100 mg/L (NM-100, NM-101 and NM-103) exposure concentrations.

MNM Type	Media Type	Dispersion Conc 0 h (mg/L)	Dispersion Conc 72 h (mg/L)	Dissolved Conc 0 h (mg/L)	Dissolved Conc 48 h (mg/L)	Dissolved Conc 72 h (mg/L)	% Dissolved (0 h)	% Dissolved (72 h)	% Change (at 72 h)
NM300K	**TG201**	676.00	152.00	56.00	-	40.00	8.28	5.92	**-2.37**
NM100	**TG201**	50.91	0.25	0.23	-	0.24	0.45	0.47	**0.02**

NM100	**MHRW**	56.36	0.03	0.23	0.23	0.22	0.41	0.39	**-0.02**
NM101	**TG201**	45.77	0.25	0.33	-	0.24	0.72	0.52	**-0.20**
NM101	**MHRW**	46.65	0.20	0.22	0.26	0.24	0.47	0.51	**0.04**
NM103	**TG201**	53.24	0.12	0.17	-	0.33	0.32	0.62	**0.30**
NM103	**MHRW**	54.04	0.22	0.41	0.23	0.33	0.76	0.61	**-0.15**

The data in Table 18 shows that the initial (0 h) NM-300K dispersion in TG201 media contained approximately 8% dissolved silver. The same dispersion after 72 h contained approximately 6 % dissolved silver, indicating that there was no increase in the dissolved silver concentration over the 72 stability study. The initial (0 h) dispersions of NM-100, NM-101 and NM-103 in both TG201 and MHRW media contained less than 1% dissolved Ti. It is suggested that the levels detected are within the analytical detection limits and that the dissolved Ti concentration is effectively 0 mg/L. The same dispersions after 72 h showed no increase in dissolved Ti. The results from these studies show:

- Over 72 h there is no significant dissolution of Ti from TiO2 MNM in either media type.
- Over 72 h there is no significant change in the concentration of dissolved silver from Ag MNM in TG201 media.
- In all cases, the percentage change in dissolved species concentration in the two media types was less than 1%. This indicates that dissolution of ionic species from these MNM types is negligible during 72 h acute ecotoxicity tests with freshwater algae and *D. magna*.
- This simple pre-test offers a cost effective approach for determining the importance of MNM dissolution in aquatic ecotoxicity studies.
- The pre-test allows the operator to make a decision, based on defined parameters, for when dissolution should be determined as part of a full-scale ecotoxicity test and when determination of this parameter can be omitted (i.e. where dissolution is shown to be greater than 20% at any test concentration).

2.4.2. Task 2.4 f) Procedures for quantification of MNM exposure and fate in dispersions for in vitro studies

A DLS procedure for assessment of particle deposition (sedimentation) and agglomeration in *in vitro* exposure mediums were suggested in the NANoREG TGD for toxicity testing. The most basic approach involved measurement of the exposure mediums at the beginning (n=10) and at the end of the experiment (n=10). It was recommended to conduct a more comprehensive time-resolved analysis using either DLS or estimations based on centrifugal analysis.

NRCWE DLS procedure for assessment of sedimentation rate and agglomeration in exposure mediums

A DLS procedure was already developed by NRCWE during the ENPRA and NANOGENOTOX projects to assess the sedimentation and agglomeration behaviour of MNM dispersions during incubation *in vitro*. This procedure was further refined by improvement of the data treatment and presentation for analysis as part of the work leading to D2.8. The resulting DLS protocol is available (NRCWE SOP for measurement of hydrodynamic size distribution).

Experiments with NM-101, NM-110 and NM-400 were selected for demonstration of the procedure. In this case, MNM were dispersed following the ENPRA dispersion protocol (2 wt.% serum water; EtOH pre-wetting) and added to an *in vitro* toxicological test medium consisting of RPMI with glutamax with 0.2% surfactant to reach a dose of 0.256 mg/mL and exposure mediums where then incubated in a DLS cuvette for a duration of 24 hours or until measurements stopped, using fixed measurement conditions of the DLS. The evolution in derived intensity (I/Io) and of hydrodynamic particle size ($Z_{ave}/Z_{ave;o}$; simple form Z/Zo) are used to assess the relative importance of deposition and agglomeration during incubation. During SOP development, it was decided to convert the data to LOG(I/Io) and LOG(Z/Zo) where the initial conditions are defined by the values (0,0). The LOG(I/Io) values also allowed calculation of apparent deposition rates using regression analysis.

Example results are given below showing the different stabilities and agglomeration behaviour of NM-101, NM-110, and NM-400 in RPMI added 0.2% (w/v) glutamax (Figure 13). The results clearly show that NM-101 is the least stable of the 3 dispersions, followed by NM-110 and NM-400. NM-400 appears to only partially deposit followed by accumulation of MNM in a layer above the bottom of the DLS cuvette, which results in agglomeration and increase in both LOG(I/Io) and LOG(Z/Zo). A similar tendency of formation of an accumulation layer at the bottom was also observed for NM-101, but less prominent, whereas most of the suspended MNM appears to deposit in the test with NM-110. This type of behaviour with formation of accumulation layers still in dispersion is difficult to predict from simple models of particle deposition. Using the initial regression slope of time versus LOG (I/Io) enables estimation of the fractional deposition times (**Error! Reference source not found.**).

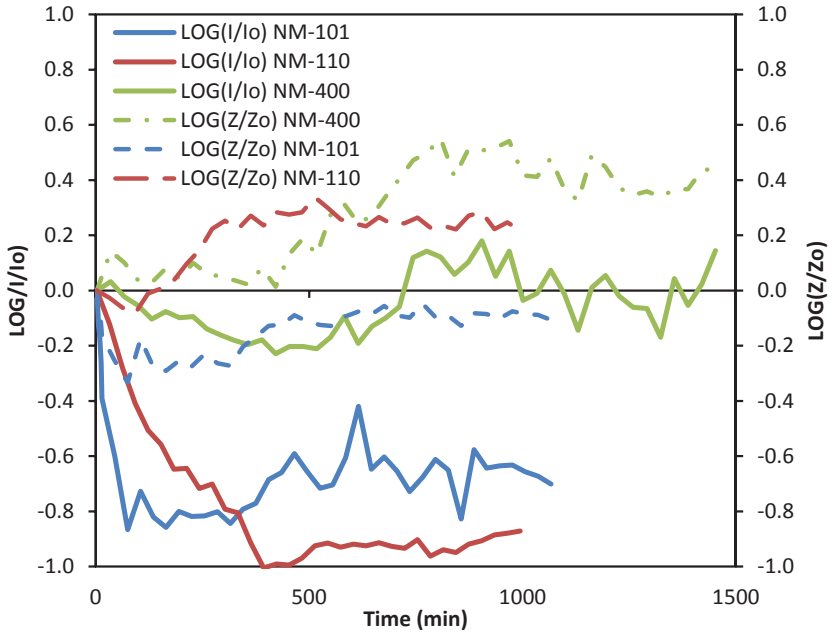

a)

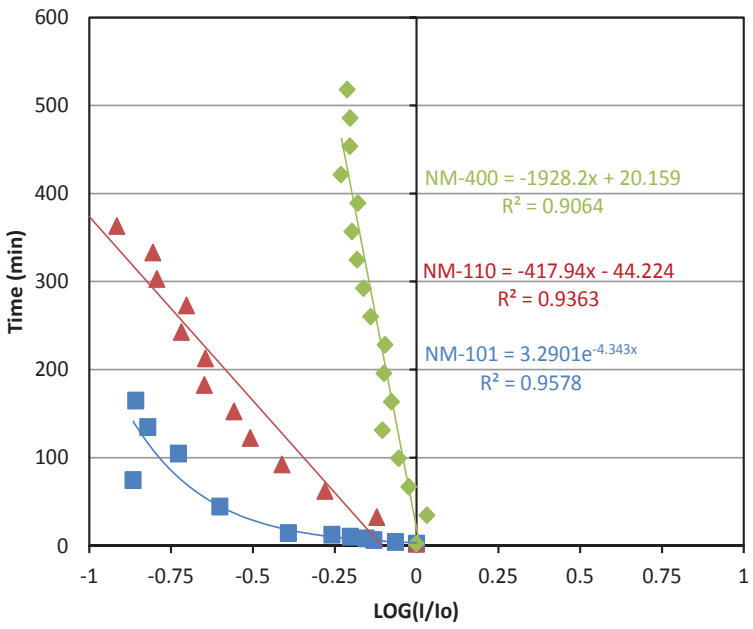

b)

Figure 13. a) Temporal evolution of the relative intensity; LOG(I/Io); and size; LOG(Z/Zo); of NM-101, NM-110 and NM-400 dispersed in RPMI with 0.2% glutamax (w/v). b) Regression curves (user defined

models) for the three MNM for assessment of fractional deposition in Table 19 Error! Reference source not found..

Table 19. Calculated fractional deposition time in hours for NM-101, NM-110, and NM-400 calculated from equations in Figure 13.

Deposited fraction	Deposition time NM-101	Deposition time NM-110	Deposition time NM-400
25% ($t_{0.25}$)	0.2	1.0	8.4
50% ($t_{0.50}$)	0.5	2.7	16.4[€]
75% ($t_{0.75}$)	1.4	4.5	24.4[€]
99% ($t_{0.99}$)	4.0[€]	6.2[£]	32.2[€]

[€] Apparent deposition time projected from initial slope, but the NM appears to form a suspended accumulation in the lower volume of test vial.

[£] Estimated from the average slope. The suspension near the bottom may start to agglomerate and accumulate at the base of the vial.

The results in Table 19 demonstrate that there may be huge differences in the apparent sedimentation rates during *in vitro* testing. Whereas deposition of suspended NM-101 and NM-110 have passed within 4 to 6 hours, less than 50% of the NM-400 CNTs appears to have deposited after 16 hours of incubation in RPMI added 0.2% glutamax. Full sedimentation of NM-400 is projected to take 32.2 hours, but the dispersion instead appears to accumulate in the lower volume of the cuvette. Consequently, care should be taken in the assessments of deposition rates as the deposition assessed by the derived count rate is affected by increases in intensity (and count rate) when particle agglomerate and accumulate. Data may be plotted as demonstrated in Figure 13 or alternatively as depicted in Figure 14 where LOG (Z/Zo) is plotted against LOG (I/Io).

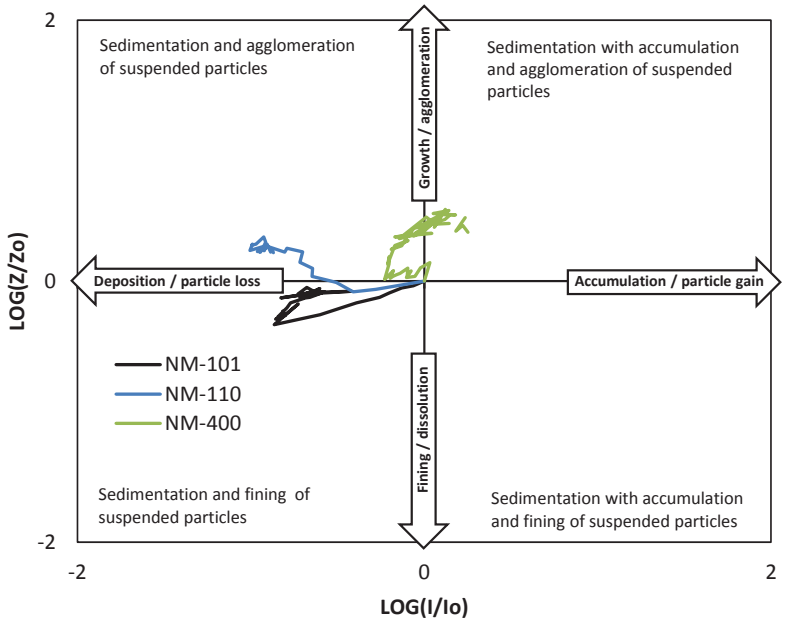

Figure 14. Dispersed particle settling assessment diagram plotting LOG(Z/Zo) versus LOG(I/Io). The graph shows the settling results from experiments with NM-101, NM-110, and NM-400 showing different evolution paths during the 24-hour incubation. The behaviour of NM-101 is dominated by deposition while first sedimentation followed by combined sedimentation and agglomeration plays an important role for NM-110. The NM-400 sample is first affected by slight deposition followed by accumulation and agglomeration at the vial bottom.

Experimental evaluation of LEITAT SOPs

Following the recommendations, procedures and SOPs reported above, three NANoREG core MNM (NM-200, NM-101, NM-212) were investigated simulating an *in vitro* cytotoxicity assay. The Z-ave diameter together with the polydispersity and the zeta potential, were monitored as a function of time to check the evolution of the MNM size and dispersion stability.

Preliminary test on MNM concentration in the specific media

As reported, a preliminary test should be performed to check which MNM concentration in cell culture media are possible to detect by DLS. In fact cell culture media contain small particles (i.e. protein) that give a signal in the particle size distribution and the Z-ave parameter could be affected from the presence of those particles especially when very low MNM concentration has been used.

Example: NM-200 diluted in DMEM

To this aim, a stock dispersion of the NM-200 is prepared following "SOP for probe-sonicator calibration of delivered acoustic power and de-agglomeration efficiency for *in vitro* and *In vitro* toxicological testing" and MNM size checked by DLS. Verified the corrected outcome of the protocol, the stock dispersion is used to prepare the concentration series used in the *in vitro* assay to simulate, that in this case are 1, 10, 25, 50 and 100 ppm. The concentration series are obtained by dilution of the stock dispersion in the complete cell culture medium employed, that in this case is the DMEM.

The stock dispersion, the DMEM alone and the MNM dilution in DMEM are measured by DLS obtaining the Z-ave and PdI parameters. The Table 19 and Figure 15 below show the dependence of Z-ave on different concentration of NM-200 when dispersed in DMEM as complete cell culture media.

Table 19. Z-ave of NM-200 in the stock solution and in the concentration series in DMEM

Sample	MNM conc. (ppm)	Z-Ave (d.nm)	St. Dev. (nm)	PdI	St. Dev.
Stock	2560	245.8	21.6	0.399	0.047
100 ppm	100	152.6	5.8	1.000	0.000
50 ppm	50	88.5	15.4	0.973	0.060
25 ppm	25	55.8	8.8	0.971	0.064
10 ppm	10	33.4	9.7	0.770	0.129
1 ppm	1	16.7	0.4	0.429	0.021
DMEM	0	15.1	0.1	0.382	0.005

From data obtained it is clear that decreasing MNM concentration the Z-ave recorded shifts towards smaller size value. This is particularly evident when 1 ppm of NM-200 has been used, in this case the Z-ave value obtained is very close to that obtained for the DMEM alone. This suggests focusing on the higher MNM concentration tested of 100 ppm for following DLS and zeta potential measurement.

The preliminary test to select the MNM concentration to be investigated should be performed when the dilution media contain small particle detectable by DLS. In fact, the Z-ave diameter, being an intensity weighted mean diameter, is strongly dependent from the size of the particles that are present in the sample and from their relative amount. In the case of cell culture media the particles contained are generally small in size but relevant in amount, while the MNM are bigger in size but, depending on the concentration employed, could be present in a lower amount to the respect of particle present in the cell culture medium. Employing a proper MNM concentration, the contribution to the total light scattered (and therefore to the Z-ave parameter) by the small particles should be neglected.

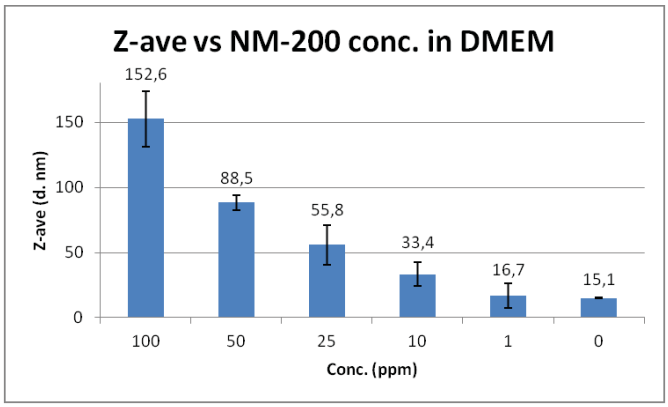

Figure 15. Z-ave of NM-200 in the stock solution and in the concentration series in DMEM

Planning of the experiment

After the preliminary test on MNM concentration in media, the time points to measure are planned and established in relation to the exposure time employed in the *in vitro* assay to simulate. In this study, the time point selected are: t = 0, 3, 6 and 24 h.

Basing on the MNM concentration selected the time point to study and the technique that will be used to analyse the samples, it is possible to estimate the total volume of stock dispersion that will be needed to prepare the samples to be measured.

Preparation of MNM samples

Stock dispersion

The MNM stock dispersion was obtained applying the “SOP for probe-sonicator calibration of delivered acoustic power and de-agglomeration efficiency for *in vitro* and *In vitro* toxicological testing”. A fixed amount of MNM were weighted, subjected to ethanol pre wetting and then a water solution of 0,05% (w/v) bovine serum albumin in MilliQ water was used as solvent. Then MNM were dispersed following the sonication setting and timing selected during the sonicator calibration and generation of benchmark data.

The correct amounts of MNM stock dispersion are then picked up: one millilitre of volume is measured by DLS to ensure the correct outcome of the dispersion protocol. If this is verified, the other amount (previously picked up) will be used for the preparation of the following diluted samples to be tested.

Samples to be tested

Samples to be tested were prepared diluting the stock dispersion up to 100 ppm in fresh, pre-wormed DMEM.

In this study two identical (twin) samples for each time point to measure (t = 0, 3, 6, 24 h) were prepared, this allow to measure size and zeta potential on one sample and to measure the pH on its "twin" sample. Therefore 8 samples, with a volume of 1 ml and a MNM concentration of 100 ppm in DMEM were prepared and stored for the duration of the experiment in a cell incubator at 37 °C and 5% of CO_2.

Size and zeta potential measurements

Further issue on the operation to perform before measurements: example of NM-101

As discussed above, the samples could be prepared directly in a dosing plate or placed in separate vials. This allow to better simulate the "condition" of the cytotoxicity assay, where the MNM dilution in cell culture media were prepared and placed in the dosing plate and then stored in a cell incubator in static condition, allowing a certain degree of MNM settling.

But when the aliquot to be measured are picked up from the dosing plate for DLS, the settled particles are re-dispersed again. An alternative procedure could be to place directly the sample in the DLS cuvette inside the

cell incubator, to achieve static condition. However measuring the sample in both conditions, different size data will be obtained, as demonstrated in Figure 16 reported below.

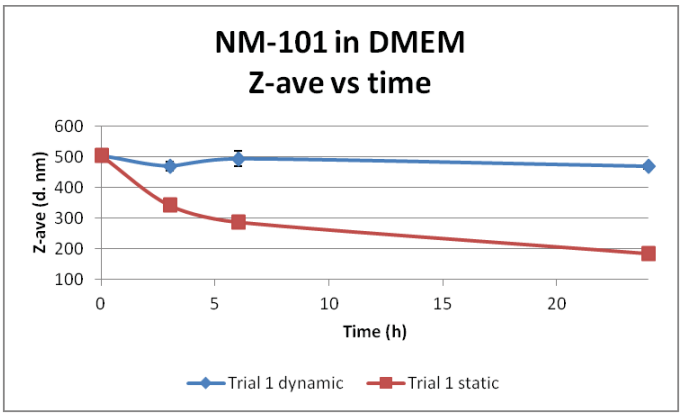

Figure 16. Z-ave of NM-101 dispersed at 100 ppm in complete culture medium DMEM at time 0, 3, 6, 24 h. The blue curve is obtained after sample homogenization ("dynamic" conditions), while the red one is obtained storing the sample to be tested inside the DLS cuvette, to ensure "static" condition.

When performing simulation experiment, it is important to understand what procedure could give us the best (or the most relevant) information on the test system under investigation. This observation suggested to homogenize the sample to be measured by vortex shaking or pipetting the sample up and down, to maintain "dynamic condition" and have information on the whole sample, including both particles still suspended and particles that will settle down over time. Note that when the sample are not re-dispersed, the DLS data will be relative to the part of the sample that is not in contact with cells, therefore in this setting the information relative to that part of the sample has been loose.

Example of size and zeta potential measurement of NM-212 dispersed in DMEM over time

After the preliminary test to set the MNM concentration to employ and the operation to perform before the measurements, the dispersion state and colloidal stability are investigated measuring size and zeta potential of MNM dispersed in DMEM as complete cell culture media following the standard operating procedure previously described. The experimental data obtained for NM-212 are shown below (Figure 17, Figure 18, Figure 19 and Table 21).

The first comment on the data shown is that the more similar are the stock solution the most reproducible and comparable result in the following test will be obtained.

In fact data obtained in all trials are comparable, but considering the trial 2 and 3, that show almost the same particle size in the stock dispersion, it could be noted that the graphs obtained for all the parameters investigated (size, PdI and zeta potential) practically overlaps demonstrating the importance to obtain similar dispersion in the starting stock solution.

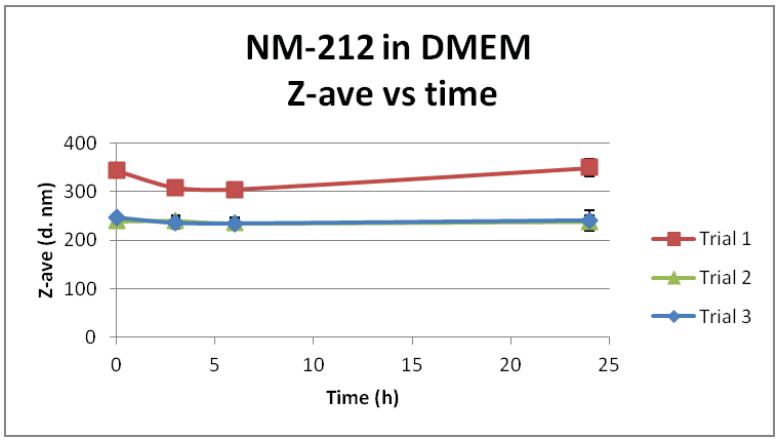

Figure 17. Z-ave of NM-212 dispersed at 100 ppm in complete culture medium DMEM at time 0, 3, 6, 24h.

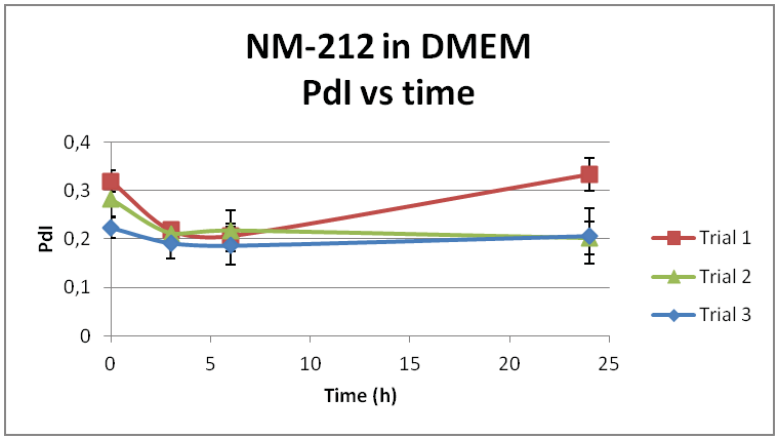

Figure 18. PdI of NM-212 dispersed at 100 ppm in complete culture medium DMEM at time 0, 3, 6, and 24h.

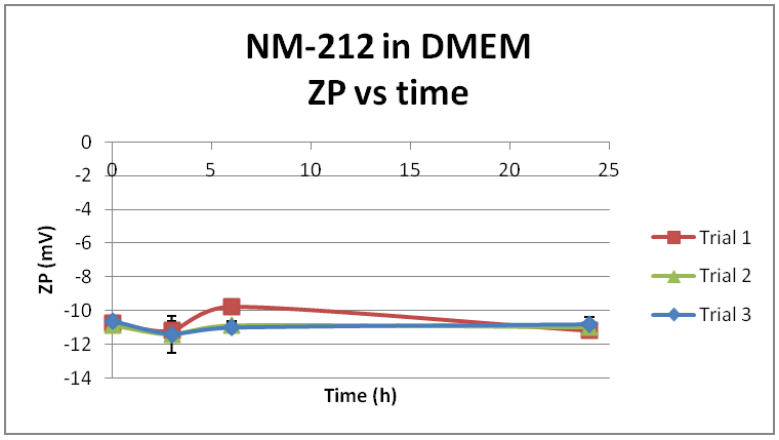

Figure 19. Zeta potential of NM-212 dispersed at 100 ppm in complete culture medium DMEM at time 0, 3, 6, and 24h.

Table 20. Z-ave of NM-200 stock dispersions.

Trial	Z-ave (d. nm)	Std. Dev.	PdI	Std. Dev.
1	305,3	4,8	0,262	0,024
2	251,0	8,9	0,283	0,038
3	251,5	9,0	0,252	0,031

Table 21. Z-ave, PdI and zeta potential of NM-200 dispersed at 100 ppm in complete culture medium DMEM at time 0, 3, 6, and 24 h.

Trial	Time (h)	Z-ave (d. nm)	Std. Dev.	PdI	Std. Dev.	pH	ZP (mV)	Std. Dev.
1	0	343,5	9,8	0,319	0,022	8,1	-10,7	0,3
2	0	239,4	11,2	0,283	0,038	8,1	-10,9	0,4
3	0	246,1	9,5	0,224	0,022	8,0	-10,6	0,3
1	3	307,4	9,9	0,218	0,017	8,2	-11,2	0,6
2	3	240,7	9,6	0,211	0,016	8,2	-11,4	0,4
3	3	235,5	12,0	0,192	0,032	8,2	-11,4	1,1
1	6	304,0	13,5	0,206	0,026	8,3	-9,75	0,1
2	6	235,3	10,7	0,217	0,042	8,3	-10,9	0,3
3	6	234,4	11,0	0,186	0,039	8,3	-11	0,3
1	24	349,3	17,5	0,333	0,034	8,2	-11,2	0,3
2	24	238,7	13,1	0,201	0,034	8,3	-11	0,2
3	24	240,8	20,5	0,206	0,057	8,3	-10,8	0,4

The Z-ave vs time graphs show that the size of the NM-212 once diluted up to 100 ppm in DMEM does not change in a relevant manner during the time point considered. But during the measurement performed, both the Z-ave parameter and the derived count rate are decreasing, showing symptoms of MNM aggregation and settling phenomena during the course of the analysis. This suggests using the DLS data in conjunction with other techniques that are able to detect all the size classes present in the sample and not only those in suspensions and undergoing Brownian motion. Alternative techniques to study the size evolution during time could be the differential centrifuge sedimentation or TEM microscopy.

The zeta potential vs time curves obtained for NM-212 once diluted up to 100 ppm in DMEM during the three trials are also comparable and moreover this value seem to be less dependent on the particle size obtained in the starting stock dispersion. In all the experiments, the NM-212 zeta potential seem shift towards more negative value during the first hours of the experiment and then to level off at value around -11 mV. These zeta potential values could suggest poor samples stability at investigated condition or may be related to protein adsorption on NM-212 surface, being the zeta potential value measured close to that of proteins present in cell culture media at the same pH.

Similar trends and data comparability are detected for the other MNM investigated (data not shown).

The observed behaviour of MNM dispersed in cell culture media encourage to investigate other parameter inherent to NM-biological interactions, such as quantity, identity and secondary structure of adsorbed proteins, which may be related to the toxicity exerted by MNM.

Results from particle size determination (CLS) and concentration determination for fate-exposure of MNM dispersion during in vitro tests (sedimented dose)

CLS technique

Two types of incubations were done: one exposing ZnO MNM to the CaCo2 cells and one exposing ZnO MNM only to the culture media. This was done to elucidate possible potential differences in the particle size distribution (PSD). Control samples containing either incubated CaCo2 cells or only culture media at 6, 24, 48

and 72 hours were measured. It was observed that the intensity and peak position of the control samples do not interfere with the observed peaks of the exposed samples (data not shown). The evolution of the main peak of the ZnO MNM PSD goes from 185 nm at 6h up to 203 nm at 72 h, see Figure 20. It is equally observed that there is not a noticeable difference in the hydrodynamic diameter between the incubation with cells or only in culture media. This implies that biological parameters such as culture media consumption, cell division, etc., do not influence the product NM-110. Also it is noticed that the standard deviation of the incubation in culture media is quite larger than its counterpart incubated with CaCo2 cells.

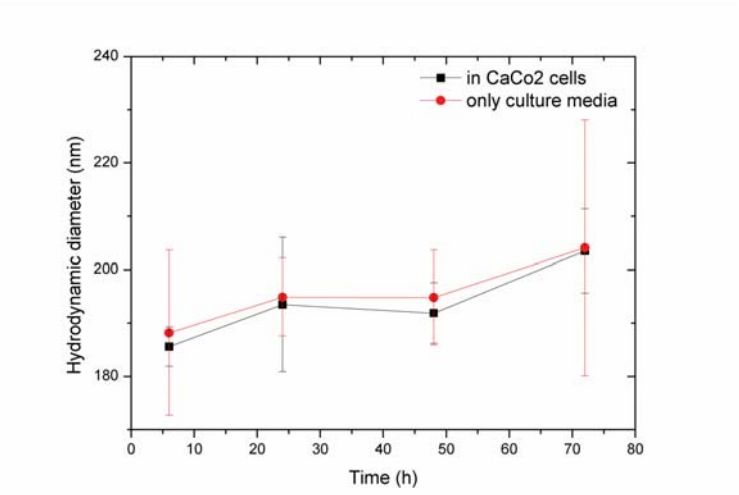

Figure 20. Evolution of hydrodynamic diameter of main peak of ZnO MNM (NM-110) measured by CLS. Results are the average +/- standard deviation from two series of triplicates per condition.

Presence of secondary distribution was found in some samples at times higher than 6 hours, which were not reproducible. In the first series of measurements it was found: after 72 hours incubation with Caco-2 cells, secondary distributions at 17 and 660 nm; and at 48h with only culture media a secondary distribution at 15 nm. For the second series it was found: at 24, 48 and 72 hours of incubation with Caco-2 cells a secondary distribution of 450-640 nm; and at 48 and 72 hours of incubation with only culture medium secondary distributions at 480 and 640 nm only in one sample per triplicate.

The sedimented dose calculated from the two series of CLS data gave values varying between 40% and 70% (Figure 21). In general the trends observed revealed certain stability of the sedimented dose values at about half of the ZnO MNM nominal dose.

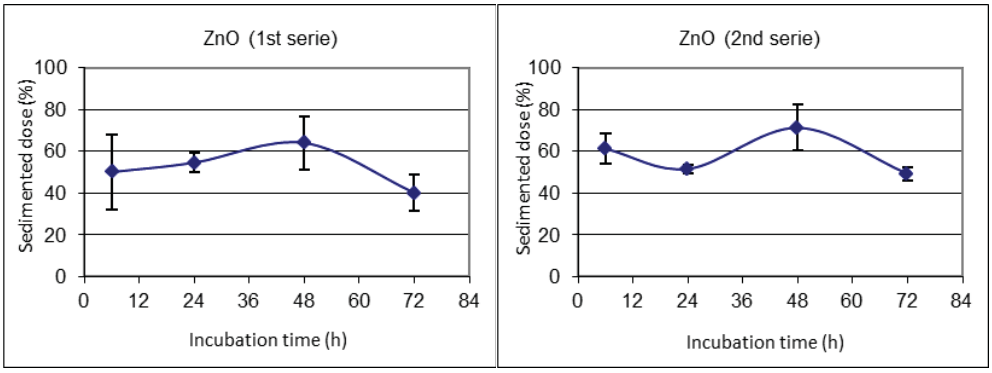

Figure 21. Sedimented dose of ZnO MNM in culture medium with cells at different incubation times calculated from CLS measurements.

These results point out that the CLS protocol is well suited for MNM PSD analysis, showing that even small hydrodynamic diameters can be measured with precision. Knowledge was generated at determining that for CaCo2 cell incubation there seems not to be an influence of the cell interaction in the PSD of product NM-110.

PIXE technique

Sedimented dose of NM-110 was evaluated in parallel by PIXE after incubation of MNM for increasing incubation times in presence or not of Caco-2 cells. Figure 22 presents such results. First of all there seems to be no difference between both conditions due to the superposition of the weighted standard deviation. The general observed trend is a minor decrease in the available ZnO up to 48 hours, then increasing 22 % with respect to the 6 hours condition. This result suggests that ZnO MNM could be in contact (either internalized or attached) with cells up to 48 h, and then a quantity would be released back to the culture media.

It was noted that in both conditions, incubation with or without CaCo2 cells led to similar weighted standard deviations, except at 6 hours with the no CaCo2 cell condition which had a very small deviation. The weighted scheme was adopted because with PIXE measurement it is possible to attribute a statistical error per measurement due to instrumentation, sample quality and complexity.

Sedimented dose values obtained from the PIXE measurements are between 28% and 55% (Figure 22). Values started at about 40% (6h) to increase until 55% (48h) and later decreased to about 28% (72h) in presence or not of cells. Both trends, in presence or not of cells, were similar and decreased with incubation time.

These results highlighted that sedimented doses are different from the nominal dose, with cells or not, thus one of the principal factors affecting this parameter is the culture medium. As previous reported, results of SiC, TiC, SiO2 and TiO2 MNM, it can be observed that values obtained seems to be MNM dependent. In general, the sedimented doses, obtained with both techniques, are similar with more notable differences for higher incubation times. There is an agreement in the values obtained with both techniques, however the complexity of the biological medium makes difficult to obtain a better fit.

In addition, these results highlights that nominal dose is quite different from the effective (i.e. sedimented) dose, which is calculated as the difference between nominal and remaining (in the culture medium) ones.

These results point out that the CLS and PIXE protocol is well suited for MNM concentration analysis in complex matrices with a simple sample preparation protocol. Knowledge was generated at determining that for CaCo2 cell incubation there seems not to be an influence of the concentration of product NM-110. At 72 hours of CaCo2 cell incubation with NM-110, concentration of 100 µg/mL, there is a ZnO release to the volume from the already sedimented MNM. We hypothesize that this could be due dead cells being detached from the culture box's bottom (Figure 23).

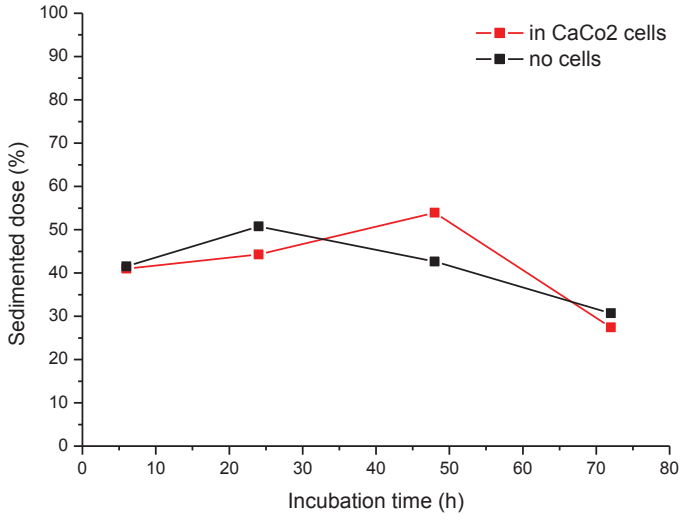

Figure 22. Sedimented dose of ZnO MNM in culture medium with cells at different incubation times calculated from PIXE measurements.

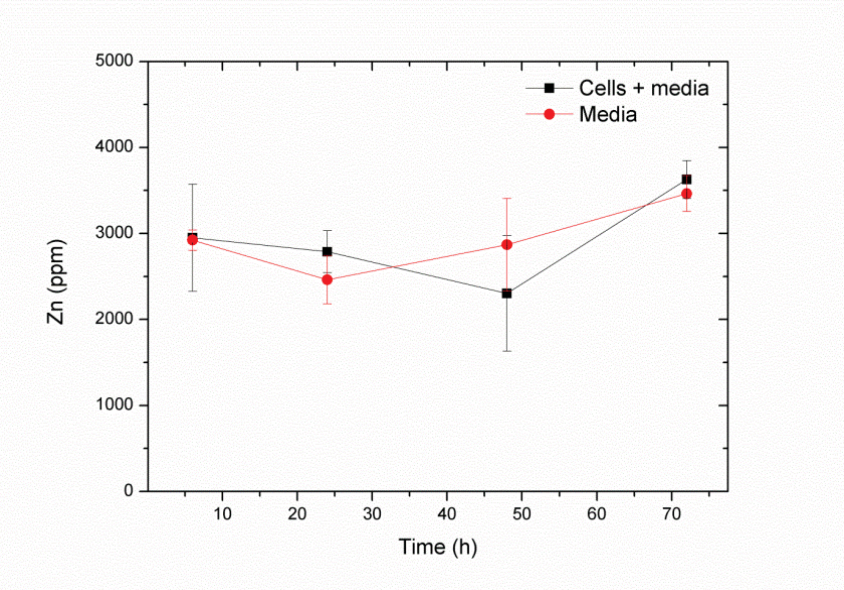

Figure 23. Evolution of the concentration of ZnO MNM (NM-110) traced by the quantity of Zn by PIXE. Results are the weighted average +/- weighted standard deviation from a series of triplicates per condition.

Overall, similar trends for the sedimented doses were obtained with both techniques. Other than that, it was observed that hydrodynamic sizes of MNM increased with the incubation time in culture medium.

Particle size distribution determination by CLS of MNM dispersions during in vitro assays.

Summary of work

Size distribution of fluorescent positively and negatively charged SiO_2 (specifically used in task 5.3), SiO_2 (NM-200) and ZnO (NM-110) MNM in water-BSA stock solutions and after dilution in different culture media (used in *in vitro* assays –tasks 5.3 and 5.5-) was characterized by Centrifugal Liquid Sedimentation (CLS). Comparison of sonicated (following the Nanogenotox dispersion protocol) or only stirred MNM was done.

Overview of main results

Particle size distribution of SiO_2 (NM-200) ZnO (NM-110) and fluorescent positively and negatively charged SiO_2 MNM for *in vitro* assays

Fluorescent positively and negatively charged SiO_2, SiO_2 (NM-200) and ZnO (NM-110) MNM were dispersed following the NANOGENOTOX dispersion protocol or only stirred using a metallic bar for the same dispersion time (12 min 20 sec). The size distribution of these MNM in stock solution and after dilution in culture medium (Caco2) at 100 (highest concentration used in *in vitro* assays) or 10 µg/ml (MNM at the lowest concentration -1 µg/ml- were not detectable) was measured by CLS at 0 or 24h of incubation. Results were expressed in relative weight to reveal the size distribution of MNM agglomerates. The maximal values in each sample were arbitrarily set to 100%. It was found that media did not interfere with the particle size distribution of either MNM in their media regardless of the incubation time.

Results for fluorescent positively and negatively charged SiO_2 MNM:

CLS analysis of size distribution of both fluorescent positively and negatively charged SiO_2 MNM showed that dilution of MNM (100 µg/ml) into Caco-2 cell culture medium did not greatly modify their size distribution in comparison with water-BSA stock solution (Figure 24A and B). One major peak was observed around 70 nm and a second peak corresponding to big agglomerates higher than 1 µm. For - SiO_2 MNM, a shift of the first peak (around 150 nm) was observed at a concentration of 10 µg/ml in cell culture medium in comparison with stock solution and MNM diluted at 100 µg/ml in cell culture medium (Figure 24B). Surprisingly, no clear peaks were detected after 24h of incubation in Caco-2 cell culture medium (Figure 24C).

Results for ZnO MNM:

Analysis of both sonicated and stirred ZnO MNMs size distribution in water stock solution or in Caco-2 cell culture media showed presence of two main peaks (Figure 24): a peak at around 30-50 nm corresponding to well-dispersed MNM was observed for both sonicated and stirred ZnO MNM. A second peak centred on 216 nm for sonicated MNM or on 373 nm for stirred MNM indicated a worse dispersion after stirring. A smaller less well-defined peak was observed around 1 µm only in stirred MNM solutions corresponding to big agglomerates observed by optical microscopy. Neither dilution at 100 µg/ml in Caco-2 culture medium nor incubation for 24h did not modify size distribution of both sonicated and stirred ZnO MNM (Figure 24A and B).

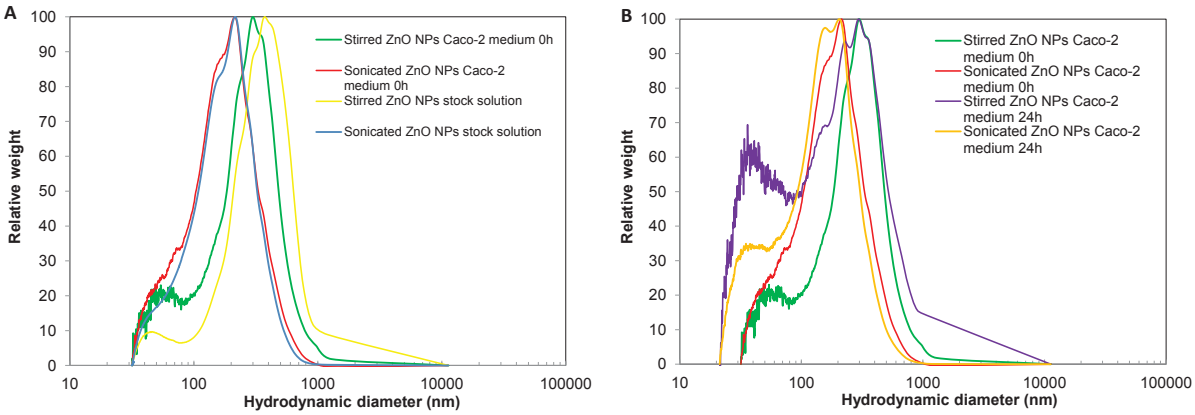

Figure 24. Size distribution analysis of sonicated and stirred ZnO MNM in stock solutions or in Caco-2 cell culture medium by centrifugal liquid sedimentation. A) Agglomeration state profiles were obtained for sonicated and stirred ZnO MNM in water-BSA stock solutions or after dilution at 100 µg/ml in Caco-2 cell culture medium. B) Size distribution profiles of sonicated and stirred SiO_2 MNM after dilution at 100 µg/ml in Caco-2 cell culture medium were compared after 0h or 24h of incubation. Results are displayed as relative ZnO MNM weight distribution against the hydrodynamic diameter. Maximal values in each sample were arbitrarily normalized to 100.

There is no important impact of cell culture medium on size distribution of ZnO MNM. The sonicated and stirred ZnO MNM stock solutions used to expose Caco-2 cells, peak corresponding to well-dispersed primary MNM was centred on 25 nm instead of approximately 50 nm in first stock whereas the values of the second peak were similar (289 nm for sonicated MNM or on 366 nm for stirred MNM).

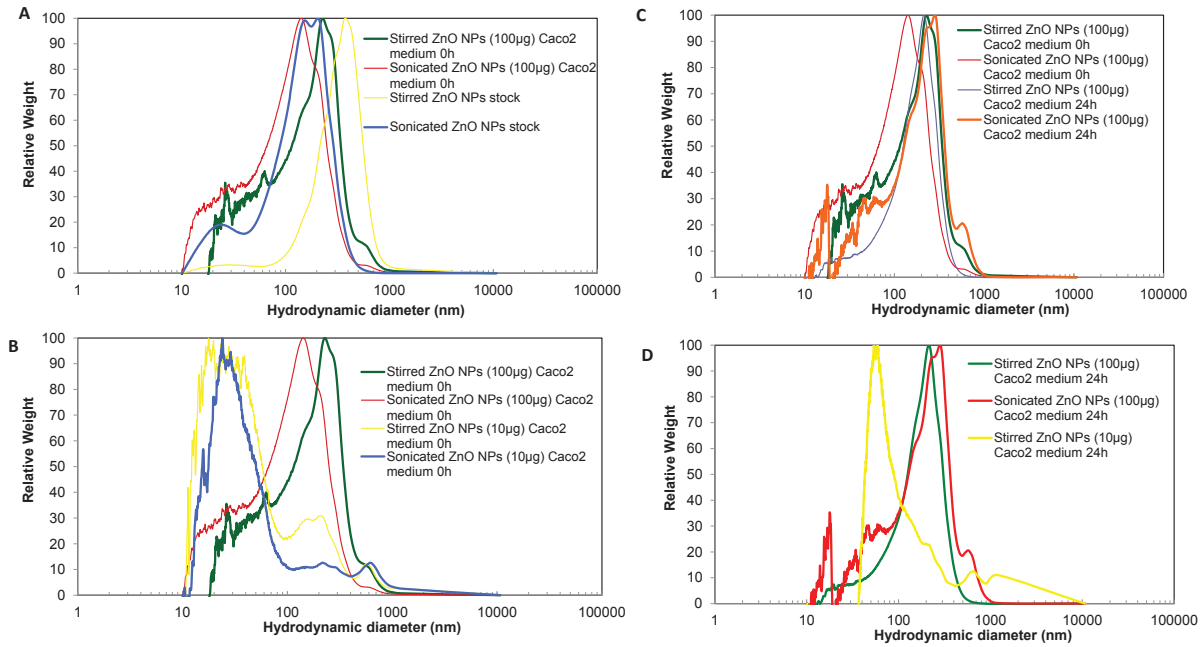

Figure 25. Size distribution analysis of sonicated and stirred ZnO MNM in stock solutions or in Caco-2 cell culture medium by centrifugal liquid sedimentation. A) Agglomeration state profiles were obtained for sonicated and stirred ZnO MNM in water-BSA stock solutions or after dilution at 100 µg/ml in Caco-2 cell culture medium. B) Agglomeration state profiles were obtained for sonicated and stirred ZnO MNM after dilution at 100 or 10 µg/ml in Caco-2 cell culture medium. C) Size distribution profiles of sonicated and stirred ZnO MNM after dilution at 100 µg/ml in Caco-2 cell culture medium were compared after 0h or 24h of incubation. D) Size distribution profiles of both sonicated and stirred ZnO MNM (100 or 10 µg/ml) after 24h incubation in Caco-2 cell culture medium. Results are displayed as relative ZnO MNM weight distribution against the hydrodynamic diameter. Maximal values in each sample were arbitrarily normalized to 100.

IIT procedure and relative protocol for characterization of MNM surface charge by zeta potential in synthetic human body fluids (simulating the human digestive compartments) or cellular biological media.

Summary of work

Development of protocol for characterization of surface charge of MNM using synthetic human body fluids (simulating the human digestive compartments) or biological media. The protocol is based on zeta potential measurement.

Overview of main results

Surface charge of MNM (from repository list) has been measured by zeta-potential after MNM incubation in different matrices such as biological media and synthetic body fluids simulating the human digestive compartments (such as saliva, stomach and intestine/bile salts). The incubation time was reflective of relevant exposure conditions such as cell exposure or the digestive temporal processes (i.e., 5 minutes of incubation in the saliva, 2 hours in the stomach and intestine, respectively). After the incubation, MNM were collected by ultracentrifugation and the surface charge of “hard protein corona” measured.

Overall we found out that the nominal surface charge for each MNM progressively changed, mostly acquiring charge features of the media components (e.g., proteins). We also observed for all the tested MNM negative values peaking around values of -25mV for the biological media (supplemented with proteins). In the saliva and intestine, MNM acquire a negative charge around -35mV, whereas in the stomach the surface charges

approach neutral values possibly similar to pI (in line with literature). Note that since these MNM partially dissolve in the stomach compartment, it could be possible that the reported values in the digestive juices refer to mixed aggregates of biological/nanostructures present in the solutions that do not relate with the primary MNM. This point deserves future investigations and clarifications.

Table 22. Surface charge of MNM in the biological media DMEM and RPMI supplemented with 10% of proteins. CTRL refers to surface charge of MNM after the dispersion by NANOGENOTOX protocol (with 0.05 % of BSA)

	Nominal Charge (mV)	CTRL charge (mV)	DMEM (mV)	RPMI (mV)
NM 300K	-11.0	-24.4	-28.2	-29.4
NM 200	-47.5	-28.0	-26.0	-27.5
NM 110	-24.3	-20.6	-28.2	-27.2

Table 23. MNM surface charges in the human *in vitro* digestive compartments. CTRL refers to surface charge of MNM after the dispersion by NANOREGONOTOX protocol (with 0.05 % of BSA)

	Nominal Charge (mV)	CTRL charge (mV)	Saliva (mV)	Stomach (mV)	Intestine (mV)
NM 300K	-11.0	-24.4	-35.0	-3.0	-32.0
NM 200	-47.5	-28.0	-30.0	-10.0	-39.0
NM 110	-24.3	-20.6	-36.0	-9.0	-35.0

IIT procedure and protocol for characterization of MNM size and aggregation by DLS in cellular biological media.

DLS analysis in cellular media over 0-48 hours (DMEM and RPMI)

NM-300K

At time 0, DLS spectra indicate the presence of 3 species peaking around 10 (Peak 2), 100 – 200 (Peak 1), and 4000 – 5000 nm (Peak 3), respectively. Peak numeration refers to DLS software assignation according to the signal intensity (Figure 26 and Figure 27). The nominal size of NM-300K is 106 nm, hence Peak 1 is reasonably the peak related to the primary MNM. Peak 2 is reasonably due to protein components of cell culture media, whereas Peak 3 represents already formed aggregates of MNM.

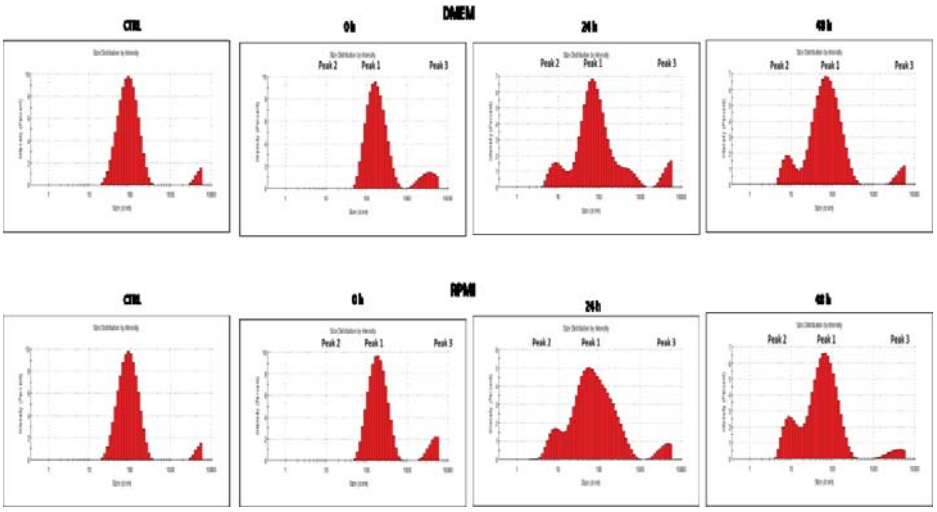

Figure 26. Representative DLS spectra of NM-300K in biological cell media (DMEM and RPMI).

From the size plot of Peak 1 over time, it is possible observing that size profile, and relative kinetic, of MNM appear different in the two media (Figure 27). These changes in size may strongly impact on the biological outcome and must be taken into account when a specific effect may be derived and related to the MNM size. Size reduction over time is monitored and possibly explained by dissolution phenomena or precipitation phenomena.

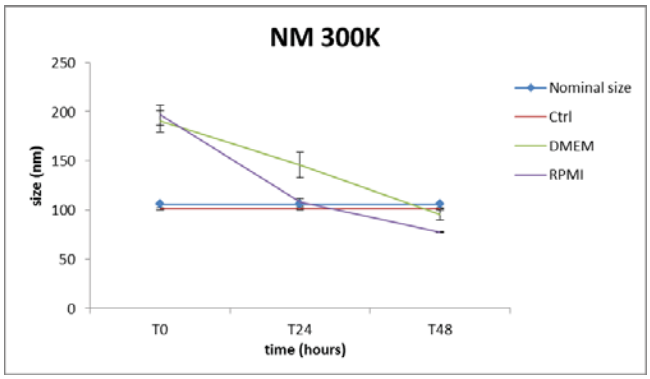

Figure 27. NM-300K size profile. The plot reports the size trend of Peak 1 over time (the deviation standard bars are relative to 10 runs)

NM-200

DLS analysis (Figure 28), indicated the presences of 4 species, distributed along spectrum according to their intensity. Peak 2 and Peak 1 were registered around 10 nm and 40 nm, respectively. Also in this case it was monitored the Peak of about 4000 – 5000 nm (Peak 4) corresponding to aggregates. The Peak 3, ranging from 400 nm to 800 nm was related to the primary MNM that partly aggregated over the incubation.

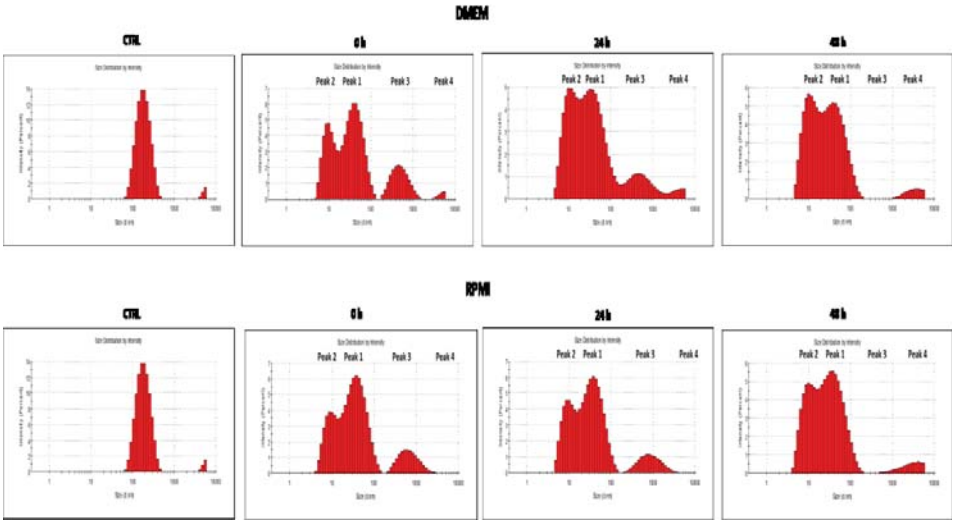

Figure 28. Representative DLS spectra of NM-200 in biological cell media (DMEM and RPMI).

Size plot of Peak 3 possibly indicates the formation of protein shells around MNM and or soluble protein/MNM aggregates in the time frame of 24 hours. After 48 hours, aggregation or degradation phenomena affect the DLS measurements and no MNM signal was detected in both media (Figure 29).

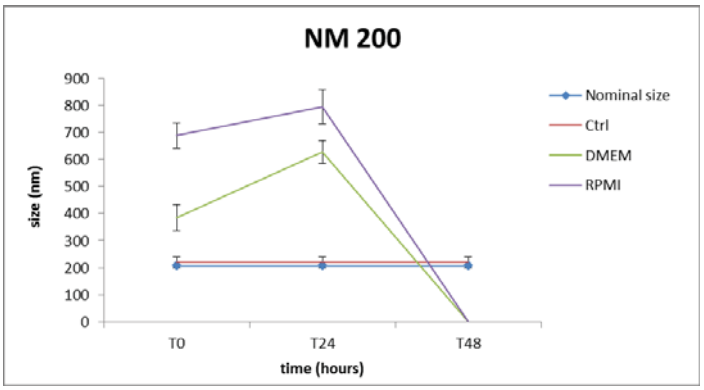

Figure 29. NM-200 size profile. The plot reports the size trend of Peak 3 (error bar are relative to 10 runs).

NM-110

NM-110 DLS spectra reported the presence of 4 species, alternatively distributed during the time assay. As for the NM-200, we monitored two peaks around 10 nm and 40 nm, which aggregate in a single peak during the incubation (Figure 30 and Figure 31). Primary MNM aggregated consistently already at time 0 and are possibly represented by Peak 3 (800 – 1200 nm). This peak disappears after 24 hours in both media possibly due to precipitation phenomena. Peaks of about 400 – 500 nm size (Peak 4) are also detected.

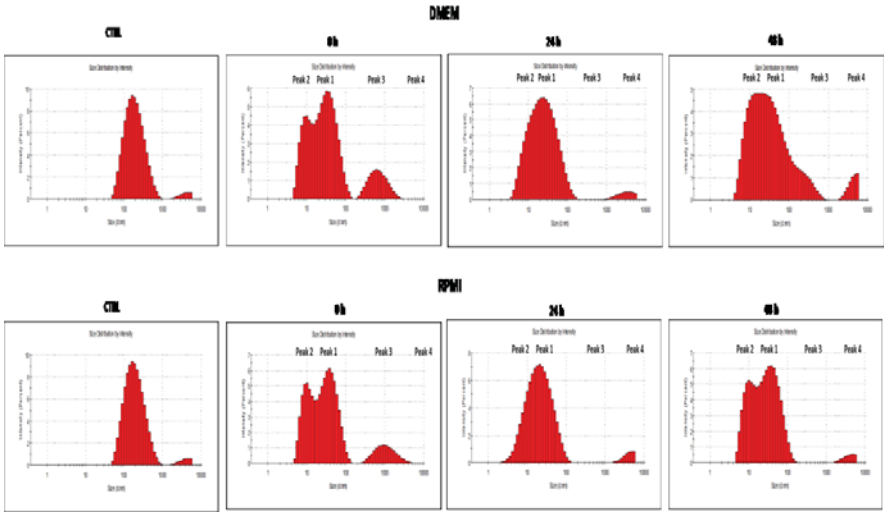

Figure 30. Representative DLS spectra of NM-110 in biological cell media (DMEM and RPMI).

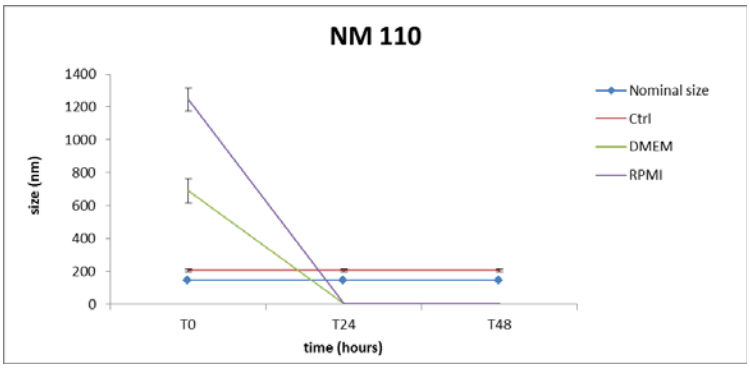

Figure 31. NM-110 size profile. The plot reports the size trend of Peak 3 (error bar are relative to 10 runs).

IIT procedure and relative protocol for characterization of MNM dissolution by ICP-AES in cellular biological media.

UF/ICP-AES in biological media

Dissolution of NM-300K; NM-110; and NM-200 has been measured in commonly used cell culture media such as DMEM and RPMI supplemented with 10% of FBS at the concentration of 20 nM for 0-48 hours by UF/ICP-OES. Results show that NM-200 abundantly dissolves in both the media and that this dissolution is a function of the starting concentration. Importantly, the rate of dissolution seems to be influenced by the ionic strength and type of biological media (reduced dissolution in RPMI with respect to DMEM).

NM-300K and NM-110 does not dissolve in these two media.

In conclusion aggregation and dissolution phenomena influence the MNM fate in the biological media at temporal points relevant for cell culture studies, therefore they must be taken into consideration for protocol validation of test item preparation and validation of *in vitro* cell studies.

Table 24. Dissolution of NM-300K, NM-110, and NM-200 in DMEM and RPMI at the concentration of 20 nM for 0-48 hours by UF/ICP-OES.

		6h	24h	48h
NM 300k	DMEM	n.d.	n.d.	n.d.
	RPMI	n.d.	n.d.	n.d.
NM 200	DMEM	48 uM	77 uM	82 uM
	RPMI	10 uM	42 uM	73uM
NM 110	DMEM	n.d.	n.d.	n.d.
	RPMI	n.d.	n.d.	n.d.

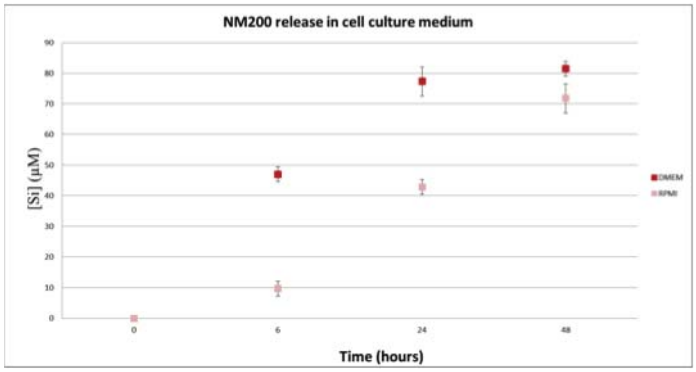

Figure 32. Dissolution of NM-200 in DMEM and RPMI at the concentration of 20 nM for 0-48 hours by UF/ICP-OES.

NRCWE procedure for assessing the hydrochemical reactivity and dissolution of MNM in vitro using the Sensor Dish Reader (SDR) method.

The purpose with the Sensor Dish Reader (SDR) procedure is to identify the oxidative-reductive reactivity of MNM and their dissolution (or time-fixed solubility) during specific *in vitro* exposure conditions. The SDR system was originally produced for monitoring of pH and O_2 during cell growth to assess the confluence and status of cells in situ. NRCWE has previously applied the SDR procedure to assess particle reactivity in a number of previous European projects (ENPRA, NANODEVICE, HINAMOX, and NANOGENOTOX). As part of the NANoREG work, the SDR procedure is now under standardization in CEN/TC 352 WG1/PG2 Hydrochemical reactivity and investigations for protocol modifications have been made, including testing the possibility to perform repeated sampling to determine the dissolution as function of time during testing.

In the SDR method, the hydrochemical reactivity is assessed by real-time measurement of the pH and O_2 concentration in exposure mediums using a 24-well SDR (Sensor Disc Reader) system (PreSens Precision Sensing GmbH, Germany), using fluorescent sensors. pH is measured using the HydroDish® fluorescent sensor plate with up to ± 0.05 pH resolution for pH 5 to 9. Measurement is not possible outside of these ranges. The O_2 variation is measured using the OxoDish® fluorescent sensor plate with ± 2 % air saturation resolution. The fluorescent sensors (spots) are placed at the bottom of the wells in a cell incubation sensor dish. The sensors contain a luminescent dye, which is excited by diode light emitted from the SensorDish® Reader which holds the SDR plates and recorded. The luminescence lifetime of the dye vary with the oxygen partial pressure (OxoDish®) and the pH of the sample (HydroDish®), respectively and are converted to O_2 and pH values by the instrument software.

Changes to pH in the exposure mediums give information on the potential causticity of the test materials and whether conditions comply with the required pH-conditions for the bioassay. Measurement of the O_2 reactivity may be another important parameter and relates to hydrochemical reactions that consume or liberate oxygen. Deviations in the O_2-balance can be caused by different reactions including redox-reactions, protonation and deprotonation affecting the $H^+ + O_2 \leftrightarrow OH$ balance in the dispersion. These phenomena may be caused by

catalytic reactions, but also dissolution, transformation of molecular speciation and precipitation in the medium under investigation.

The dissolution or solubility of MNM is determined conventionally by sampling liquid samples and filtering out the residual particles by 3 kDa centrifugal filtration as defined in D2.9.

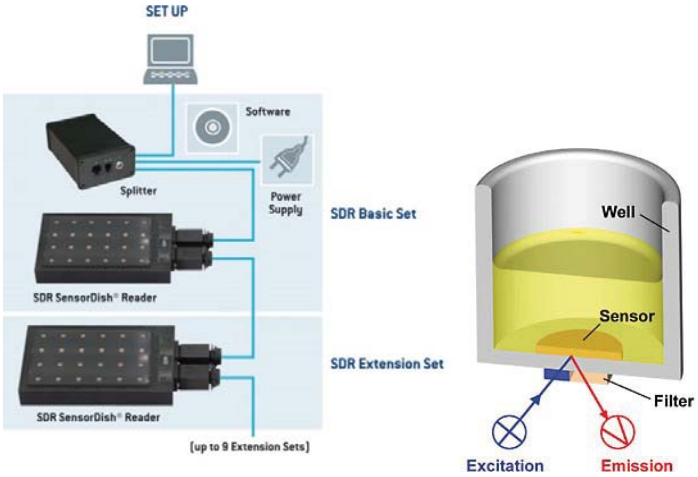

Figure 33: SDR Sensor Dish Reader and illustration of the SDR measurement principle. In this study we used the 24-well Oxy- and HydroDish for O_2 and pH monitoring, respectively. Source: PreSens Precision Sensing GmbH, Germany.

Experimental procedure

MNM batch dispersion were prepared following the NANOGENOTOX dispersion protocol and added to HAMs F12 cell exposure medium with 10% FBS matching in full the A549 epithelial cell incubation medium. In this test design, a fixed dose of 0.32 mg MNM/mL exposure medium was investigated with pure exposure medium as reference. The incubation lasted for 24 hours and samples for dissolution testing were collected at 0.25, 1, 2, 4, and 24 hours incubation during logging the pH and O_2 concentration every 5 minutes.

Each sample collected for dissolution testing was immediately filtered using the 3kDa centrifugal filter at 4,000 RCF for 30 min. After centrifugal filtering, the filtered medium was retrieved from each vial and added 0.5 ml 2% HNO_3 water to prevent precipitation and growth. The liquids were then stored in darkness until send for chemical analyses. The full protocol is found in NRCWE protocol for SDR.

Data treatment and evaluation

The reactivity of the individual MNM was evaluated from the evolution of the pH and O_2 over time and comparison with the blank medium controls. For plotting, the SDR pH-values were plotted directly as function of time as well as by the difference between the pH in exposure mediums and control medium considering the possibility for systematic off-set in some of the sensors. This sensor-evaluation was always done using the blank control as the assumed correct internal reference value. For the O_2 analyses, the difference between the time-resolved readings from the “exposure doses” and the control medium ($dO_2 = (O_{2,dose} - O_{2,medium\ control})$) was plotted as function of time.

In both cases, if the SDR readings from the dosed media only showed systematic offset from the reference media, the NM was assumed to have negligible pH reactivity or influence on the oxygen balance through redox reactivity or dissolution.

Results

Experimental studies for demonstration of the SDR method were completed using NM-200, NM-110, NM-111 and NM-300K. Results from the reactivity tests are plotted in Figure 34, Figure 35, Figure 36, and Figure 37. Results from the dissolution tests are plotted in Figure 38 to Figure 41.

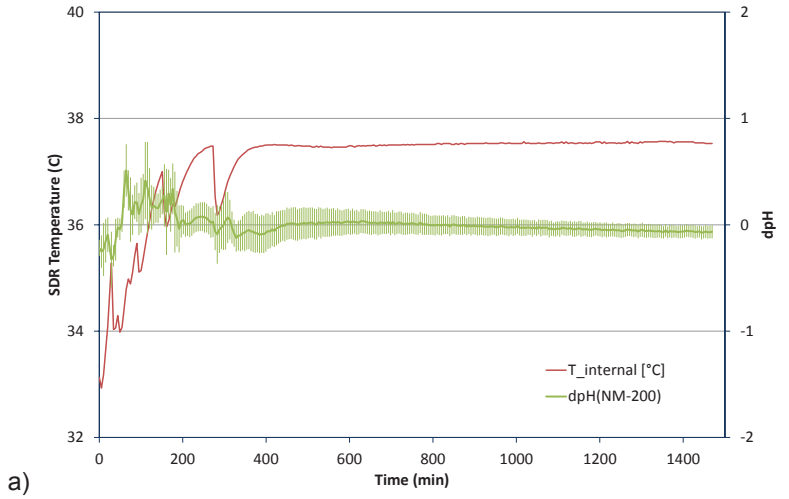

a)

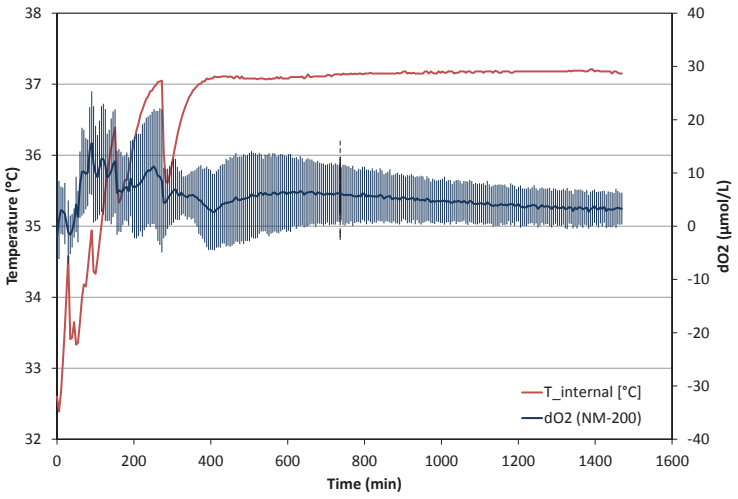

b)

Figure 34. a) dpH and b) dO_2 reactivity plots for NM-200 in HAMs F12 +10%FBS. A minor increase in both pH and O_2 is observed within the first 400 minutes of the test. The temperature fluctuations are due to sampling of mediums for dissolution studies. The temperature fluctuations are due to sampling of mediums for dissolution studies and to have some effect on the reactivity measurements.

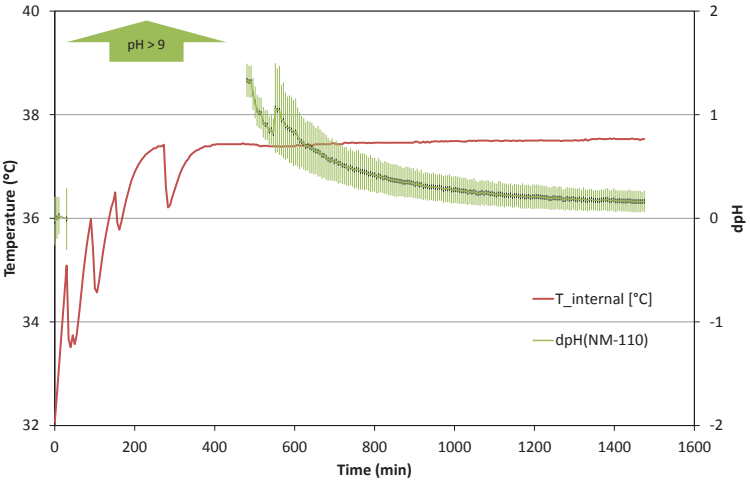

a)

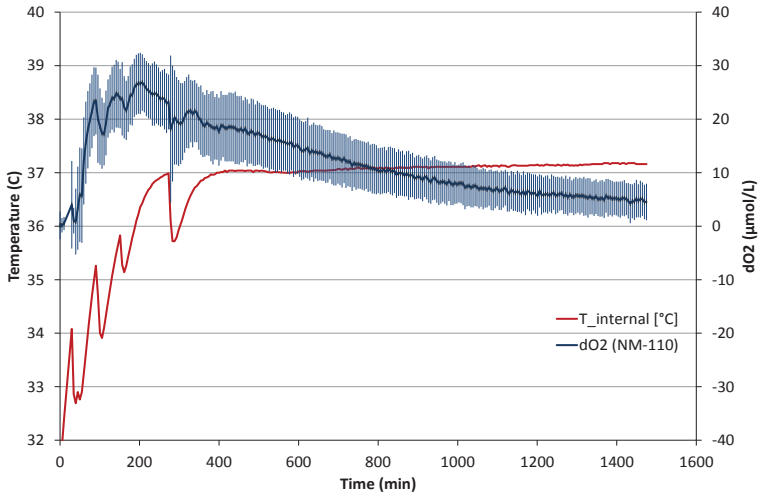

b)

Figure 35. a) dpH and b) dO_2 reactivity plots for NM-110 in HAMs F12 +10%FBS. A high increase in both pH and O_2 is observed at the start of the experiment and slowly diminishes during the entire experiment. The temperature fluctuations are due to sampling of mediums for dissolution studies. The temperature fluctuations are due to sampling of mediums for dissolution studies and appear to affect reactivity the measurements.

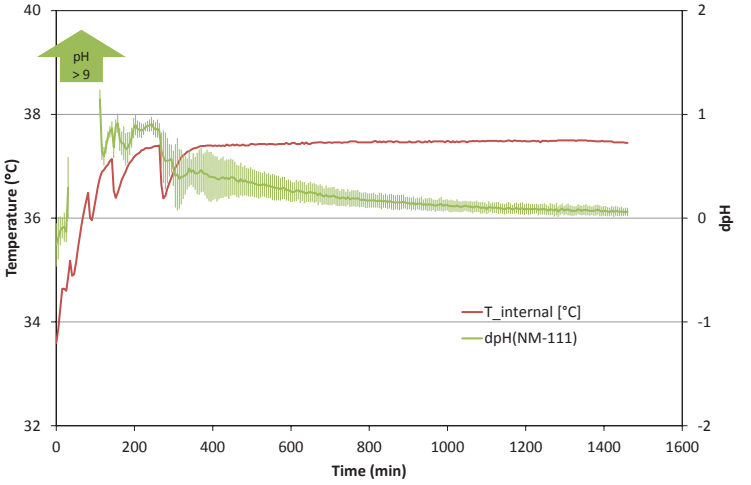

a)

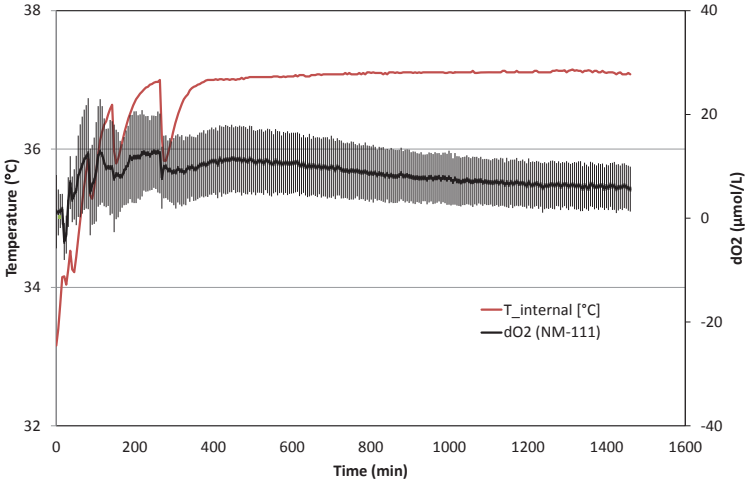

b)

Figure 36. a) dpH and b) dO_2 reactivity plots for NM-111 in HAMs F12 +10%FBS. An increase in both pH and O_2 is observed at immediate the start of the experiment and slowly diminishes during mainly the first 800 min of the entire experiment. The temperature fluctuations are due to sampling of mediums for dissolution studies and appear to affect reactivity the measurements.

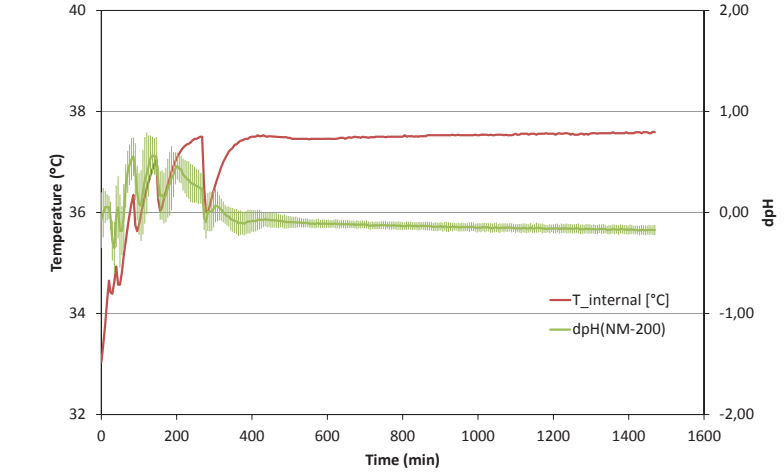

a)

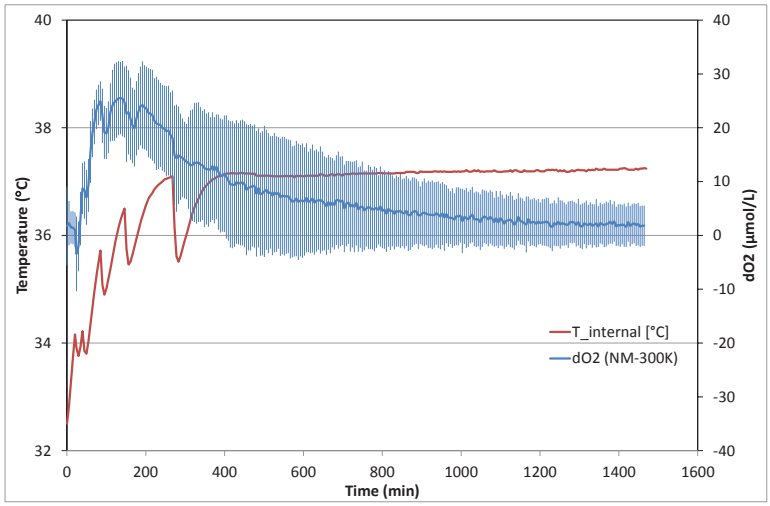

b)

Figure 37. a) dpH and b) dO_2 reactivity plots for NM-300K in HAMs F12 +10%FBS. A weak increase in pH and a greater increase in O_2 is observed at immediate the start of the experiment and slowly diminishes during mainly the first 400 (dpH) to 800 (dO_2) min of the entire experiment. The temperature fluctuations are due to sampling of mediums for dissolution studies and appear to affect the reactivity measurements.

The results of the SDR-reactivity measurements clearly demonstrates that the two ZnO materials NM-110 and NM-111 are highly pH reactive, but also have some influence on the O_2 concentrations in the medium. For NM-110, the measured pH-values exceed pH 9 until ca. 400 min into the test, while it is shorter for NM-111. The pH is not back to normal in experiments with both ZnO nanomaterials until between at least 800 min into the incubation period. pH is also affected during incubation with NM-200 and NM-300K, but to a much lesser extent. The dO_2 is not affected much by incubation with NM-200, indicating (as expected) low to negligible redox activity by the materials. The greatest effect on dO_2 is seen in the test with NM-110 and NM-300K. In NM-110, the effect may be linked to the high pH reactivity, whereas this is not the case for NM-300K.

The results from the SDR dissolution tests in HAMs F12+10%FBS are shown in Figure 38; Figure 39; Figure 40; and Figure 41. The plotted data include the total measured concentrations (*) as well as the concentrations subtracted medium control values (**), which indicate the total amount of MNM dissolved during sample

preparation and incubation. The initial dissolved elemental concentration in the test mediums was estimated from results of elemental analysis on HAMs F12+10%FBS and batch dispersions just sonicated following the NANOGENOTOX dispersion protocol. This value was used to calculate the amount of element dissolved from the test material during the experiment.

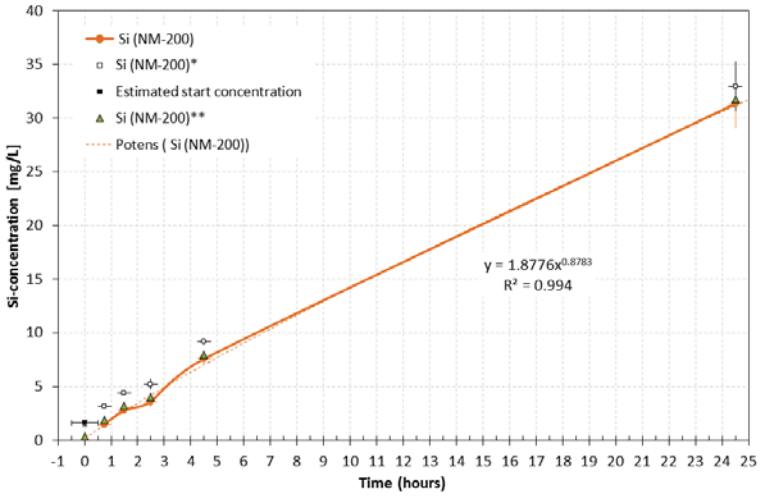

Figure 38. Concentration of Si dissolved during incubation [Si[NM-200]] compared to the measured [Si (NM-200)*] and calculated total Si dissolved from NM-200 [Si (NM-200)] in HAM's F12+10%FBS cell medium during dissolution and hydrochemical reactivity testing of NM-200 plotted as function of time. The data fit a sub-linear power function suggesting a slowly decreasing dissolution rate within the 24-hour incubation time. The sampling time-points are added 0.50±0.25 hour to include time and uncertainty for dosing, sampling and centrifugal centrifugation. The estimated start concentration is calculated from the measured Si-concentration in HAMs F12 + 10% FBS (1.2 g/mL) and the batch dispersion (0.41 mg/L).**

The results show that whereas the Si-concentration increases almost linearly as function of time in the test with NM-200, the Zn (for NM-110 and NM-111) and Ag (NM-300K) concentrations increase with high rate within the first hours of the incubation with NM-110, NM-111, and NM-300K and then slows of. This suggests that the NM-200 silica dissolves at an almost constant dissolution rate, while the dissolution rate varies with time for the two ZnO samples (NM-110 and NM-111) and the Ag sample (NM-300K). The variation in dissolution rate of the ZnO and Ag samples may in part be affected by the high increase in pH for NM-110 and NM-111 (Figure 35 and Figure 36) and NM-300K (Figure 37). For NM-300K, the variation in O_2 also suggests that phase transformations occur during this time-period.

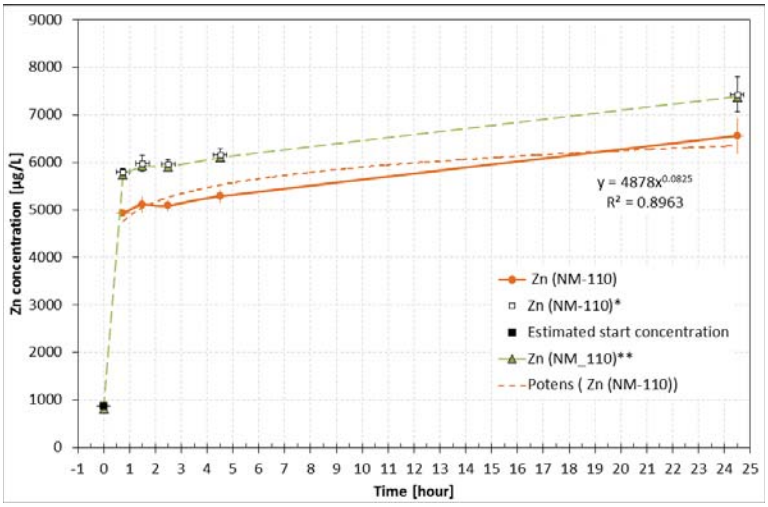

Figure 39. Temporal evolution in dissolved Zn [Zn (NM-110)] during incubation as compared to the measured [Zn (NM-110)*] and calculated total dissolved Zn [Zn (NM-110)] in HAM's F12+10%FBS cell medium during dissolution and hydrochemical reactivity testing of NM-110. The data show a slightly irregular evolution during time which can be partially fitted to a sub-linear power function. A very high initial dissolution rate appears to rapidly decreasing within the first four-hour incubation time followed by a slight increase in the Zn release rate between 4 and 24 hours incubation. The sampling time-points are added 0.50±0.25 hour to include time and uncertainty for dosing, sampling and centrifugal centrifugation. The estimated start concentration is calculated from the measured Zn-concentration in HAMs F12 + 10% FBS (49.6 µg/L) and the batch dispersion (904.3 µg/L).**

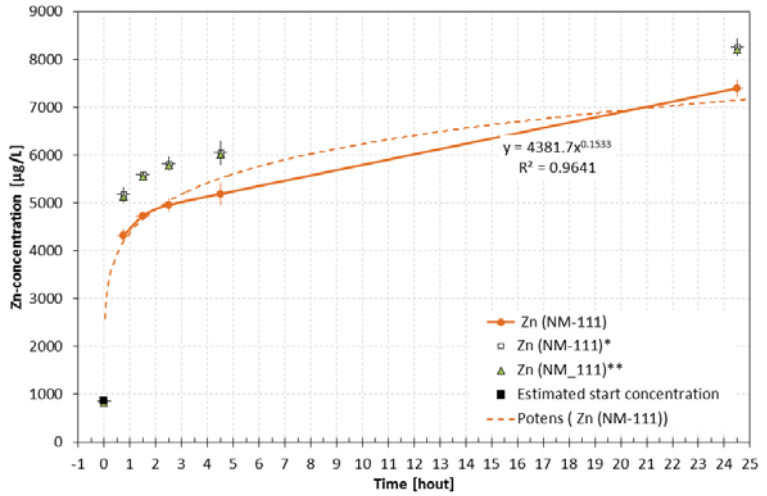

Figure 40. Temporal evolution of dissolved Zn [Zn (NM-111)] as compared to the measured [Zn (NM-111)*] and calculated total dissolved Zn from ZnO [Zn (NM-111)] in HAM's F12+10%FBS cell medium during dissolution and hydrochemical reactivity testing of NM-111. The data show a slightly irregular evolution during time which can be partially fitted to a sub-linear power function. A very high initial dissolution rate appears to rapidly decreasing within the first four-hour incubation time followed by a slight increase in the Zn release rate between 4 and 24 hours incubation. The sampling time-points are added 0.50±0.25 hour to include time and uncertainty for dosing, sampling and centrifugal centrifugation. The estimated start concentration is calculated from the measured Zn-concentration in HAMs F12 + 10% FBS (49.6 µg/L) and the batch dispersion (904.3 µg/L).**

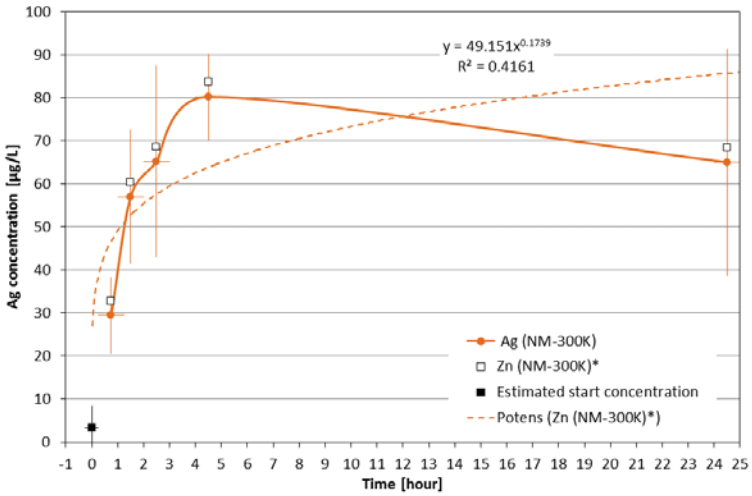

Figure 41. Temporal evolution in the dissolved Ag-concentration during incubation [Ag (NM-300K)] of NM-300K in HAM's F12+10%FBS cell medium as compared to the measured Ag-concentration [Ag (NM-300K)*] during dissolution and hydrochemical reactivity testing of NM-300K. The data show a slightly irregular evolution as function of time which can be partially fitted to a sub-linear power function. Dissolution appears to occur within the first four-hour incubation time followed by stagnation or potentially even re-precipitation of Ag between 4 and 24 hours incubation. The sampling time-points are added 0.50±0.25 hour to include time and uncertainty for dosing, sampling and centrifugal centrifugation. The estimated start concentration is calculated from the measured Ag-concentration in HAMs F12 + 10% FBS (3.4 µg/L).

NRCWE procedure for assessing the particle adsorption of BSA, LDH and interleukins during incubation with MNM in in vitro exposure mediums

Several studies have reported interaction between test materials and toxicological markers expressed during *in vitro* toxicological testing, which, if not understood, can lead to erroneous results and interpretations. Therefore, it is essential to understand to what extent such interactions may be expected in any *in vitro* test, so such interactions can be corrected for. It must also be considered whether the interaction between the specific toxicological markers such as serum protein, cytokines and lactate dehydrogenases (LDH) plays a mechanistic role.

In this part of the project, we developed a procedure to screen the ability of MNM to interact with the Lactate Dehydrogenases (LDH) and the pro-inflammatory cytokines IL-6 and IL-8, which are commonly measured in *in vitro* toxicological tests with human lung-epithelial cells, A549. Because, for the NANoREG *in vitro* studies, it was decided to use the NANOGENOTOX dispersion protocol with 0.05% bovine serum albumin we also quantify the amount of BSA adsorbed onto the MNM before toxicological testing.

Experimental procedure

For the BSA adsorption experiment, the MNM were dispersed following the NANOGENOTOX dispersion protocol and centrifuged at 20,000G (RCF) for 30 min after 30 min of storage. This represents the typical storage time of the batch dispersion before use. The dispersion medium supernatant is collected and analyzed using an ELISA-kit for quantification for the remaining BSA-concentrations.

For the LDH, IL-6, and IL-8 interaction tests, cell medium (here HAMs F12 + 10% Fetal Bovine Serum) is prepared following the exact protocol for the *in vitro* toxicity testing and doped with typical concentrations of LDH (target 100 ng/mL), IL-6 (target 500 pg/mL) and IL-8 (target 4000 pg/mL). It was found that the IL-8 target values were not always reached using the method applied in the study, because it was decided to not use a carrier protein for preparing the interleukin suspensions. This should be considered for potential revision in future experiments. The test materials are then incubated for 24-hours in a cell incubator (37°C; 5% CO2; 97%RH) following the exact procedure for the *in vitro* toxicological testing. Here we studied the doses, 0.01;

0.02; 0.04; 0.08; 0.16; 0.32; and 0.64 mg/mL. After incubation, the mediums are retrieved and centrifuged at 20,000G (RCF) for 30 min to settle the majority of suspended particles. The particle-free supernatant is retrieved for subsequent quantification by the use of standard LDH, IL-6 and IL-8 ELISA-kits.

Data treatment

The amount of adsorbed proteins and markers are given by the difference between the medium incubated with test materials and the reference medium without test material. A significant interaction is identified for tests where the adsorption values exceed the accumulated uncertainty measured in all the control mediums using the error propagation rule. For test materials where adsorption or interaction is identified, the data may be further used to fit adsorption functions as function and/or calculate the adsorption isotherms.

Results

Figure 42 shows the results from the analysis of the BSA adsorbed onto the NANoREG core MNM after preparation using the NANOGENOTOX batch dispersion protocol. It is evident that the BSA has highly different affinity towards the different MNM. Noteworthy, more than 50% of the added BSA is adsorbed onto NM-103, NM-203, NM-110, NM-111, NM-212, and NM-400 while no to very low amounts of BSA is adsorbed onto UPM Bleached Birch Pulp, UPM Biofibrils, NFC Fine, NM-300K, NM-204, and NM-100. This suggests that the BSA plays different roles for enabling particle dispersion in the different batch dispersions.

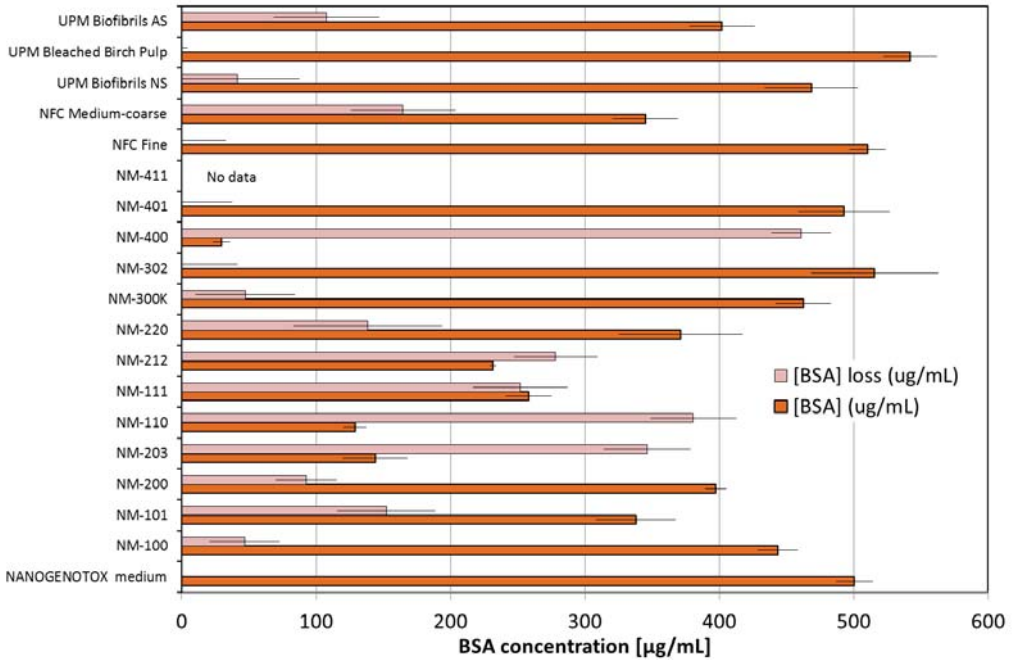

Figure 42. Concentration of BSA adsorbed onto the NANoREG core MNM compared to the relative percentage of BSA present in the NANOGENOTOX dispersion medium with 2.56 mg MNM/mL.

The results from the MNM interaction tests showed that there is a strong interaction between LDH and MNM: NM-110; NM-111; and NM-300K (Figure 43). A moderate effect on LDH was observed in the tests with NM-302 and NM-400. The steep curve for NM-110, NM-111, and NM-300K shows close to complete loss of the LDH in the doped cell test medium already at 0.02 mg MNM/mL. Consequently, the surface concentration and adsorption isotherms needs to be calculated based on low doses.

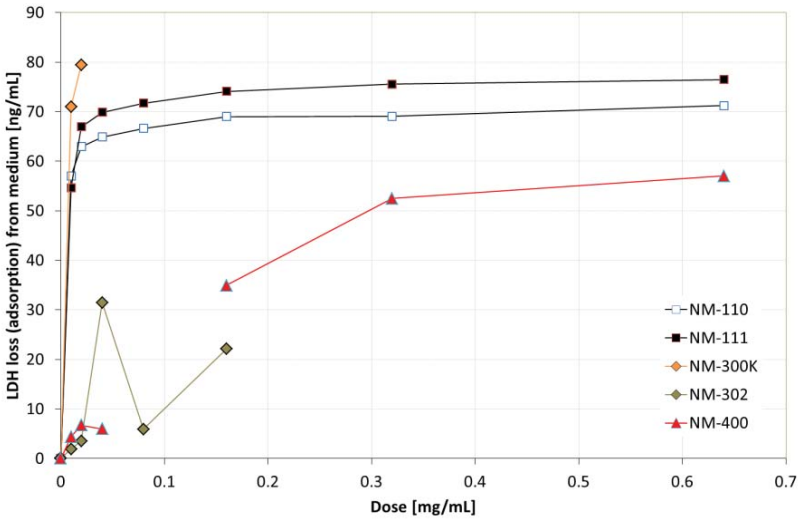

Figure 43. Loss in LDH-concentration from HAMs F12+10%FBS cell medium after 24-hours incubation in a cell incubator plotted as function of MNM dose. All NANoREG core MNM were tested and data are only plotted for experiments where the LDH concentration difference exceed the standard deviation of the controls. The LDH loss is assumed to be due to adsorption onto the MNM test materials.

The loss of IL-6 and IL-8 during incubation in the cell medium is shown in Figure 44 and Figure 45, respectively. The highest level of IL-6 adsorption was observed in the test with NM-411 (ca. 650 pg/mg). Intermediate IL-6 adsorption is observed for NM-101; NM-200; and NM-203 (ca. 260 to 320 pg/mg) while low levels of IL-6 adsorption was observed NM-300K (ca. 115 pg/mg). Noteworthy, IL-8 was also very efficiently adsorbed onto NM-411 (ca. 18,000 pg/mg), where IL-8 also showed high affinity towards NM-101 (ca. 16,600 pg/mg). Moderate IL-8 adsorption was observed in the tests with NM-200; NM-203 and NM-400 (on the order 1766 – 2576 pg/mg). NM-100 showed only limited levels of adsorption (ca. 450 pg/mg). The rest of the NANoREG core MNM showed no to negligible interleukin adsorption in the tested dose range.

Table 25 shows a summary of all the adsorption experiments where the results are given in the relative fraction of BSA adsorbed and the dose-percentage adsorption slope for LDH, IL-6 and IL-8. The results suggest that there is not an immediate systematic common interaction behavior of the BSA, LDH and interleukins studies. Whereas the TiO_2 (NM-100 and NM-101) and silica samples (NM-200 and NM-201) appears to attract BSA and both interleukins (not NM-100), the ZnO samples (NM-110 and NM-111) attracts BSA and LDH. The silver and CNT samples have variable behavior depending on the specific MNM. NM-400 adsorbs almost all the BSA - and some of the LDH and IL-8 contents. NM-411 adsorbs both interleukins (the interaction with BSA is not known at this point in time). Most cellulose samples as well as NM-212 and NM-220 only adsorbs BSA. NM-401, NFC Fine and UPM Beached Birch Pulp do not interact with any of the molecules tested.

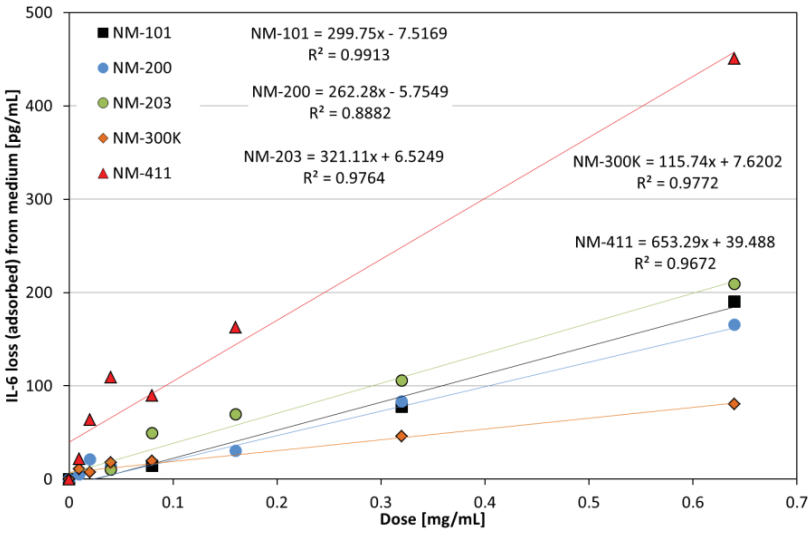

Figure 44. Loss in IL-6-concentration from HAMs F12+10%FBS cell medium after 24-hours incubation in a cell incubator plotted as function of MNM dose. All NANoREG core MNM were tested and data are only plotted for experiments where the IL-6 concentration difference exceed the standard deviation of the controls. The IL-6 loss is assumed to be due to adsorption onto the MNM test materials.

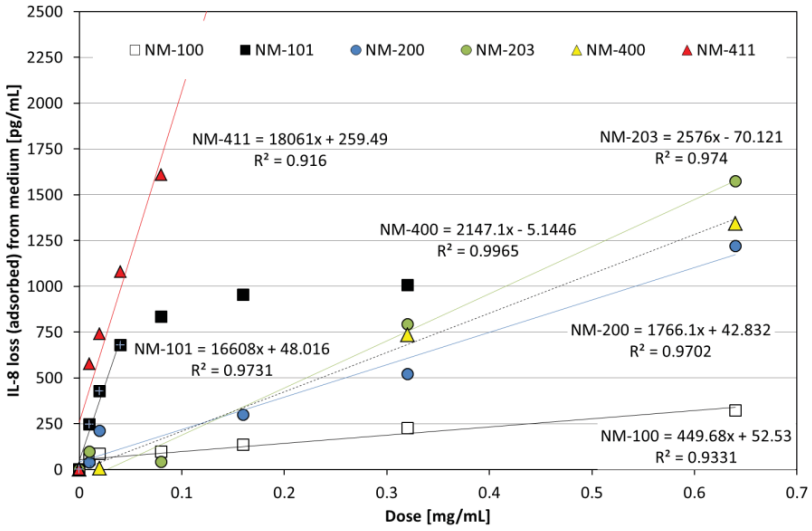

Figure 45. Loss in IL-8-concentration from HAMs F12+10%FBS cell medium after 24-hours incubation in a cell incubator plotted as function of MNM dose. All NANoREG core MNM were tested and data are only plotted for experiments where the IL-8 concentration difference exceed the standard deviation of the controls. For NM-101, the regression curve is only calculated in the linear range in the first four doses only, before the medium starts to be depleted. The IL-8 loss is assumed to be due to adsorption onto the MNM test materials.

Table 25. Colour-coded relative scale for the fraction of BSA adsorbed and the percentage doses-adsorption slope for LDH, IL-6 and IL-8. Green indicates lowest values (minimum) and red highest values (maximum). For samples were the LDH, IL-6 or IL-8 is depleted the slopes were calculated based on the data that show linear dose-response behaviour.

Test Material	fBSA	αLDH	αIL-6	αIL-8
NM-100	0.09	0.00	0.00	0.04
NM-101	0.30	0.00	0.06	0.74
NM-200	0.19	0.00	0.05	0.08
NM-203	0.69	0.00	0.06	0.12
NM-110	0.76	0.24	0.00	0.00
NM-111	0.50	0.44	0.00	0.00
NM-212	0.56	0.00	0.00	0.00
NM-220	0.28	0.00	0.00	0.00
NM-300K	0.09	0.85	0.03	0.00
NM-302	0.00	0.09	0.00	0.00
NM-400	0.92	0.16	0.00	0.11
NM-401	0.00	0.00	0.00	0.00
NM-411	N/A	0.00	0.13	0.75
NFC Fine	0.00	0.00	0.00	0.00
NFC Medium-coarse	0.33	0.00	0.00	0.00
UPM Biofibrils NS	0.08	0.00	0.00	0.00
UPM Bleached Birch Pulp	0.00	0.00	0.00	0.00
UPM Biofibrils AS	0.22	0.00	0.00	0.00

Conclusions

For the BSA adsorption experiment, the MNM were dispersed following the NANOGENOTOX dispersion protocol and centrifuged at 20,000G (RCF) for 30 min after 30 min of storage. This

The conclusion from this interaction study demonstrates and confirms previous studies that great care should be taken in controlling for artefacts when performing colorimetric measurements of the inflammatory potential and cytotoxicity markers of particulate and fibrous materials.

It is likely essential to perform the interaction tests following the exact recipes and procedures followed in each laboratory. In this the case, the batch dispersion is prepared following the NANOGENOTOX dispersion protocol with 0.05% (v/v) BSA and added to HAMs F12+10%FBS. If no of lower concentrations of albumin and/or serum is used, this could affect the adsorption efficiency of the test materials.

NRCWE method for Atmosphere-Temperature-pH-controlled Stirred Batch Reactor procedure for determination of hydrochemical reactivity and dissolution of MNM in phagolysomal cell fluids

In addition to improving information on the reactivity and dissolution of MNM in the cell medium, it is also important to assess the reactivity and dissolution in specific organs and intracellular compartments. The phagolysosome with its low pH (ca. 4.5) is of interest from the perspective of both *in vitro* and *In vitro* toxicological testing. In contrast to testing under the *in vitro* conditions with temporal evolution in temperature, pH and O_2-concentrations in the medium, intracellular systems are considered to provide stronger buffering capacity and maintenance of the overall fixed conditions. Consequently, to simulate the intracellular conditions, it is important to try and keep the pH and temperature, as well as the atmospheric, conditions realistic and constant.

Experimental procedure

In this example, dissolution tests are conducted at 0.25 mg/mL. 25 mg test material is added add 100 mL stirred synthetic phagolysomal fluid (PSF) after dispersion using the conditions of the NANOGENOTOX dispersion protocol. The batch reactor test conditions are maintained at 37.4°C and the atmosphere is kept by constant bubbling with filtered air added $CO_{2,g}$. The PSF medium pH is kept at ca. pH 4.5 using a titrator mounted with a suitable acid (HCl) or base (NaOH). The volume of added titrant is recorded together with the pH, temperature, and redox potential (Eh). Especially the redox potential is used to assess whether the test material has an intrinsic capacity to cause reductive or oxidative stress. Liquid samples are collected at different time-points (0 (set to 0.001), 1, 2, 4, 24, and 48 hours incubation) for elemental analysis after centrifugal filtration through a 3KDa centrifuge filter by ICP-MS or another suitable techniques such as WD-XRF.

Data treatment

The caustic and oxidative-reductive behavior of the MNM is assessed by the temporal evolution in the pH and titration volume as well as the redox potential of the MNM-doped PSF suspension as compared to the evolution and a pure PSF reference liquid tested under the same conditions.

Results

The results from the direct reactivity monitoring data are plotted in Figure 46 while the temporal evolution in the elemental concentrations of Zn and Ag during incubation in the PSF medium can be seen in Figure 47. The reactivity monitoring data shows that both NM-110 and NM-300K are reactive and cause some changes in pH and Eh as compared to that of the PSF reference medium.

NM-110 causes an increase in pH and Eh immediately after dosing the ZnO MNM into the PSF medium. The pH increase is immediately controlled by titration of mL 1M HCl. The dissolution of NM-110 appears to be very rapid as high concentrations are reached immediately after addition into the PSF. The concentration, however, appears to continue to increase slightly between 24 and 48 hours into the test and reach more than 1000 times the concentration in the PSF reference medium (Table 26). Compared to the added Zn concentration (200.78 mg/L = (M_{Zn}/M_{ZnO}) x (0.25mg/mL x 1000 mL), it is evident that practically all added ZnO appears to be dissolved within 1 hour in PSF.

NM-300K causes a different evolution pattern than NM-110. The Eh decreases as an immediate response to the addition of the dispersed silver nanoparticle suspension whereas the pH appears to be constant. The Eh reduction continues during the entire experiment with NM-300K without any change to pH. However, the acid-base effect considered from the titration volume is very high as ca. 15 mL titrant was required to keep the pH at 4.5. Considering 250 mg/L Ag is added to PSF, only ca. 0.06 wt.% of the added Ag is dissolved after 48 hours. It is likely that the Cl in the PSF is a rate-limiting factor converting Ag to AgCl, but this needs to be further assessed from electron microscopy and thermodynamic modelling.

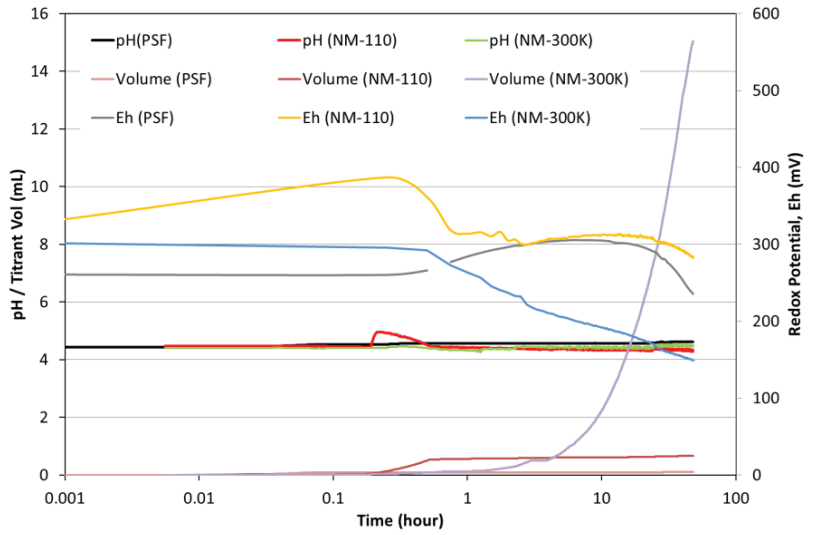

Figure 46. Temporal evolution in pH and Eh coupled with measured titrant volume in tests with NM-110 and NM-300K and the reference medium PSF. Addition of NM-110 causes immediate increase in Eh and pH and counterbalancing titration, which suggests an acute strong reaction. Addition of NM-300K results in a long-term addition of titrant with reduction in Eh and no increase in pH, which suggests a long-term slow reaction.

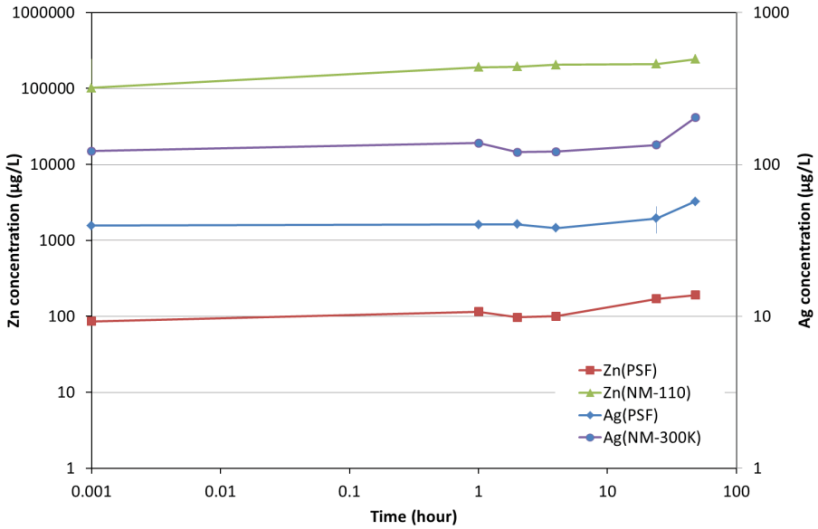

Figure 47. Temporal evolution of Zn and Ag concentrations in PSF kept at pH and Eh conditions plotted above. All concentrations are almost constant in the measured samples suggesting very rapid dissolution of most of the soluble fraction in both NM-110 and NM-300K. However, a clear increase is also observed from 24 hours to 48 hours, where the blind-control background concentration also increases slightly for both Zn and Ag.

Table 26. Elemental concentrations measured at different time-points during dissolution of NM-110 and NM-300K in PSF (n = 2)

Time	Zn (PSF) [µg/L]	sd	Ag (PSF) [µg/L]	sd	Zn (NM-110) [mg/L]	Sd	Ag (NM-300K) [µg/L]	sd
0.001*	86.1	2.7	39.6	2.7	101.7	143.8	122.1	0.9
1	114.9	2.6	40.1	1.7	190.9	-	138.2	18.7
2	96.8	0.9	40.4	0.9	193.0	-	120.3	3.5
4	100.2	0.9	38.1	2.7	205.5	0.0	121.4	2.6

24	170.0	8.9	44.1	1.8	210.7	4.5	134.5	21.1
48	189.9	-	57.0	1.8	243.4	-	203.4	-

**Defined time for immediate sampling after dosing and mixing into PSF*

Conclusions from the SBR test

The results demonstrate that the SBR method is a suitable method to potentially identify MNM with no, low and high hydrochemical reactivity and solubility as function of time. It is possible to quantify the MNM reactivity based on the data obtained, but further experimentation may be needed at different doses to better assess the pH and redox reactivities as well as the dissolution rates. The strategy with the currently tested dose was to have a relatively high medium-to-material ratio, which allows "maximum" dissolution, and also mimic the doses that could occur in a phagolysosome.

IIT procedure and relative protocol for characterization of MNM size and aggregation by DLS in synthetic human body fluids (simulating the human digestive compartments).

DLS analysis in artificial human digestive juices (saliva, stomach and intestine/bile)

Two values of starting MNM concentration were considered for this test: 45 µg/mL and 950 µg/mL. "Nominal size" refers to value of MNM radius reported in the technical datasheet samples. "Ctrl" refers to MNM size after the application of the Nanogenotox dispersion protocol. Treated samples are MNM size when they are immersed in synthetic human digestion compartments at temporal points simulating digestion according to Walczak et al, 2013.

The size plots indicate that while all MNM in the saliva fluid maintained similar size profile with respect to the Ctrl, a progressive aggregation occurred in the stomach and intestine compartments (Figure 48). NM-110 showed a particular behaviour possibly due to its tendency to precipitate and aggregate already after the application of the dispersion protocol. These results are confirmed by TEM analyses (see below). Furthermore, MNM were subjected to dissolution (see data reported in Chapter 5.3 also) in these matrices.

In general, as these are very complex matrices, DLS data interpretation may result challenging so that we recommend the application of more than one complementary technique to follow the MNM dissolution in the human *in vitro* digestive matrices (e.g., DLS, TEM and ICP or others).

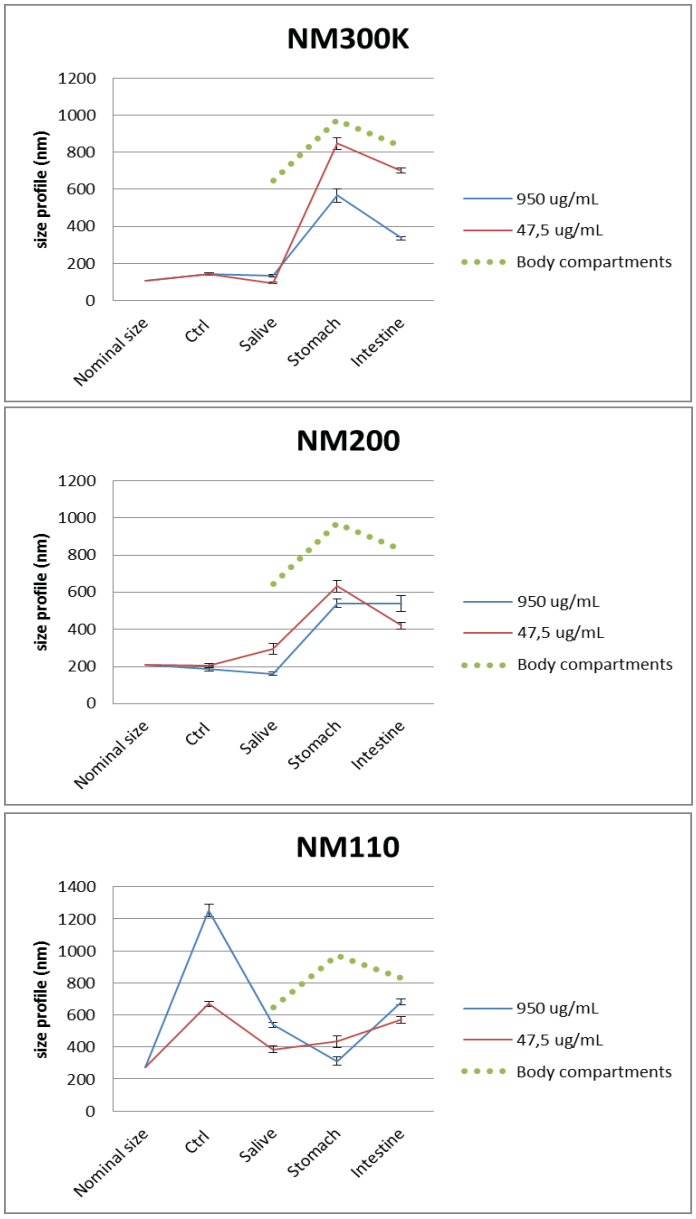

Figure 48. MNM size profile in the human digestive juices. The plots report the size trend of DLS Peak 1 possibly related to primary MNM (deviation standard bars are relative to 10 runs). Body compartments are the size signals detected for inorganic/organic/protein components of the *in vitro* human digestive compartments.

IIT procedure and relative protocol for characterization of MNM size and aggregation by TEM in synthetic human body fluids (simulating the human digestive compartments).

The TEM characterization of MNM from repository list in artificial human digestive juices (saliva, stomach and intestine/bile) is illustrated in Figure 49.

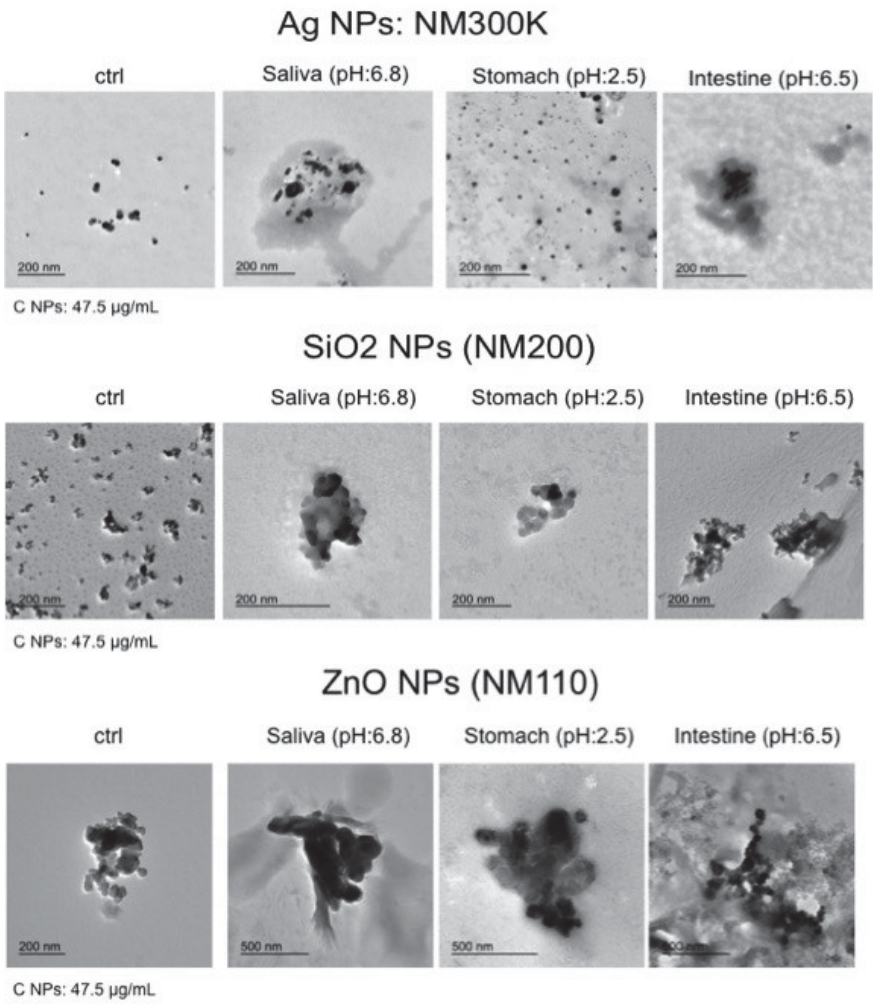

Figure 49. TEM images of MNM in synthetic human digestive juices: Images show MNM dissolution in the stomach and a partial re-aggregation in the intestine-bile compartments for NM-300K. For the NM-200 and NM-110 MNM, it was possible observing only aggregation by this technique.

IIT procedure for characterization of MNM dissolution by UF-ICP-AES in synthetic human body fluids (simulating the human digestive compartments)

Summary of work

The studies comprise a set of experiments addressing methods to qualitatively and quantitatively measure the biological hydro-chemical reactivity of NM in both *in vitro* cell culture media and synthetic body fluids (which simulate the human compartments). IIT focused on NM dissolution using DMEM, RPMI, artificial saliva, and gastro-intestinal-bile juices. Preliminary studies have been performed using NM-300k, NM-110, and NM-200 from repository list. Dissolution was quantified by using UF/ICP-AES. The phenomenon was also qualitatively described by DLS and TEM measurements. We found that all MNM dissolve with different dissolution rates (with preferential dissolution in gastro-intestinal compartments).

UF/ICP-AES using an in vitro dynamic human digestive process (Sub-task 2,4i)

Overview of main results

- NM-300k dissolves prevalently in the stomach compartment. Ionic strengths of stomach acidic pH seem to be the trigger factors to initiate the dissolution (Figure 50). Ionic strength/neutral pH induces poor dissolution in saliva and intestine; aggregation phenomena occur.

- NM-200 dissolves mainly in neutral body compartments at increasing dissolution rates as MNM concentration increases (Figure 51). The acidic pH seems to be not the trigger factor to initiate the dissolution. Indeed, dissolution not only occurs in saliva and intestinal/bile compartments, but also in *in vitro* biological media as DMEM and RPMI, at neutral conditions (see data for biological media).

- NM-110 dissolves in all the body compartments but with a highest rate in the GI compartments (Figure 52). Dissolution is low in saliva and undetectable (with the employed technique) in DMEM and RPMI at neutral conditions at comparable concentration (see data for biological media).

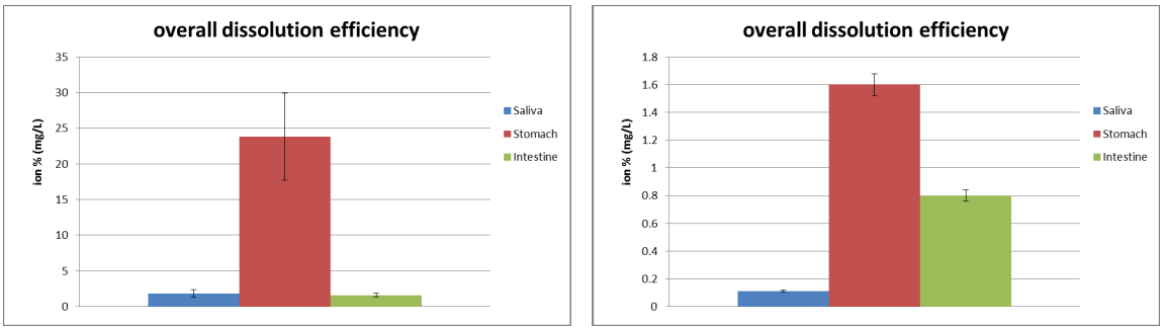

Figure 50. Histograms reporting the dissolution efficiency (mg/mL) of NM-300k at two concentration values into the human body compartments simulating the oral exposure of NMs. Note: results are affected by down-estimation due to the partial filter clogging.

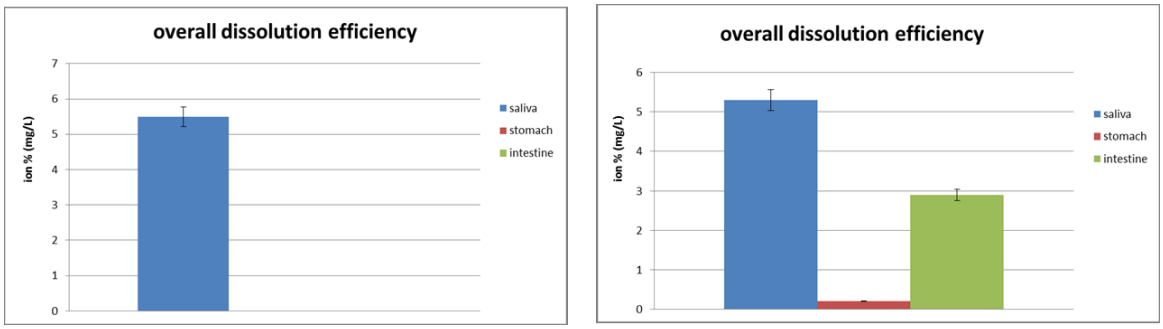

Figure 51. Histograms reporting the dissolution rate (mg/mL) of NM-200 at two concentration values into the human body compartments simulating the oral exposure of NMs. Note: results are affected by down-estimation due to the partial filter clogging.

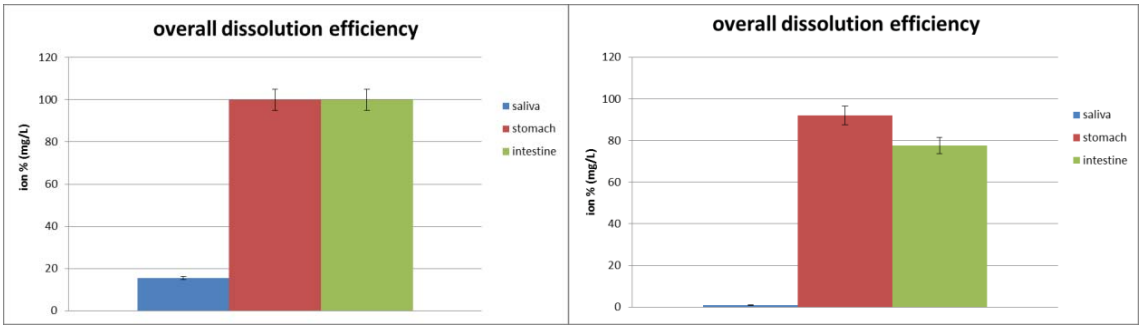

Figure 52. Histograms reporting the dissolution rate (mg/mL) of NM-110 at two concentration values into the human body compartments simulating the oral exposure of NMs. Note: results are affected by down-estimation due to the partial filter clogging.

Procedure and relative protocol for characterization of MNM dissolution by UV-Vis in synthetic human body fluids (simulating the human digestive compartments) NM-300K.

Summary of work

Dissolution of MNM was further monitored by using UV-Vis. Preliminary studies have been performed using NM-300K from repository list. The process has been compared with dissolution monitored by UF-ICP, DLS and TEM measurements finding that Ag MNM prevalently dissolve in the stomach compartment as revealed by the absence of the plasmonic peak at 412 nm, which is typical of Ag MNM. These data indicate that the dissolution of NM-300K is not absent in the saliva but it is minimal while it is almost total in the stomach and that UF/ICP data may down estimate such process.

UV-Vis analysis in the intestine compartment is affected by the presence of bile salts, which in turn present a strong absorption in the spectral range of 400-430 nm overlapping with the MNM plasmonic peak thus masking the spectrum and hampering the outcome of the experiment at the intestinal level. The study also highlights that in the stomach many processes occur during the digestion such as dissolution, agglomeration, AgCl salt formations and protein corona formation (in line with literature data).

UV-Vis spectra of NM-300K in water (Figure 53). The spectra are recorded using solutions of MNM in water (As it is) or to re-suspensions of MNM pellet after ultracentrifugation (using Amicon Ultra 3k). Pellets are re-suspended to obtain the same MNM concentration used for the digestive test (details in experimental). Volumes reported are 7, 19 and 39 ml that refer to the dilutions that MNM undergo in each digestive compartment in a dynamic process. Figure indicates that MNM present the typical plasmonic peak of silver MNM at 412 nm both in solutions of MNM immediately suspended in water (As it is) and after the ultracentrifugation procedures (pellets). Pellets indicate that MNM are retained due to their size, the reduction of intensity spectra indicates that there is a partial (and constant) MNM retention by filter membranes (this effect must be taken into account in quantitative measurements). Peak in the red region of the spectra also indicates a partial aggregation of these MNM already in water.

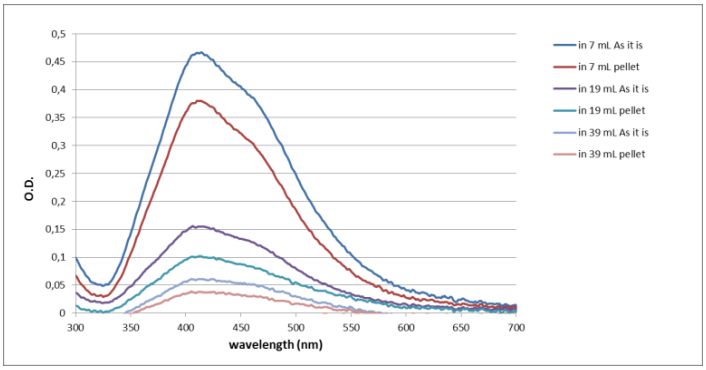

Figure 53. UV-Vis spectra of NM300K in water.

The spectra taken when MNM are immersed in saliva indicate that a mixture of primary MNM (plasmonic peak at 412 nm) and partially aggregated MNM (additional peaks in the visible region) occurs when MNMs interact with saliva (Figure 54). Apart this MNM partial aggregation, no loss of plasmonic peak is evidenced at both t0 and after 5 minutes of incubation (which is indicative of the mastication time, according to Versantvoort et al, 2005, Food Chem Toxicol 43:31–40).

By these data, we conclude that saliva did not particularly affect MNM dissolution (in line with UFICP-AES data also showing low dissolution) but did induce aggregation (as also evidenced by the pictures reported and DLS spectra).

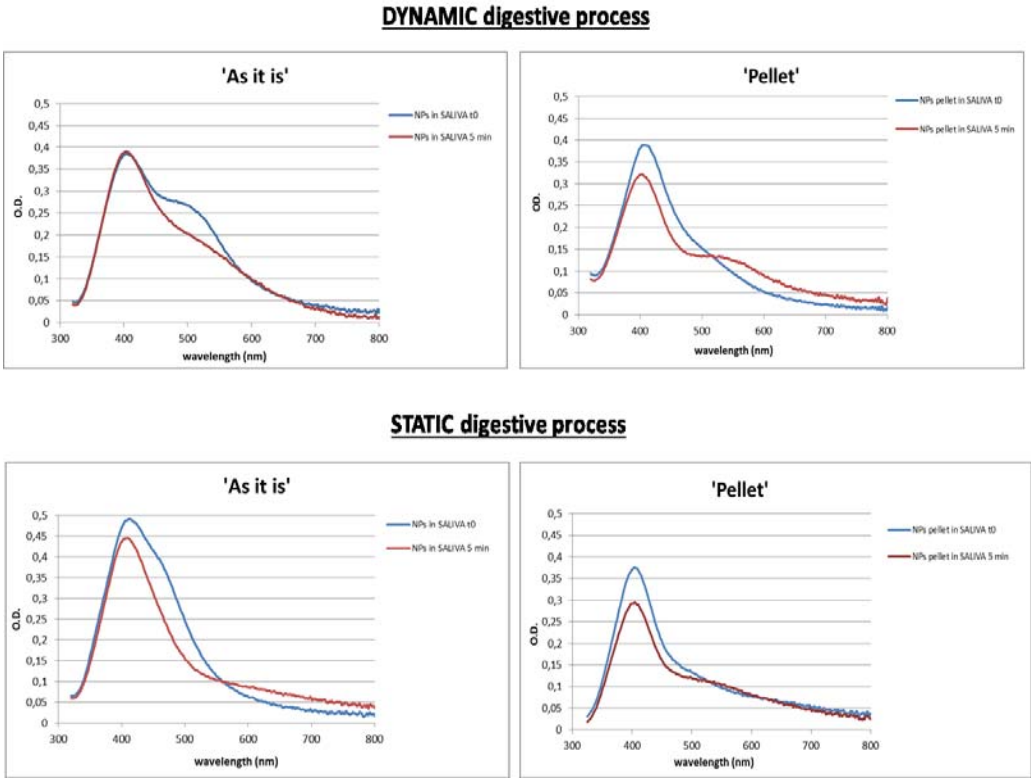

Figure 54. UV-Vis spectra of NM-300K in saliva compartment.

DLS spectra at t0 and after 5 minutes of incubation indicate the presence of a peak at about 130 nm possibly arising from primary MNM and larger aggregates (Figure 55). Pictures are Vial 1 Stock solution of MNM; Vial 2 MNM in low % of BSA at the same MNM concentration in saliva (to compare with Vials 4 and 5), Vial 3 Saliva

juice, Vial 4 MNMs in saliva at time 0, Vial 5 MNMs in saliva at time 5 minutes. Overall, results indicate that saliva did induce aggregation phenomena that did not alter the plasmonic peak of Ag MNM although a visible colour change of the solutions occur. Aggregation is monitored also by TEM (data reported above). No Low dissolution occurs as also revealed by UF-ICPAES data.

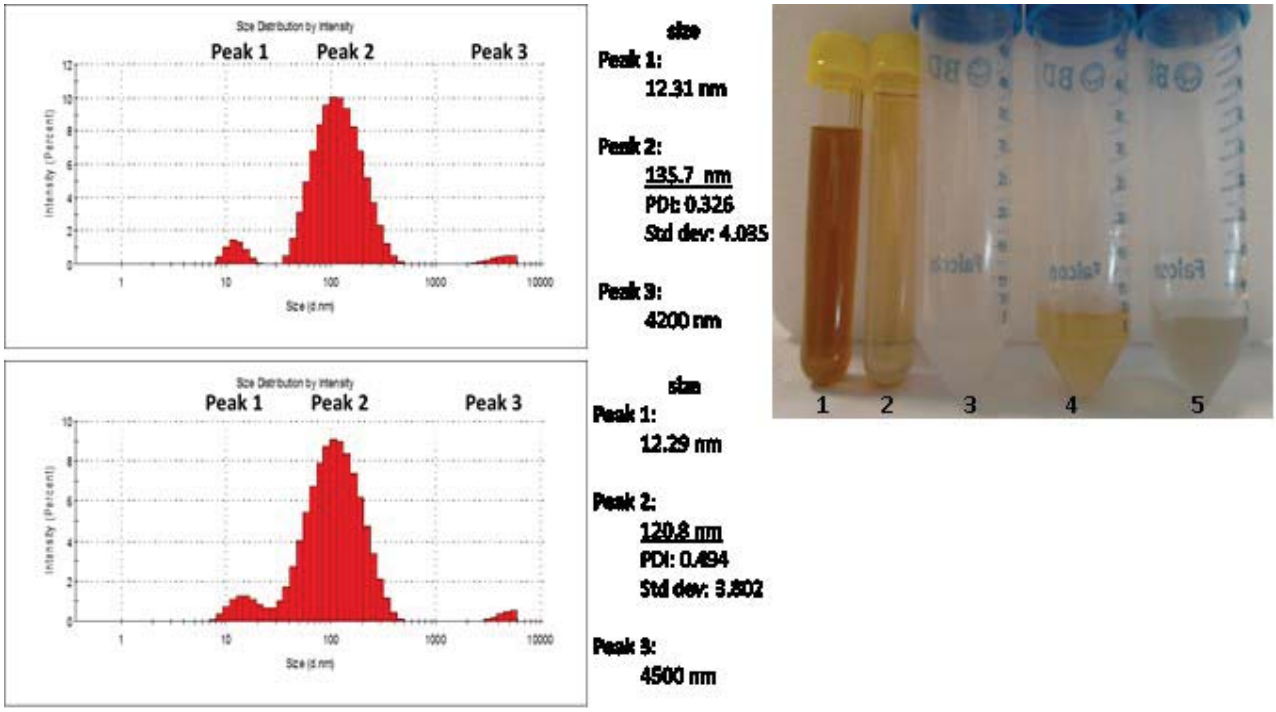

Figure 55. Characterization of NM-300K in saliva.

The spectra have been recorded during the digestive process test performed in two modalities: dynamic (that consider the real continuous process in which saliva-incubated MNM are incubated with stomach juice solution for 2 hours) and static (in which MNM have been directly added to solutions of stomach juice) (Figure 56).

The spectra taken when MNM pass from saliva to the stomach indicate the complete loss of the plasmonic peak both when MNM are in the solution “As it is” and upon ultracentrifugation after 2 hours of incubation (the pellet do not contain MNM showing a plasmonic signal as contrarily happens in the corresponding control: pellet of MNM from water at comparable values of concentration, see images of MNM control in water above).

Stomach induced the loss of primary MNM plasmonic signal with a concomitant strong MNM aggregation as also evidenced by the corresponding vial pictures and DLS spectra. This loss corresponds also to an increase of MNM dissolution as revealed by UF-ICPAES data. They show a MNM dissolution corresponding to the presence of about the 25% of free ions. This data might be down estimated (due to possible filter clogging or ion/MNM adsorption on filters). Also TEM images show MNM of smallest size. These data are in line with recent literature findings (Walczak et al, 2013, Nanotoxicology, 7(7):1198–1210).

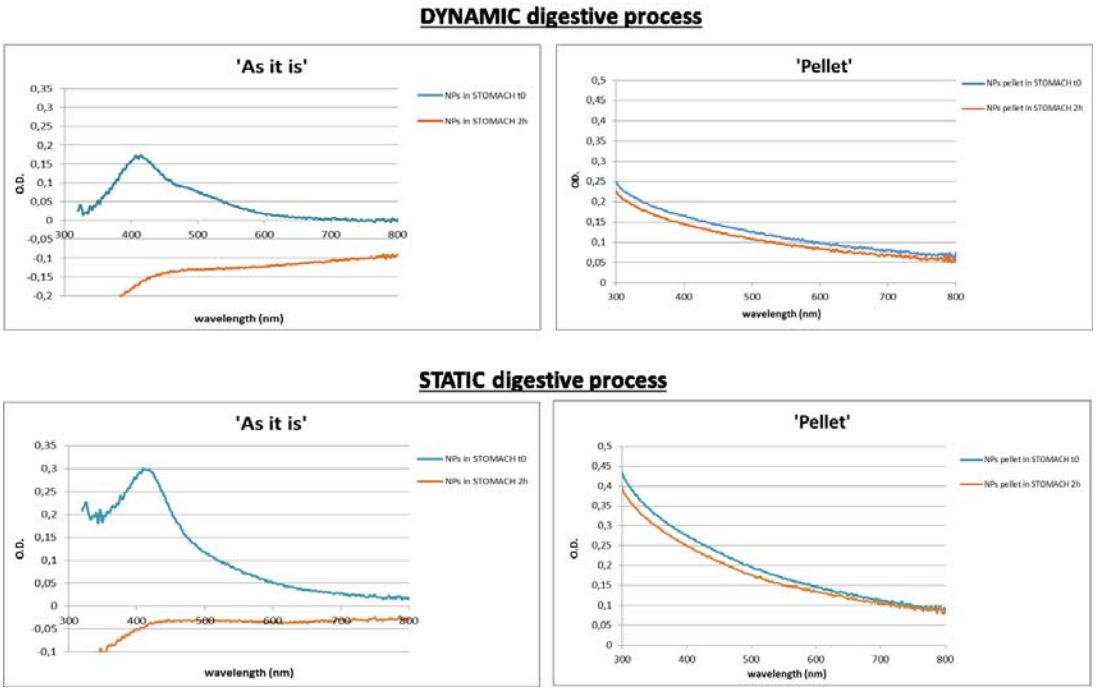

Figure 56. UV-Vis spectra of NM-300K in stomach compartment.

Characterization of NM-300K in stomach (Figure 57): DLS spectra at t0 and after 2 hours of incubation indicate the presence of large aggregates peaking at about 700 nm. Pictures are Vial 1 Stock solution of MNM; Vial 2 MNM in low % of BSA at the same MNM concentration in stomach (to compare with Vials 4 and 5), Vial 3 Stomach juice, Vial 4 MNM in stomach at time 0, Vial 5 MNM in stomach at time 2 hours. Overall, results indicate that stomach induced aggregation phenomena and the loss of the plasmonic peak of Ag MNM. A visible colour change of the solutions occurs. This also supports that dissolution mainly occurs in the stomach as revealed by UF-ICPAES data (see above).

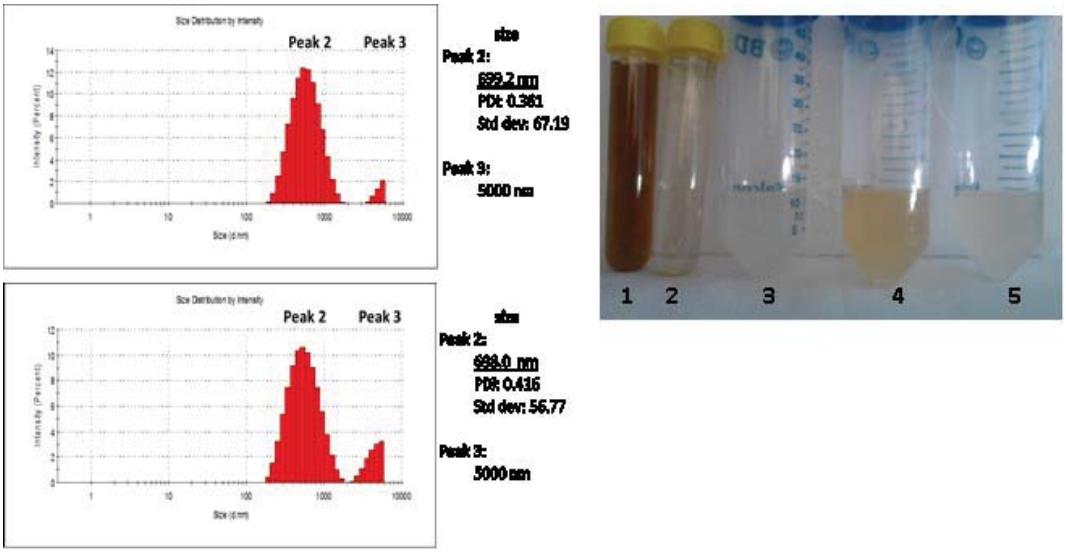

Figure 57. Characterization of NM-300K in stomach

UV-Vis spectra of NM-300K in intestine compartment (Figure 58). Also for intestine, the UV-vis spectra have been recorded in the two modalities: dynamic (MNM incubated into saliva for 5 minutes, then with stomach

solution for 2 hours and finally mixed to intestine juice for other 2 hours) and static (in which MNM have been added directly to intestine solution for 2 hours).

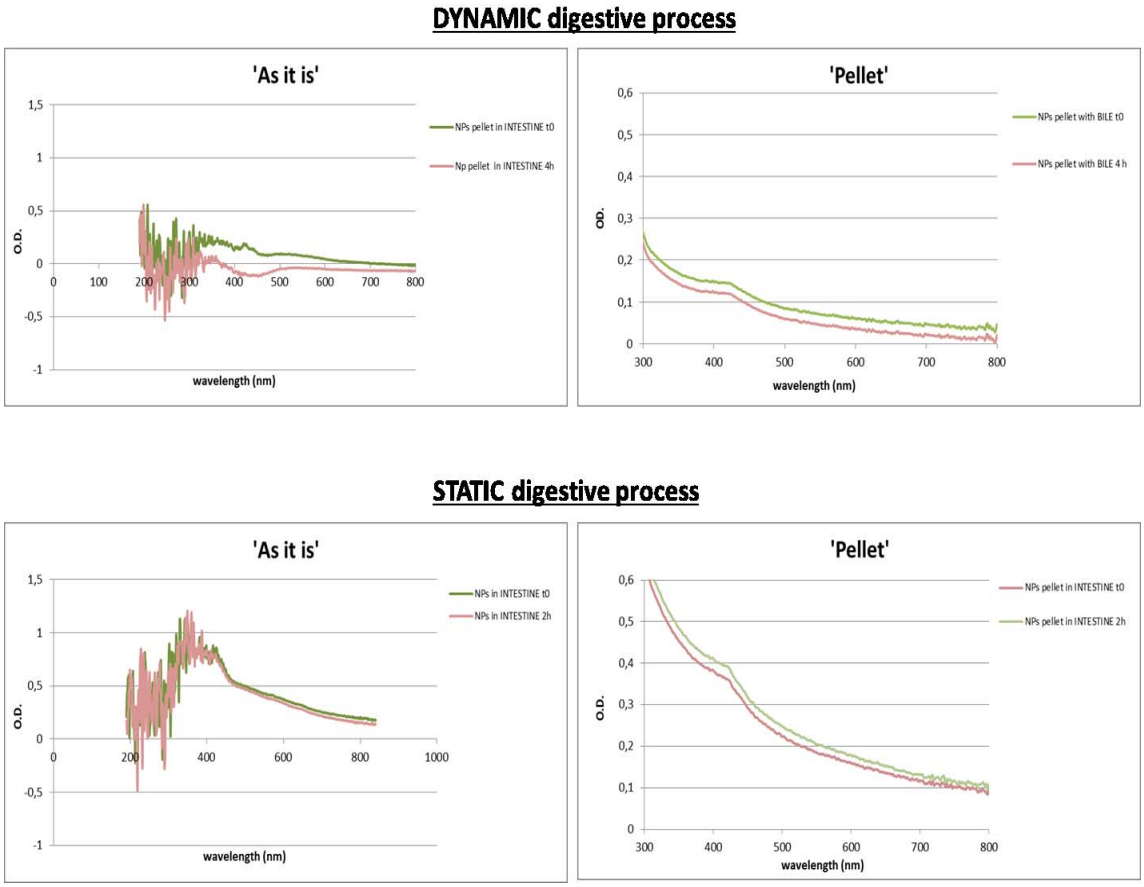

Figure 58. UV-Vis spectra of NM-300K in intestine compartment

UV-Vis analysis in the intestine compartment shows that the MNM plasmonic pick of 412 nm is affected by the presence of bile salts, which in turn present a strong absorption in the spectral range of 400-430 nm, in particular on 422 nm

Characterization of NM-300K in intestine. As observed in stomach, intestine DLS spectra at t0 and after 2 hours of incubation indicate the presence of aggregates peaking around 700 nm (spectra not shown). The presence of bile salts, in the intestine juice, do not permit to appreciate the colour change of solution (due to the presence of MNM), instead revealed both in Saliva and Stomach. In fact, the bile salts spectral range (400-430 nm) covers the MNM plasmonic peak. Aggregation is monitored also by TEM. No dissolution is occurred, as revealed by UF-ICPAES data, because of MNM re-formation (in line with literature data).

2.5. Evaluation and conclusions

2.5.1. Task 2.4 e) Procedures for quantification of MNM exposure and fate in dispersions for ecotoxicological studies

Currently, an adequate interpretation of data generated in aquatic ecotoxicity studies is often limited owing to a lack of an appropriate procedure for the physicochemical characterisation and quantification of test MNM being implemented in such studies. The developed NANoREG ECOTOX Dispersion Characterisation TGD provides a framework for aquatic ecotoxicologists to generate the necessary physicochemical characterisation data to enable improved interpretation of results and also for improved read across between data generated in different studies. Importantly, the TGD is designed in such a way as to try and minimise the amount of MNM dispersion characterisation necessary to achieve this goal. The TGD is best employed in conjunction with other relevant SOPs generated within NANoREG WP2 for preparing and characterising MNM dispersions in ecotoxicity studies in order to achieve reproducible data within in ecotoxicity tests. The TGD has been developed in NANoREG WP2 and implemented in NANoREG WP4 for evaluation purposes.

Application of the TGD developed in NANoREG WP2 within the aquatic ecotoxicity studies completed as part of NANoREG WP4 highlights clearly that there is a need for including and conducting detailed physicochemical characterisation of MNM dispersion exposures throughout the duration of an ecotoxicity test. The TGD provides a framework to better understand MNM behaviour and fate in ecotoxicological studies. We believe the developed TGD enables a clearer and more reproducible decision making process for MNM characterisation in aquatic ecotoxicity tests.

Through the implementation of the TGD in aquatic ecotoxicity tests conducted in NANoREG WP4, we were able to conduct an internal evaluation. It was found that a number of key factors can significantly influence the MNM exposure organisms undergo in aquatic ecotoxicity tests:

- MNM type (inherent physicochemical properties)
- MNM exposure dispersion concentration (all toxicity tests employ an exposure concentration range in order to establish an effect concentration for the test item)
- Media type media type is typical specific to individual standard tests/organisms and can vary considerably in composition)
- Ecotoxicity test duration (time was found to be a significant factor in controlling the exposure dispersion conditions)

It was also determined through the evaluation process that the *extrinsic* properties identified in the TGD as important to measure in aquatic ecotoxicity tests have the potential to significantly influence the final exposure to which the test organisms are subjected. These were indeed found to change over time and therefore need to be monitored over the duration of such tests in order to meaningfully interpret resulting toxicity data. The key *extrinsic* properties highlighted are:

- MNM aggregation (z-ave)
- MNM dispersion concentration (linked to settling/sedimentation)
- MNM dissolution

It was found that even the minimum level of MNM dispersion characterisation which was one of the primary goals for the TGD still represents a considerable time and resource (analysis) cost to such studies. Further work is needed to develop new instrumentation, improve existing instrumentation, and to develop instrument add-ons, data processing and management software which are focused on streamlining time and costs required to undertake MNM characterisation in aquatic ecotoxicity studies.

However, the results from the TGD also indicate that such testing is absolutely essential if a full understanding of MNM exposure is to be achieved during aquatic ecotoxicity. It also shows that current approaches frequently employed in aquatic ecotoxicity testing of MNM may fail to adequately characterise the organism's exposure and therefore permit accurate interpretation of resulting ecotoxicity endpoint data. In conclusion, we

feel that the TGD developed goes a significant way to providing a framework from which to design and conduct MNM characterisation in aquatic ecotoxicity testing. We acknowledge that this document may need further evaluation, revision and updating as new data and knowledge regarding MNM aquatic ecotoxicity testing becomes available in the future.

2.5.2. Task 2.4 f) Procedures for quantification of MNM exposure and fate in dispersions for in vitro studies;

In-depth characterization at each stage is fundamental to facilitate data interpretation, to relate MNM properties to the biological outcomes and also improving data reliability for benchmarking. A multi-techniques based approach is suggested to expand the characterization of MNM not only to size, but also to surface charge and dissolution. These properties, together with size, appear strictly linked to exposure. They may be considered interesting physical descriptors for MNM risk assessment. Presence of culture medium and cells add significant complexity to the physicochemical determinations. Their pattern change evaluation may be informative of the MNM fate in the dispersant medium and of their actual dose.

Furthermore the pattern analysis of these properties may pave the way for grouping based on structural properties of MNM, which are influenced by the environment. Many of these research works are cross-cutting with activities done between WP5 and WP2 and the results may respond to key questions of WP1.

At least size and surface characteristics of MNMs should be determined before and monitored during in vitro exposure studies. Dose of MNMs evolves during in vitro studies; therefore, a methodology like the one proposed here, should be used systematically to determine the sedimented dose. This determination should be done at least at the beginning and the end of in vitro testing. Obtained sedimented dose should help to improve the interpretation of the biological outcome, which is still associated to a “nominal dose”. At this state, given the small quantity of data, it is suggested to continue with protocol evaluation and further data generation.

Kinetics of MNMs during in vitro tests, sedimented dose and protein corona determinations require further evaluation. The complexity of the determinations and the technical limitations, associated to current characterisation techniques, suggest that *in silico* approaches should be considered to better understand fate.

2.5.3. Task 2.4 i) Characterization of MNM hydrochemical reactivity in synthetic biological fluids.

Data obtained by a multi-technique based method (list of all methods applied? NRCWE and IIT) on different NPs from repository list to check different endpoints (size, pH, surface charge, dissolution rate, etc.) indicated that MNM are reactive in synthetic fluids (e.g., biological media or simulating human fluids) at different extent depending on their pristine properties. Determination of hydro chemical reactivity is complex and cannot be seen as a single property but rather a pattern of specific endpoints (such as solubility, pH, dissolution, protein absorption, etc.) that might strongly influence the output of an in vitro test. Here, we envisage the possibility to apply multi-technique methodologies as they appear fundamental to facilitate the data interpretation. Hence, we recommend the use of different techniques to characterize size and dissolution during a digestive test or when using complex matrixes.

The generated SOP (IIT SOP), protocol or guideline are in a proof of concept state and need to be further improved due to the small quantity of data available up to now. We still need to better evaluate the protocols by generating a wider amount of data possibly under validating conditions such as inter-laboratory comparison analysis.

2.6. Data management

A specific template for reporting the particle size distribution obtained with the CLS technique was proposed, discussed and implemented. Each partner will report their results individually using the appropriate templates.

3. Deviations from the work plan

3.1. Task 2.4 e) Procedures for quantification of MNM exposure and fate in dispersions for ecotoxicological studies

The NANoREG partners contributing to Task 2.4e had to prioritise the allocation of their individual financial and time resources towards other WP2 tasks in which they were involved. Owing to the structure and linear development of tasks within WP2, these other Tasks needed to be fully completed before Task 2.4e could be initiated. As a result, Task 2.4e has had to be slightly reduced in scope. This means that the planned evaluation and benchmarking (verification) of the procedure for quantification of MNM exposure and fate in dispersions for ecotoxicological studies will be reduced to an evaluation only. This evaluation will be conducted by partners SINTEF and NMBU as part of their contribution to conducting aquatic ecotoxicity studies in NANoREG WP4. It is uncertain if any work related to Task 2.4e will be published as the developed TGD has not undergone any form of benchmarking. However, elements of the work will be reported in publications expected in WP4.

3.2. Task 2.4 f) Procedures for quantification of MNM exposure and fate in dispersions for in vitro studies

One principal difference with respect to the DOW is that proposed interlaboratory comparisons of MNM dispersion methods for *in vitro* exposure were overtaken due to compulsory use of the sonicator calibration protocol (as a tool for harmonization of the dispersion preparation). Strong collaboration was established with the WP5 task 5.3 where UNamur partners were contributing as well.

Partner IIT reported that AFM, SDS-PAGE for protein corona characterization in the matrices have not been performed due to technical overload taken for the other experiments done within this deliverable and in collaboration with WP5 for the dissolution test.

3.3. Task 2.4 i) Characterization of MNM hydrochemical reactivity in synthetic biological fluids

Except from technical delays, no other significant modifications occurred in this task.

4. References / Selected sources of information (optional)

Ahmad Khanbeigi, R., et al. (2012). "The delivered dose: Applying particokinetics to *in vitro* investigations of nanoparticle internalization by macrophages." J Control Release 162.

Arts, J. H. E., et al. (2016). "Case studies putting the decision-making framework for the grouping and testing of nanomaterials (DF4nanoGrouping) into practice." Regulatory Toxicology and Pharmacology 76: 234-261.

Baun, A., et al. (2008). "Ecotoxicity of engineered nanoparticles to aquatic invertebrates: a brief review and recommendations for future toxicity testing." Ecotoxicology 17(5): 387-395.

Cohen, J. M., et al. (2015). "A critical review of *in vitro* dosimetry for engineered nanomaterials." Nanomedicine (Lond).

Corradi, S., et al. (2012). "Influence of serum on in situ proliferation and genotoxicity in A549 human lung cells exposed to nanomaterials." Mutation Research/Genetic Toxicology and Environmental Mutagenesis 745(1–2): 21-27.

David, C. A., et al. (2012). "Dissolution Kinetics and Solubility of ZnO Nanoparticles Followed by AGNES." The Journal of Physical Chemistry C 116(21): 11758-11767.

Domingos, R. F., et al. (2009). "Characterizing Manufactured Nanoparticles in the Environment: Multimethod Determination of Particle Sizes." Environmental Science & Technology 43(19): 7277-7284.

Ellegaard-Jensen, L., et al. (2012). "Nano-silver induces dose-response effects on the nematode Caenorhabditis elegans." Ecotoxicol Environ Saf 80: 216-223.

Farmen, E., et al. (2012). "Acute and sub-lethal effects in juvenile Atlantic salmon exposed to low µg/L concentrations of Ag nanoparticles." Aquatic Toxicology 108(0): 78-84.

Flaherty, N. L., et al. (2015). "Comparative analysis of redox and inflammatory properties of pristine nanomaterials and commonly used semiconductor manufacturing nano-abrasives." Toxicol Lett 239(3): 205-215.

George, S., et al. (2012). "Surface Defects on Plate-Shaped Silver Nanoparticles Contribute to Its Hazard Potential in a Fish Gill Cell Line and Zebrafish Embryos." ACS Nano 6(5): 3745-3759.

Gittings, S., et al. (2015). "Characterisation of human saliva as a platform for oral dissolution medium development." Eur J Pharm Biopharm 91: 16-24.

Handy, R., et al. (2012). "Ecotoxicity test methods for engineered nanomaterials: practical experiences and recommendations from the bench." Environ Toxicol Chem 31(1): 15 - 31.

Hartmann, N. B., et al. (2015). "Techniques and Protocols for Dispersing Nanoparticle Powders in Aqueous Media-Is there a Rationale for Harmonization?" J Toxicol Environ Health B Crit Rev 18(6): 299-326.

Ilknur, S., et al. (2012). "The influence of the surface chemistry of silver nanoparticles on cell death." Nanotechnology 23(37): 375102.

Jackson, P., et al. (2015). "Characterization of genotoxic response to 15 multiwalled carbon nanotubes with variable physicochemical properties including surface functionalizations in the FE1-Muta(TM) mouse lung epithelial cell line." Environ Mol Mutagen 56(2): 183-203.

Jain, S., et al. (2011). "Toxicity of Multiwalled Carbon Nanotubes with End Defects Critically Depends on Their Functionalization Density." Chemical Research in Toxicology 24(11): 2028-2039.

Jensen, E. K., et al. (2012). "Early Combination of Material Characteristics and Toxicology Is Useful in the Design of Low Toxicity Carbon Nanofiber." Materials 5(9): 1560-1580.

Jensen, K. A., et al. (2014). Characterization of Manufactured Nanomaterials, Dispersion, and Exposure for Toxicological Testing. Nanotoxicology, CRC Press: 45-74.

Kahru, A. and H.-C. Dubourguier (2010). "From ecotoxicology to nanoecotoxicology." Toxicology 269(2-3): 105-119.

Klaine, S. J., et al. (2008). "Nanomaterials in the environment: Behavior, fate, bioavailability, and effects." Environmental Toxicology and Chemistry 27(9): 1825-1851.

Laloy, J., et al. (2012). "Validation of the calibrated thrombin generation test (cTGT) as the reference assay to evaluate the procoagulant activity of nanomaterials." Nanotoxicology 6(2): 213-232.

Lankoff, A., et al. (2012). "Effect of surface modification of silica nanoparticles on toxicity and cellular uptake by human peripheral blood lymphocytes *in vitro*." Nanotoxicology.

Li, M., et al. (2013). "Effects of water chemistry on the dissolution of ZnO nanoparticles and their toxicity to Escherichia coli." Environmental Pollution 173: 97-102.

Lozano, O., et al. (2013). "How does the deposited dose of oxide nanomaterials evolve in an *in vitro* assay?" J Phys Conf Series 429: 012013.

Lynch, I., et al. (2009). "Protein-nanoparticle interactions: What does the cell see?" Nat Nano 4(9): 546-547.

Mejia, J., et al. (2013). "Dose assessment of SiC nanoparticle dispersions during *in vitro* assays." Journal of Nanoparticle Research 15(8): 1-15.

Miralles, P., et al. (2012). "Toxicity, Uptake, and Translocation of Engineered Nanomaterials in Vascular plants." Environmental Science & Technology 46(17): 9224-9239.

Morishige, T., et al. (2012). "Suppression of nanosilica particle-induced inflammation by surface modification of the particles." Archives of Toxicology 86(8): 1297-1307.

Nangia, S. and R. Sureshkumar (2012). "Effects of Nanoparticle Charge and Shape Anisotropy on Translocation through Cell Membranes." Langmuir 28(51): 17666-17671.

Navarro, E., et al. (2008). "Environmental behavior and ecotoxicity of engineered nanoparticles to algae, plants, and fungi." Ecotoxicology 17(5): 372-386.

Nymark, P., et al. (2013). "Genotoxicity of polyvinylpyrrolidone-coated silver nanoparticles in BEAS 2B cells." Toxicology 313(1): 38-48.

Paterson, G., et al. (2011). "The need for standardized methods and environmental monitoring programs for anthropogenic nanoparticles." Analytical Methods 3(7): 1461-1467.

Patlolla, A. K., et al. (2010). "Comparative study of the clastogenicity of functionalized and nonfunctionalized multiwalled carbon nanotubes in bone marrow cells of Swiss-Webster mice." Environmental Toxicology 25(6): 608-621.

Peijnenburg, W. J. G. M., et al. (2015). "A review of the properties and processes determining the fate of engineered nanomaterials in the aquatic environment." Critical Reviews in Environmental Science and Technology: 00-00.

Sajid, M., et al. (2015). "Impact of nanoparticles on human and environment: review of toxicity factors, exposures, control strategies, and future prospects." Environmental Science and Pollution Research 22(6): 4122-4143.

Simonin, M. and A. Richaume (2015). "Impact of engineered nanoparticles on the activity, abundance, and diversity of soil microbial communities: a review." Environmental Science and Pollution Research: 1-14.

Tiede, K., et al. (2009). "Considerations for environmental fate and ecotoxicity testing to support environmental risk assessments for engineered nanoparticles." Journal of Chromatography A 1216(3): 503-509.

Varnes, M. E., et al. (1986). "The effect of pH on potentially lethal damage recovery in A549 cells." Radiat Res 108(1): 80-90.

Vranic, S., et al. (2016). "Impact of serum as a dispersion agent for *in vitro* and *In vitro* toxicological assessments of TiO2 nanoparticles." Archives of Toxicology: 1-11.

Wang, N., et al. (2016). "Lifetime and dissolution kinetics of zinc oxide nanoparticles in aqueous media." Nanotechnology 27(32): 324001.

Wardman, P. (2007). "Fluorescent and luminescent probes for measurement of oxidative and nitrosative species in cells and tissues: progress, pitfalls, and prospects." Free Radic Biol Med 43(7): 995-1022.

Warheit, D. B. (2008). "How Meaningful are the Results of Nanotoxicity Studies in the Absence of Adequate Material Characterization?" Toxicological Sciences 101(2): 183-185.

Weinberg, H., et al. (2011). "Evaluating engineered nanoparticles in natural waters." TrAC Trends in Analytical Chemistry 30(1): 72-83.

Wigginton, N. S., et al. (2007). "Aquatic environmental nanoparticles." Journal of Environmental Monitoring 9(12): 1306-1316.

Wu, Y., et al. (2016). "pH dependence of quinone-mediated extracellular electron transfer in a bioelectrochemical system." Electrochimica Acta 213: 408-415.

Xia, T., et al. (2006). "Comparison of the Abilities of Ambient and Manufactured Nanoparticles To Induce Cellular Toxicity According to an Oxidative Stress Paradigm." Nano Letters 6(8): 1794-1807.